LUND UNIVERSITY

Determination of Linear and Nonlinear Steering Models for the USS Compass Island

Källström, Claes G.

1977

Document Version:
Publisher's PDF, also known as Version of record

Link to publication

Citation for published version (APA):
Källström, C. G. (1977). *Determination of Linear and Nonlinear Steering Models for the USS Compass Island*. (Technical Reports TFRT-7130). Department of Automatic Control, Lund Institute of Technology (LTH).

Total number of authors:
1

General rights
Unless other specific re-use rights are stated the following general rights apply:
Copyright and moral rights for the publications made accessible in the public portal are retained by the authors and/or other copyright owners and it is a condition of accessing publications that users recognise and abide by the legal requirements associated with these rights.
• Users may download and print one copy of any publication from the public portal for the purpose of private study or research.
• You may not further distribute the material or use it for any profit-making activity or commercial gain
• You may freely distribute the URL identifying the publication in the public portal

Read more about Creative commons licenses: https://creativecommons.org/licenses/

Take down policy
If you believe that this document breaches copyright please contact us providing details, and we will remove access to the work immediately and investigate your claim.

LUND UNIVERSITY

PO Box 117
221 00 Lund
+46 46-222 00 00

Download date: 12. Oct. 2024

CODEN: LUTFD2/(TFRT-7130)/1-099/(1977)

DETERMINATION OF LINEAR AND NONLINEAR STEERING MODELS FOR THE USS COMPASS ISLAND

CLAES G. KÄLLSTRÖM

Department of Automatic Control
Lund Institute of Technology
December 1977

Dokumentutgivare
Lund Institute of Technology
Handläggare Dept of Automatic Control
Claes G. Källström
Författare
Claes G. Källström

Dokumentnamn
Report
Utgivningsdatum
Dec 1977

Dokumentbeteckning
LUTFD2/(TFRT-7130)/1-099/(1977)
Ärendebeteckning
STU 73 41 28 U
STU 75 40 53

10T4

Dokumenttitel och undertitel
Determination of linear and nonlinear steering models for the USS Compass Island

Referat (sammandrag)

System identification techniques are applied to determine the steering dynamics of the cargo ship USS Compass Island of the Mariner class. Three 20°/20° zig-zag tests performed at different speeds are analysed. The output error method and the maximum likelihood method are applied using the identification program LISPID. Parameters of both a linear and a nonlinear model are estimated. It is concluded that the non-linear model should be used when the zig-zag tests are analysed. Good parameter estimates are obtained. The maximum likelihood method is proved to be advantageous compared with the output error method.

Referat skrivet av
Author

Förslag till ytterligare nyckelord
ship, ship steering, ship dynamics

Klassifikationssystem och -klass(er)
50T0

Indextermer (ange källa)
52T0

Omfång
99 pages

Övriga bibliografiska uppgifter
56T2

Språk
English

Sekretessuppgifter
60T0

ISSN
60T4

ISBN
60T6

Dokumentet kan erhållas från
Department of Automatic Control
Lund Institute of Technology
P O Box 725, S-220 07 Lund 7, SWEDEN

Mottagarens uppgifter
62T4

Pris
66T0

DOKUMENTDATABLAD enligt SIS 62 10 12

SIS-DB 1

Blankett LU 11:25 1976–07

DETERMINATION OF LINEAR AND NONLINEAR STEERING MODELS FOR THE USS COMPASS ISLAND

CLAES G. KÄLLSTRÖM

ABSTRACT

System identification techniques are applied to determine the steering dynamics of the cargo ship USS Compass Island of the Mariner class. Three $20^{o}/20^{o}$ zig-zag tests performed at different speeds are analysed. The output error method and the maximum likelihood method are applied using the identification program LISPID. Parameters of both a linear and a nonlinear model are estimated. It is concluded that the nonlinear model should be used when the zig-zag tests are analysed. Good parameter estimates are obtained. The maximum likelihood method is proved to be advantageous compared with the output error method.

TABLE OF CONTENTS

	Page
1. INTRODUCTION	4
2. EXPERIMENTS	4
3. SHIP STEERING DYNAMICS	9
4. IDENTIFICATION OF LINEAR MODELS	18
5. IDENTIFICATION OF NONLINEAR MODELS	31
6. CONCLUSIONS	95
7. ACKNOWLEDGEMENTS	97
8. REFERENCES	98

1. INTRODUCTION

System identification techniques are applied to determine the steering dynamics of the USS Compass Island from three $20^{\circ}/20^{\circ}$ zig-zag tests performed at different speeds. Parameters of both linear and nonlinear models are estimated by use of the identification program LISPID (see Källström, Essebo and Åström, 1976). The output error method and the maximum likelihood method are applied.

2. EXPERIMENTS

The USS Compass Island is a converted, single-screw 13 400 tdw cargo ship of the Mariner class with a half-spade rudder. The power at 97 rpm is 19 250 shp and the corresponding speed is 21.1 knots. The length between perpendiculars L is 161 m, the breadth is 23.2 m and the design draught is 9.1 m at a displacement of 20 840 m^3.

Extensive experiments with the USS Compass Island are described by Morse and Price (1961). Three $20^{\circ}/20^{\circ}$ zig-zag tests will be analysed. The aft and forward draught during the experiments were 8.08 m and 6.86 m corresponding to a displacement ∇ of 16 650 m^3. The experiments were performed in calm sea and lasted for about 10 min each. The approach speed of the different zig-zag tests was 10, 15 and 20 knots which resulted in an average speed during each experiment of 8.75, 12 and 16.5 knots, respectively. The rudder angles, the sway velocities at the centre of gravity, the yaw rates and the headings from each experiment were obtained from graphs in Morse and Price (1961). A sampling interval T of 6 s was used when the graphs were digitalized. Notice, however, that 4 samples were omitted when the data of the first experiment were generated. The input-output data obtained from the 3 zig-zag

tests are shown in Figs. 2.1, 2.2 and 2.3. The rudder angles are positive towards port. The number of samples of experiment 1, 2 and 3 are 102, 83 and 73, respectively.

The USS Compass Island experiments were performed using an inertial navigation system which makes it possible to obtain measurements with high precision and high resolution. Naturally a lot of the precision inherent in the data were, however, lost when the graphs were converted to digits.

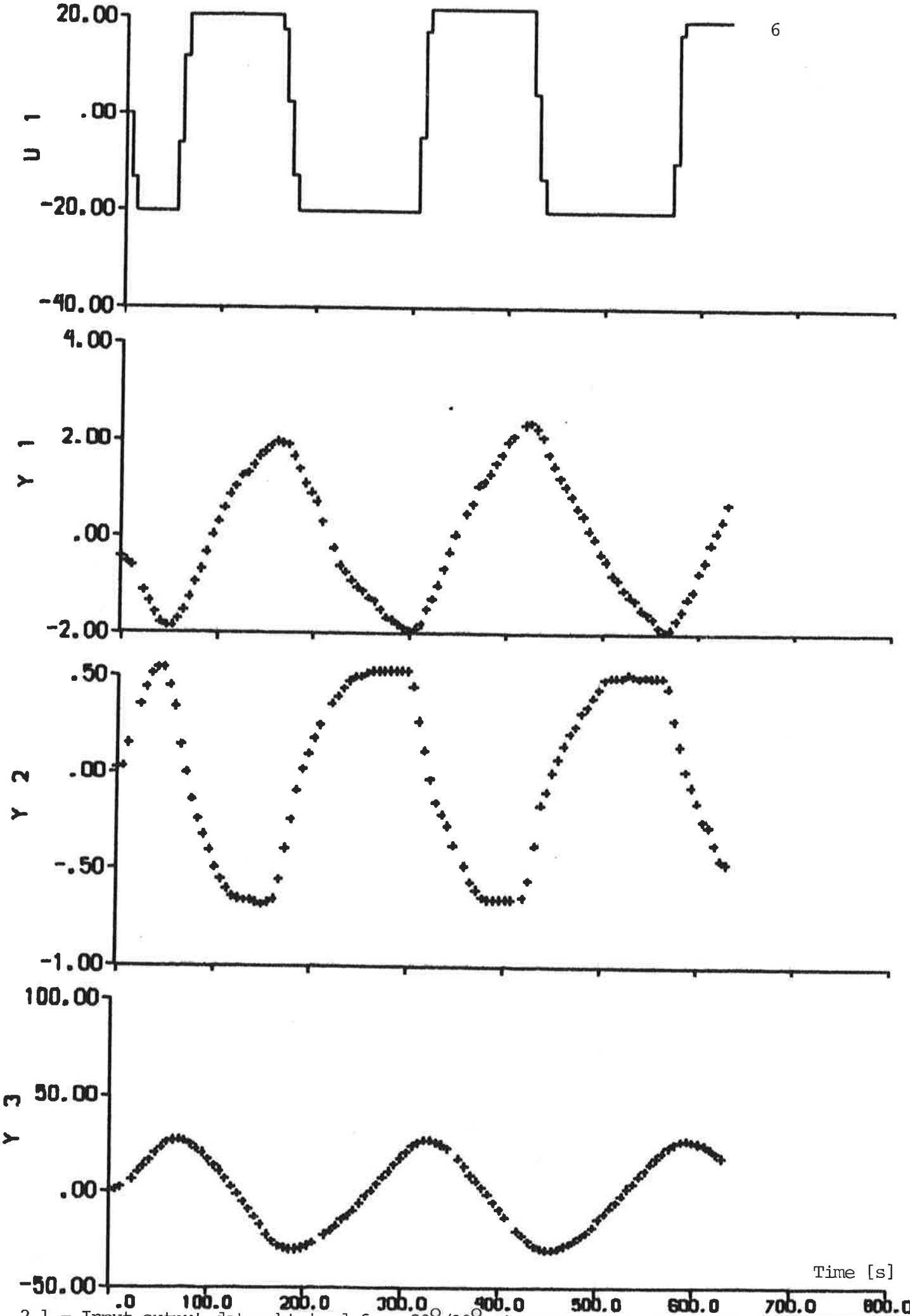

Fig. 2.1 - Input-output data obtained from 20°/20° zig-zag test 1 performed at an average speed of 8.75 knots. The input is the rudder angle U1 [deg] and the outputs are the sway velocity at centre of gravity Y1 [knots], the yaw rate Y2 [deg/s] and the heading angle Y3 [deg].

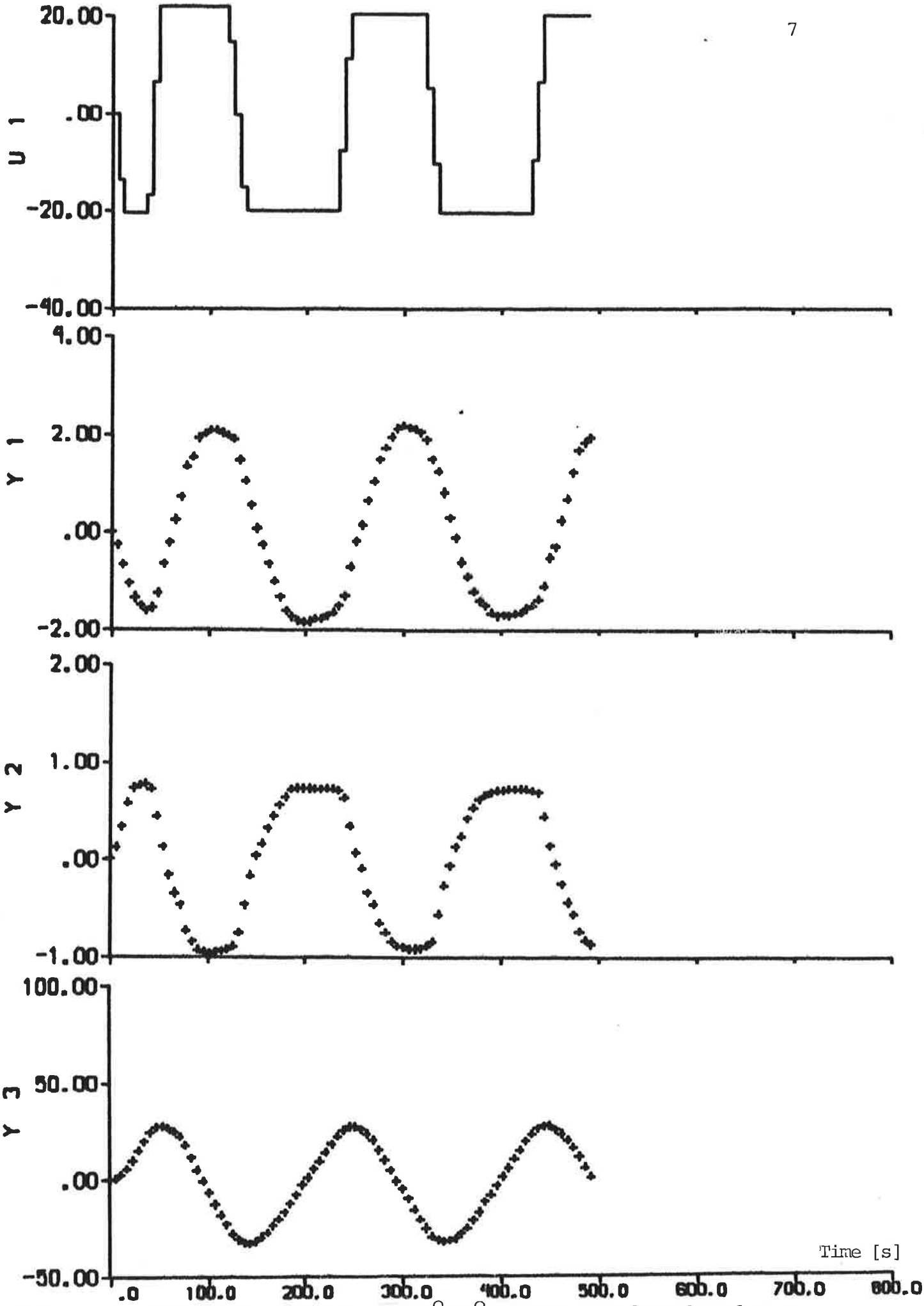

Fig. 2.2 - Input-output data obtained from $20^{o}/20^{o}$ zig-zag test 2 performed at an average speed of 12 knots. The input is the rudder angle U1 [deg] and the outputs are the sway velocity at centre of gravity Y1 [knots], the yaw rate Y2 [deg/s] and the heading angle Y3 [deg].

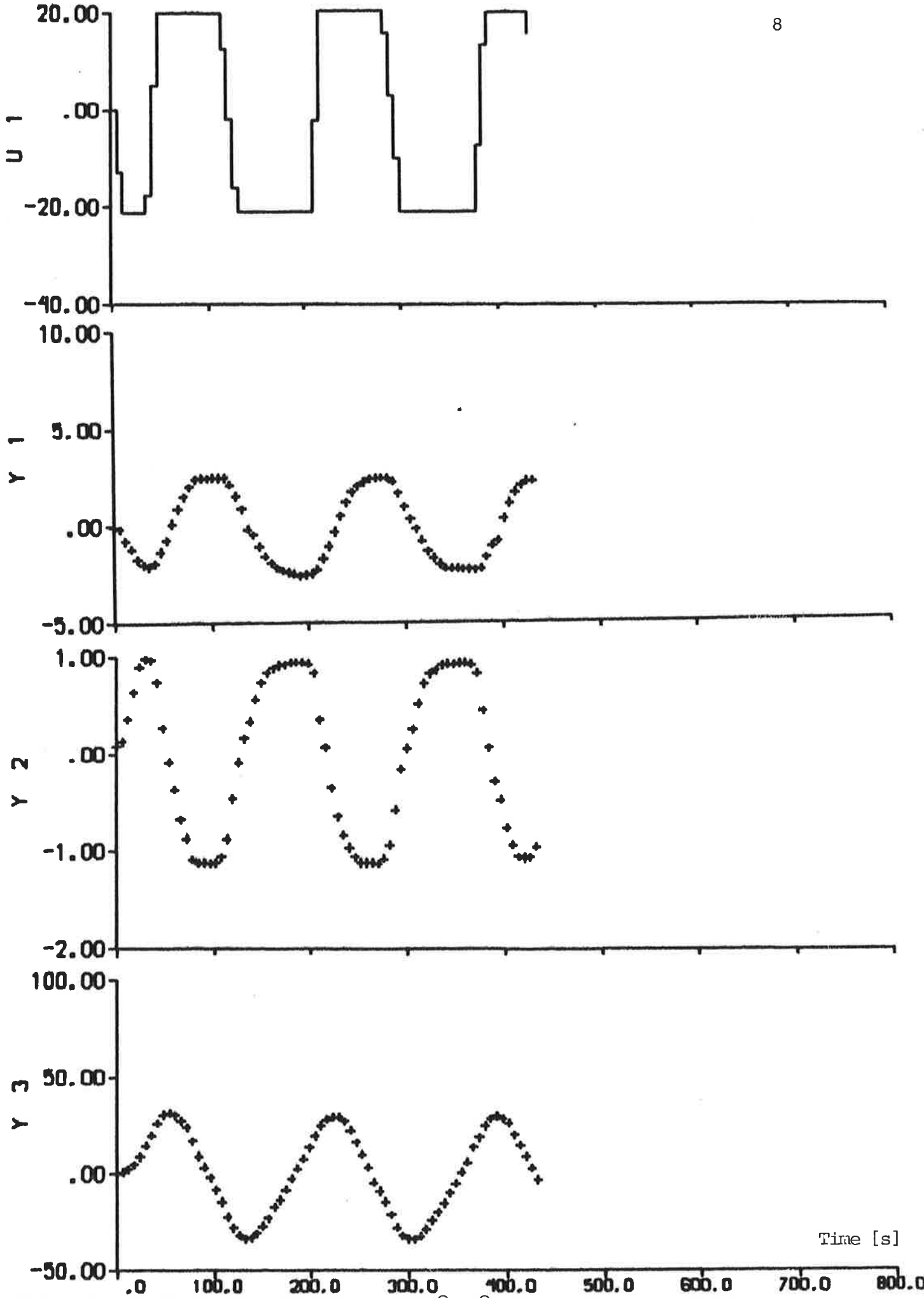

Fig. 2.3 - Input-output data obtained from $20^{\circ}/20^{\circ}$ zig-zag test 3 performed at an average speed of 16.5 knots. The input is the rudder angle U1 [deg] and the outputs are the sway velocity at centre of gravity Y1 [knots], the yaw rate Y2 [deg/s] and the heading angle Y3 [deg].

3. SHIP STEERING DYNAMICS

The identification results described in Sections 4 and 5 are based on the following model of the ship steering dynamics (see Åström, Norrbin, Källström and Byström, 1974; Åström, Källström, Norrbin and Byström, 1975):

$$\begin{bmatrix} \frac{L}{V^2}\theta_1 & \frac{L^2}{V^2}\theta_2 & 0 \\ \frac{L}{V^2}\theta_3 & \frac{L^2}{V^2}\theta_4 & 0 \\ 0 & 0 & 1 \end{bmatrix} \begin{bmatrix} dv \\ dr \\ d\psi \end{bmatrix} = \begin{bmatrix} \frac{1}{V}\theta_5 & \frac{L}{V}\theta_6 & \theta_9 \\ \frac{1}{V}\theta_7 & \frac{L}{V}\theta_8 & \theta_9 \cdot \theta_{10} \\ 0 & 1 & 0 \end{bmatrix} \begin{bmatrix} v(t) \\ r(t) \\ \psi(t) \end{bmatrix} dt +$$

$$+ \begin{bmatrix} \alpha_1 \cdot \theta_{11} & \theta_{13} \\ -\alpha_1 \cdot \theta_{11}\theta_{12} & \theta_{14} \\ 0 & 0 \end{bmatrix} \begin{bmatrix} \delta(t-T_D) \\ U \end{bmatrix} dt + \theta_{35} \begin{bmatrix} f_Y(v,r) \\ f_N(v,r) \\ 0 \end{bmatrix} dt + dw$$

$$\begin{bmatrix} v_m(t_k) \\ r_m(t_k) \\ \psi_m(t_k) \end{bmatrix} = \begin{bmatrix} \alpha_2 & 0 & 0 \\ 0 & 1/\alpha_1 & 0 \\ 0 & 0 & 1/\alpha_1 \end{bmatrix} \begin{bmatrix} v(t_k) \\ r(t_k) \\ \psi(t_k) \end{bmatrix} + \tag{3.1}$$

$$+ \begin{bmatrix} 0 & \theta_{15} \\ 0 & \theta_{17} \\ 0 & 0 \end{bmatrix} \begin{bmatrix} \delta(t_k-T_D) \\ U \end{bmatrix} + e(t_k) \quad k=0,1,\ldots,N-1$$

The Wiener process w has the incremental covariance R_1 dt, where

$$R_1 = \begin{bmatrix} |\theta_{18}| & \sqrt{|\theta_{18}||\theta_{19}|}\ \sin\theta_{20} & 0 \\ \sqrt{|\theta_{18}||\theta_{19}|}\ \sin\theta_{20} & |\theta_{19}| & 0 \\ 0 & 0 & 0 \end{bmatrix}$$

The measurement errors { $e(t_k)$ } are assumed to be independent and gaussian with zero mean and covariance R_2, where

$$R_2 = \begin{bmatrix} |\theta_{21}| & 0 & 0 \\ 0 & |\theta_{23}| & 0 \\ 0 & 0 & |\theta_{24}| \end{bmatrix}$$

The initial state is given by

$$\begin{bmatrix} v(t_o) \\ r(t_o) \\ \psi(t_o) \end{bmatrix} = \begin{bmatrix} \theta_{25}/\alpha_2 \\ \alpha_1\theta_{26} \\ \alpha_1\theta_{27} \end{bmatrix}$$

The time delay T_D is computed as

$$T_D = T - T\ |\sin\theta_{34}|$$

where T is the sampling interval.

The following variables are introduced in (3.1):

<u>Inputs</u>

- δ - rudder angle [deg]
- U - artificial unit step input [-]

<u>States</u>

- v - sway velocity at centre of gravity [m/s]
- r - yaw rate [rad/s]
- ψ - heading angle [rad]

Outputs

v_m - sway velocity at centre of gravity [knots]

r_m - yaw rate [deg/s]

ψ_m - heading angle [deg]

The model (3.1) is provided with the following fixed parameter values:

V - ship speed (4.5, 6.2 or 8.5 m/s dependent on the experiment)

L - ship length (161 m)

α_1 - conversion factor from degrees to radians (0.01745)

α_2 - conversion factor from m/s to knots (1.944)

T - sampling interval (6 s)

The parameters θ_1 - θ_{35} can be estimated in LISPID. Notice, however, that it is possible to estimate only a subset of the 35 parameters and to give the other parameters arbitrary fixed values. The parameters θ_{16}, θ_{22}, θ_{28} - θ_{33} have been omitted in the model (3.1), because they have no meaning for the analysis performed in this report.

It is concluded from (3.1) that θ_1 - θ_4 are normalized acceleration hydrodynamic derivatives, θ_5 - θ_8, θ_{11} and $-\theta_{11}$ θ_{12} are normalized linear hydrodynamic derivatives, θ_9 and θ_{10} are wind parameters, θ_{13} and θ_{14} are force and moment biases, and θ_{15} and θ_{17} are measurement biases. The time delay T_D can be regarded as the characteristic time between the sampling event and the rudder change, since the rudder angle δ is the input. See Fig. 3.1.

The effective cross-flow drag coefficient θ_{35} = C is the only unknown parameter of the nonlinear contributions to the force and moment. The value is expected to be of the order of $0.4 < C < 1.4$. The commonly used linear model

of the steering dynamics is obtained when $\theta_{35} = 0$. The nonlinear functions f_Y and f_N have been derived in Norrbin (1976) by considering the cross-flow drag. The nonlinear model (3.1) is in LISPID transformed into a linear model by introducing f_Y/m' and f_N/m' as additional inputs U4 and U5, where $m' = 2\nabla/L^3 = 0.00798$. Notice that U4 and U5 are dimension-less. The functions f_Y and f_N are dependent on the true sway velocity v and the true yaw rate r, which are unknown. The estimates $\hat{x}_1$ and $\hat{x}_2$ of v and r obtained through the filter

$$\begin{aligned} \hat{x}(t+T) &= A\,\hat{x}(t+) + Bu(t) \\ \hat{x}(t+) &= \hat{x}(t) + \bar{K}\,[y(t)-C\hat{x}(t)-Du(t)] \end{aligned} \qquad (3.2)$$

are instead used when the additional inputs U4 and U5 are generated. The input vector u, the state vector $\hat{x}$

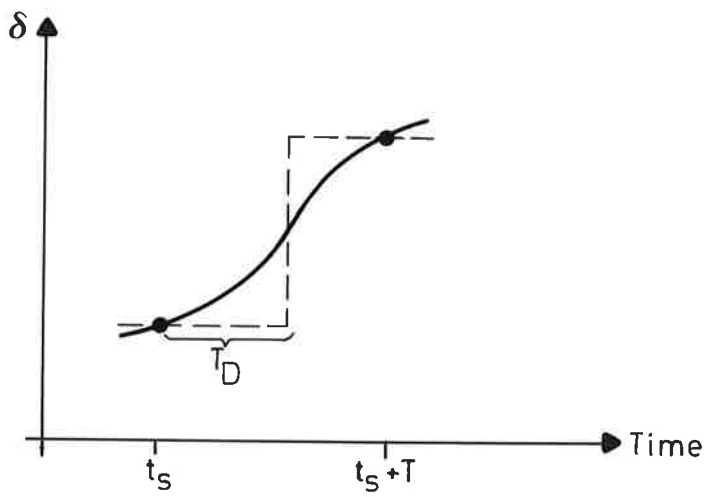

Fig. 3.1 - Explanation of the time delay T_D. The continuous line is the true rudder angle and the dashed line is the approximation of the rudder angle used in LISPID.

and the output vector y are the same as in the model (3.1). The filter (3.2) is obtained from (3.1) by assuming $\theta_{35} = 0$ and by sampling with T = 6 s. The stationary filter gain $\bar{K}$ is calculated by solving an appropriate, discrete Riccati equation. Notice that $\bar{K} = 0$ when there is no process noise in (3.1), i.e. when w = 0. The problem of estimating unknown parameters of the nonlinear model (3.1) with $\theta_{35} \neq 0$ is thus transformed into the much easier problem to estimate parameters of a linear model.

The maximum likelihood estimates of the unknown parameters are in LISPID obtained by minimizing the loss function

$$V = \frac{1}{N} \det \left[\sum_{k=0}^{N-1} \varepsilon(t_k)\varepsilon^T(t_k) \right] \tag{3.3}$$

where N is the number of samples. The residuals ε are determined recursively from the innovations representation (see Källström, Essebo and Åström, 1976; Åström, 1970):

$$\begin{aligned} \hat{x}(t+T) &= A\,\hat{x}(t) + Bu(t) + K\,\varepsilon(t) \\ y(t) &= C\,\hat{x}(t) + Du(t) + \varepsilon(t) \end{aligned} \tag{3.4}$$

Cf. (3.2). Notice that $K = A\bar{K}$. Notice also that (3.2) and (3.4) are equivalent if θ_{35} of (3.1) is zero, i.e. if a linear model is used. The input vector u of (3.4) contains the additional inputs U4 and U5 when $\theta_{35} \neq 0$, i.e. when a nonlinear model is analysed. The one-step prediction errors, i.e. the residuals, are minimized in the maximum likelihood method. The output error method is easily obtained by assuming no process noise in (3.1), i.e. w = 0. This implies that K = 0 in (3.4)

Different models can be compared by using Akaike's information criterion (see Akaike, 1972):

$$AIC = -2 \log \hat{L} + 2\nu \tag{3.5}$$

where $\hat{L}$ is the maximum of the likelihood function and ν is the number of estimated parameters. According to Akaike the quantity AIC should be minimum for the correct model structure. The following relation is obtained from (3.3) and (3.5):

$$AIC = N \log V + 2\nu + (1-n_y)\, N\log N + n_y N(1+\log 2\pi) \qquad (3.6)$$

where n_y is the number of outputs, i.e. 3 according to the model (3.1).

The program LISPID allows for both uniform and varying sampling. Three different cases are possible:

ISAMP = 1: Constant sampling interval.
ISAMP = 2: Constant sampling interval, but some samples are missing.
ISAMP = 3: Non-uniform sampling interval.

ISAMP = 1 is used when experiments 2 and 3 are analysed, but experiment 1 requires that ISAMP = 2.

It was concluded in Källström (1977) that it is questionable if the wind parameters θ_9 and θ_{10} should be estimated, when the wind speed is less than 10 m/s. Since the USS Compass Island zig-zag tests were performed in calm sea, it is decided to assume $\theta_9 = \theta_{10} = 0$ in the sequel.

The transfer function relating the heading ψ to the rudder angle δ (in radians), when the wind parameters θ_9 and θ_{10}, the time delay T_D, and the parameter θ_{35} are zero, is obtained from (3.1):

$$G_{\psi\delta}(s) = \frac{K(1+sT_3)}{s(1+sT_1)(1+sT_2)} = \frac{K_1(s+1/T_3)}{s(s+1/T_1)(s+1/T_2)} \qquad (3.7)$$

where $K_1 = \frac{KT_3}{T_1T_2}$. The corresponding transfer function relating the sway velocity v to the rudder angle δ (in radians) is

$$G_{v\delta}(s) = \frac{K_v(1+sT_{3v})}{(1+sT_1)(1+sT_2)} = \frac{K_{1v}(s+1/T_{3v})}{(s+1/T_1)(s+1/T_2)} \tag{3.8}$$

where $K_{1v} = \frac{K_v T_{3v}}{T_1 T_2}$. It is customary to normalize the gains and time constants of (3.7) and (3.8) by use of the 'prime' system:

$$\begin{aligned} K' &= K \cdot L/V & T_1' &= T_1 \cdot V/L \\ K_1' &= K_1 \cdot L^2/V^2 & T_2' &= T_2 \cdot V/L \\ K_v' &= K_v/V & T_3' &= T_3 \cdot V/L \\ K_{1v}' &= K_{1v} \cdot L/V^2 & T_{3v}' &= T_{3v} \cdot V/L \end{aligned} \tag{3.9}$$

The identifiability aspects of the model (3.1) were discussed in Åström and Källström (1973, 1976). The linear hydrodynamic derivatives $\theta_5 - \theta_8$, $\theta_{11}, -\theta_{11} \cdot \theta_{12}$, the wind parameters $\theta_9 - \theta_{10}$, the biases $\theta_{13} - \theta_{15}$, θ_{17}, and the parameter θ_{35} can be determined if the acceleration hydrodynamic derivatives $\theta_1 - \theta_4$ are known and if the parameter values are such that the model (3.1) is completely observable and completely controllable. It is necessary that measurements of the sway velocity are available together with measurements of th yaw rate or the heading angle. All parameters $\theta_{18} - \theta_{21}$, $\theta_{23} - \theta_{24}$ of the covariance matrices R_1 and R_2 can not be determined when the maximum likelihood method is applied, since it is possible to multiply R_1 and R_2 by an arbitrary coefficient and still obtain the same filter gain K (cf. (3.4)). Therefore, the parameter θ_{24} is always fixed in the sequel.

The hydrodynamic derivatives of the linear model (3.1) for a Mariner class vessel have been estimated from several scale model tests. The results have been summarized by Motora (1972). The estimates obtained by the Hydro- and Aerodynamics Laboratory (HyA, now SL), Denmark, are shown

in Table 3.1. The scale model tests were performed at a speed corresponding to 15 knots. The acceleration derivatives $\theta_1 - \theta_4$ are always fixed in the sequel to the values given in Table 3.1.

A preliminary analysis of zig-zag test 1 was presented in Åström, Norrbin, Källström and Byström (1974) and Åström, Källström, Norrbin, Byström (1975). The relation $-N_\delta'/Y_\delta'$ was then estimated to 0.24 when the maximum likelihood method was applied and to 0.14 when the output error method was used. The relation is known to be approximately 0.5. It is concluded from Table 3.1 that the value 0.48 is obtained from HyA:s model. Since the estimates of $-N_\delta'/Y_\delta'$ obtained from the preliminary identifications are poor, it is decided to fix $\theta_{12} = -N_\delta'/Y_\delta'$ to 0.48 in the sequel. This was also suggested in Källström (1977).

A preliminary analysis of all 3 zig-zag tests showed that it was questionable if the measurement biases θ_{15} and θ_{17} should be estimated at the same time as the parameters $\theta_{25} - \theta_{27}$ of the initial state. Large measurement biases were sometimes obtained, and they were compensated by a large initial state. This effect was also noticed in Källström (1977). To avoid such difficulties it is decided to fix the measurement biases θ_{15} and θ_{17} to zero.

The following fixed parameter values are thus always used in the identifications described in Sections 4 and 5:

$$\theta_1 = 0.01546$$
$$\theta_2 = 0.00026$$
$$\theta_3 = 0.00012$$
$$\theta_4 = 0.00083$$
$$\theta_9 = 0$$
$$\theta_{10} = 0$$
$$\theta_{12} = 0.48$$
$$\theta_{15} = 0$$
$$\theta_{17} = 0$$
$$\theta_{24} = 0.0001 \text{ deg}^2$$

$m' - Y_{\dot{v}}'$	(θ_1)	0.01546
$m'x_G' - Y_{\dot{r}}'$	(θ_2)	0.00026
$m'x_G' - N_{\dot{v}}'$	(θ_3)	0.00012
$I_z' - N_{\dot{r}}'$	(θ_4)	0.00083
Y_v'	(θ_5)	-0.01160
$Y_r' - m'$	(θ_6)	-0.00526
N_v'	(θ_7)	-0.00291
$N_r' - m'x_G'$	(θ_8)	-0.00184
Y_δ'	(θ_{11})	0.00278
N_δ'	$(-\theta_{11}\theta_{12})$	-0.00133

Table 3.1 - Hydrodynamic derivatives for a Mariner class vessel estimated by HyA from planar motion mechanism tests (see Chislett and Strøm-Tejsen, 1965). The tests were performed at a speed corresponding to 15 knots. The hydrodynamic derivatives are normalized by use of the 'prime' system with mass unit $\rho L^3/2$. The corresponding values in the 'bis' system are obtained by dividing with $m' = 0.00798$. The values are corrected to $x_G = 0$ (see Mandel, 1967), i.e. the origin of the coordinate system is assumed to be at the centre of gravity.

4. IDENTIFICATION OF LINEAR MODELS

The parameters of the linear version of (3.1) with θ_{35} fixed to zero are first estimated. Preliminary results from zig-zag test 1 were described in Åström, Norrbin, Källström and Byström (1974) and Åström, Källström, Norrbin and Byström (1975). The final results from all 3 zig-zag tests are given in this section.

The results of output error identifications when the model is fixed to HyA:s model, output error identifications when the hydrodynamic derivatives also are estimated, and miximum likelihood identifications are shown in Figs. 4.1-4.9. The parameter estimates obtained are summarized in Tables 4.1-4.3. It is concluded from Figs. 4.1, 4.4 and 4.7 that the consistency between the outputs from HyA:s model and the measurements is rather bad. The models obtained from output error identifications (Figs. 4.2, 4.5 and 4.8) and maximum likelihood identifications (Figs. 4.3, 4.6 and 4.9) give a much better consistency. However, very bad estimates of the hydrodynamic derivatives are obtained in many cases (see Table 4.1), and the models from zig-zag tests 2 and 3 even have a pair of complex poles (see Table 4.2). Parameter values rather close to HyA:s estimates are obtained from zig-zag test 1, with one exception; N_v' is strongly underestimated.

Table 4.3 shows the parameters of the covariance matrices estimated with the maximum likelihood method. The corresponding stationary filter gains (cf. (3.4)) obtained from zig-zag test 1,2 and 3 are:

		Zig-zag test 1			Zig-zag test 2			Zig-zag test 3		
		Output error (HyA:s model)	Output error	Maximum likeli-hood	Output error (HyA:s model)	Output error	Maximum likeli-hood	Output error (HyA:S model)	Output error	Maximum likeli-hood
Figure		4.1	4.2	4.3	4.4	4.5	4.6	4.7	4.8	4.9
Number of samples N		101	101	101	82	82	82	72	72	72
Number of estimated parameters ν		6	11	16	6	11	16	6	11	16
Loss function V		252.519	1.037	0.005	2644.323	11.448	0.098	7199.211	3.969	0.559
Akaike´s information criterion AIC		498	-47	-576	634	197	-183	649	118	-13
Hydrodynamic derivatives ('prime' system, mass unit $\rho L^3/2$)	Y_v' (θ_5)	-0.01160*	-0.01153	-0.01313	-0.01160*	0.07516	-0.05502	-0.01160*	-0.03240	-0.02428
	$Y_r'-m'$ (θ_6)	-0.00526*	-0.00730	-0.00844	-0.00526*	0.01023	-0.02175	-0.00526*	-0.01343	-0.01005
	N_v' (θ_7)	-0.00291*	-0.00029	-0.00009	-0.00291*	-0.05645	0.00273	-0.00291*	0.00159	0.00117
	$N_r'-m'x_G'$ (θ_8)	-0.00184*	-0.00116	-0.00106	-0.00184*	-0.00728	0.00052	-0.00184*	0.00002	-0.00021
	Y_δ' (θ_{11})	0.00278*	0.00238	0.00218	0.00278*	0.00157	0.00140	0.00278*	0.00128	0.00130
	N_δ' $(-\theta_{11}\theta_{12})$	-0.00133*	0.00114**	-0.00105**	-0.00133*	-0.00075**	-0.00067**	-0.00133*	-0.00062**	-0.00062**
Biases	θ_{13} [-]	$1.2\cdot10^{-4}$	$8.9\cdot10^{-5}$	$-3.5\cdot10^{-5}$	$3.1\cdot10^{-5}$	$3.6\cdot10^{-5}$	$3.7\cdot10^{-6}$	$1.2\cdot10^{-5}$	$-1.9\cdot10^{-4}$	$-1.3\cdot10^{-4}$
	θ_{14} [-]	$-1.6\cdot10^{-6}$	$-2.6\cdot10^{-5}$	$-3.7\cdot10^{-5}$	$-5.1\cdot10^{-5}$	$-1.3\cdot10^{-5}$	$-1.8\cdot10^{-5}$	$-5.2\cdot10^{-5}$	$-9.6\cdot10^{-6}$	$-1.1\cdot10^{-5}$
Initial state	θ_{25} [knots]	-0.41	-0.91	-0.49	-1.05	-0.08	0.20	-0.52	0.12	-0.11
	θ_{26} [deg/s]	-0.108	0.105	0.025	0.275	-0.003	0.024	0.383	0.233	0.069
	θ_{27} [deg]	-5.29	1.90	0.60	-4.64	-0.60	-0.93	-5.49	-0.10	0.32
Time delay	T_D $(T-T\lvert\sin\theta_{34}\rvert)$ [s]	0.0	0.0	0.2	4.4	4.8	5.7	0.0	2.7	0.1

* = fixed value ** = θ_{12} fixed to 0.48

Table 4.1 - Parameter values from identifications of linear models. The corresponding hydrodynamic derivatives in the 'bis' system are obtained by dividing with m' = 0.00798.

		Zig-zag test 1		Zig-zag test 2		Zig-zag test 3	
	HyA:s model	Output error	Maximum likeli-hood	Output error	Maximum likeli-hood	Output error	Maximum likeli-hood
K'	-3.90	-1.23	-1.06	-1.07	-1.09	-0.87	-0.81
K_1'	-1.65	-1.41	-1.28	-	-	-	-
K_v'	2.01	0.98	0.85	0.12	0.46	0.40	0.39
K_{1v}'	0.21	0.17	0.17	-	-	-	-
T_1'	5.70	1.68	1.15	complex poles	complex poles	complex poles	complex poles
T_2'	0.37	0.67	0.85				
T_3'	0.89	1.29	1.18	0.37	0.32	0.54	0.72
T_{3v}'	0.22	0.20	0.19	0.40	0.10	0.15	0.19

Table 4.2 - Normalized ('prime' system) transfer function parameters (cf. (3.7), (3.8) and (3.9)) computed from the models in Table 4.1.

	Zig-zag test 1	Zig-zag test 2	Zig-zag test 3
$R_1(1,1)$ $(\lvert\theta_{18}\rvert)$ [s]	$6.7 \cdot 10^{-7}$	$3.2 \cdot 10^{-6}$	$9.7 \cdot 10^{-8}$
$R_1(1,2)$ $(\sqrt{\lvert\theta_{18}\rvert\lvert\theta_{19}\rvert} \cdot \sin\theta_{20})$ [s]	$1.3 \cdot 10^{-8}$	$-6.8 \cdot 10^{-7}$	$9.9 \cdot 10^{-8}$
$R_1(2,2)$ $(\lvert\theta_{19}\rvert)$ [s]	$2.0 \cdot 10^{-6}$	$2.2 \cdot 10^{-6}$	$3.8 \cdot 10^{-7}$
$R_2(1,1)$ $(\lvert\theta_{21}\rvert)$ [knots]^2	$8.2 \cdot 10^{-10}$	$1.3 \cdot 10^{-7}$	$5.4 \cdot 10^{-5}$
$R_2(2,2)$ $(\lvert\theta_{23}\rvert)$ [deg/s]^2	$1.0 \cdot 10^{-3}$	$1.1 \cdot 10^{-2}$	$5.0 \cdot 10^{-3}$

Table 4.3 - Parameter values of the covariance matrices obtained from maximum likelihood identifications.

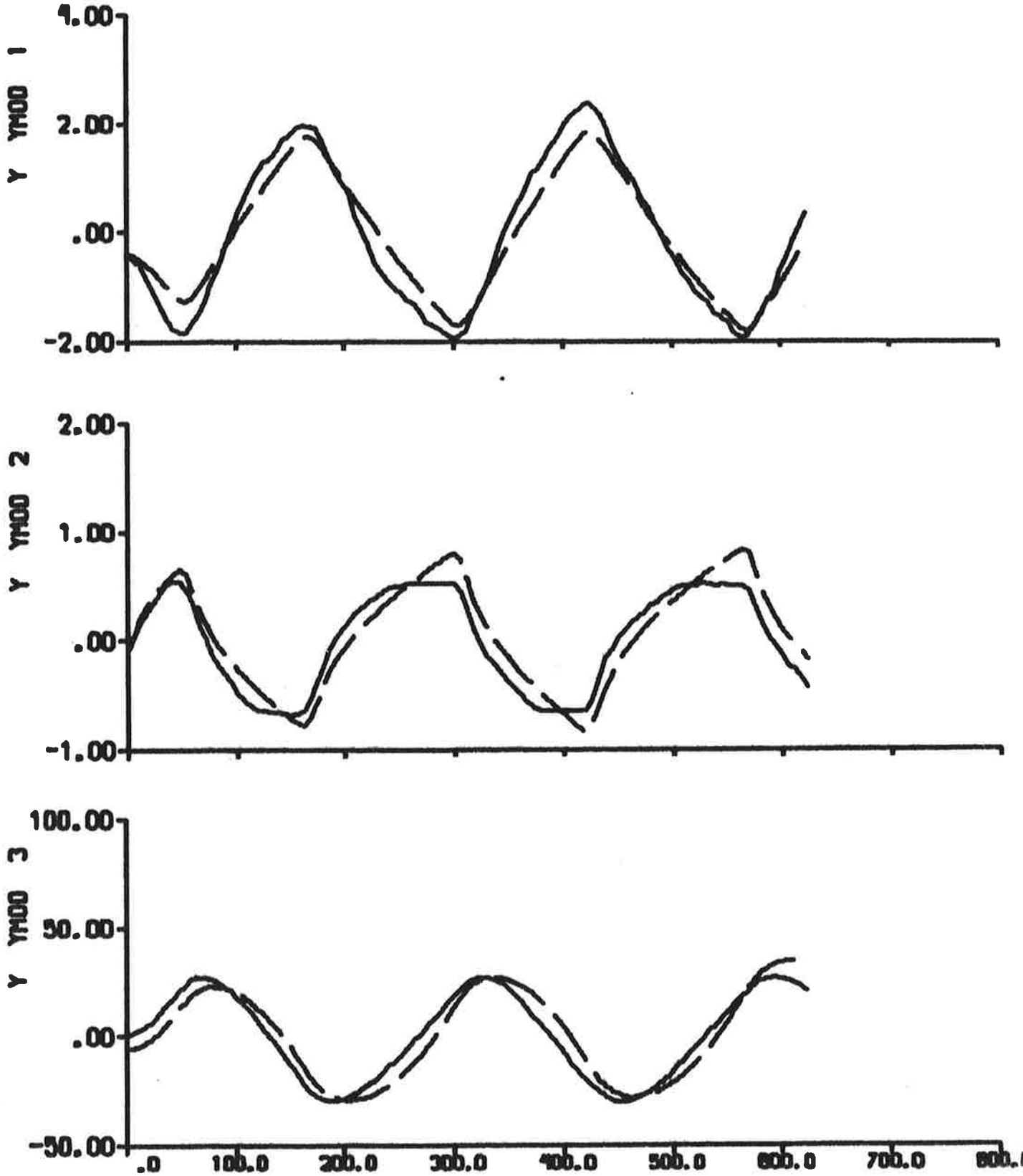

Fig. 4.1 - Result of output error identification to data from zig-zag test 1, when the model is fixed to HyA:s model. The dashed lines are model outputs. Cf. Fig. 2.1.

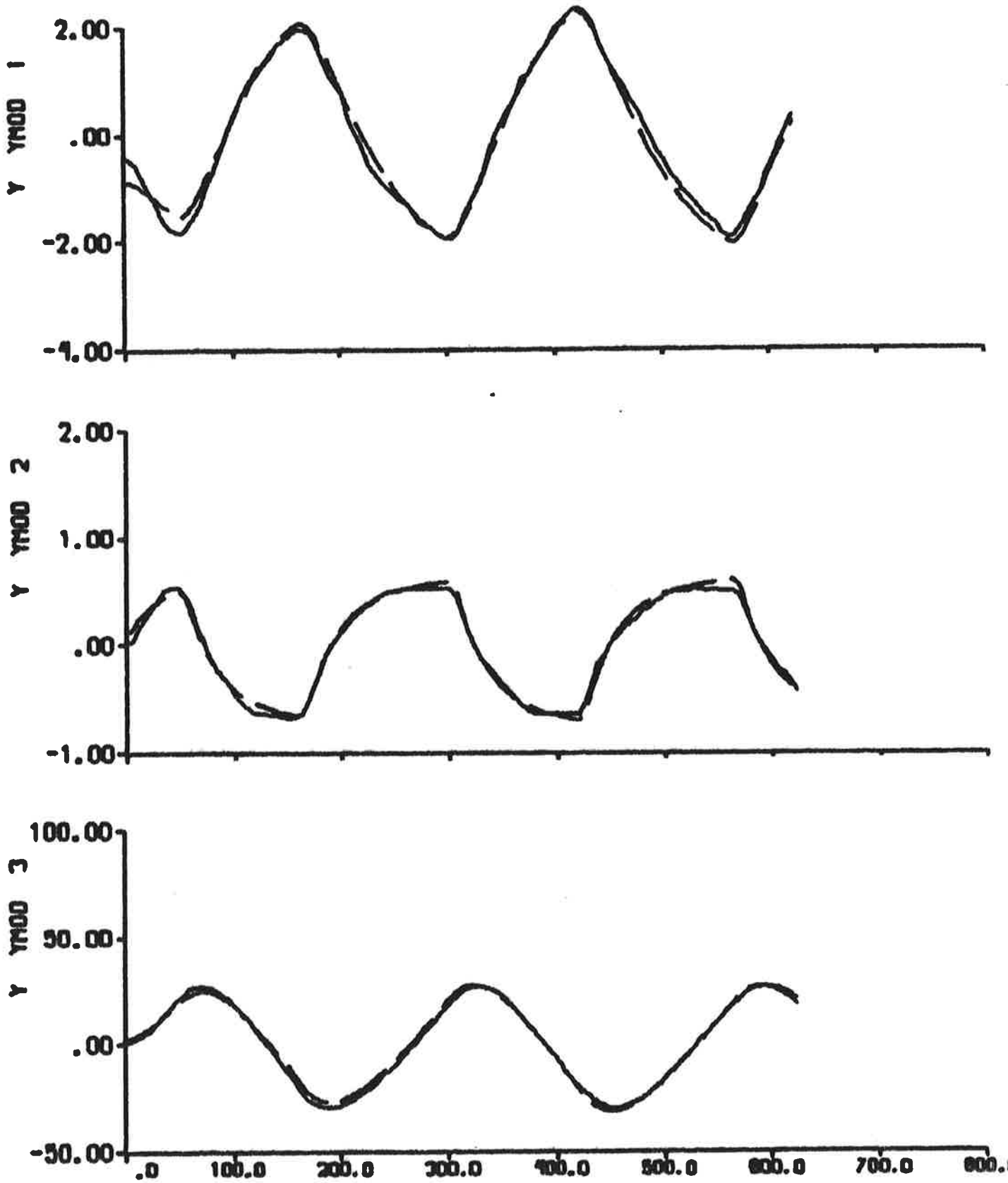

Fig. 4.2 - Result of output error identification fo data from zig-zag test 1. The dashed lines are model outputs. Cf. Fig. 2.1.

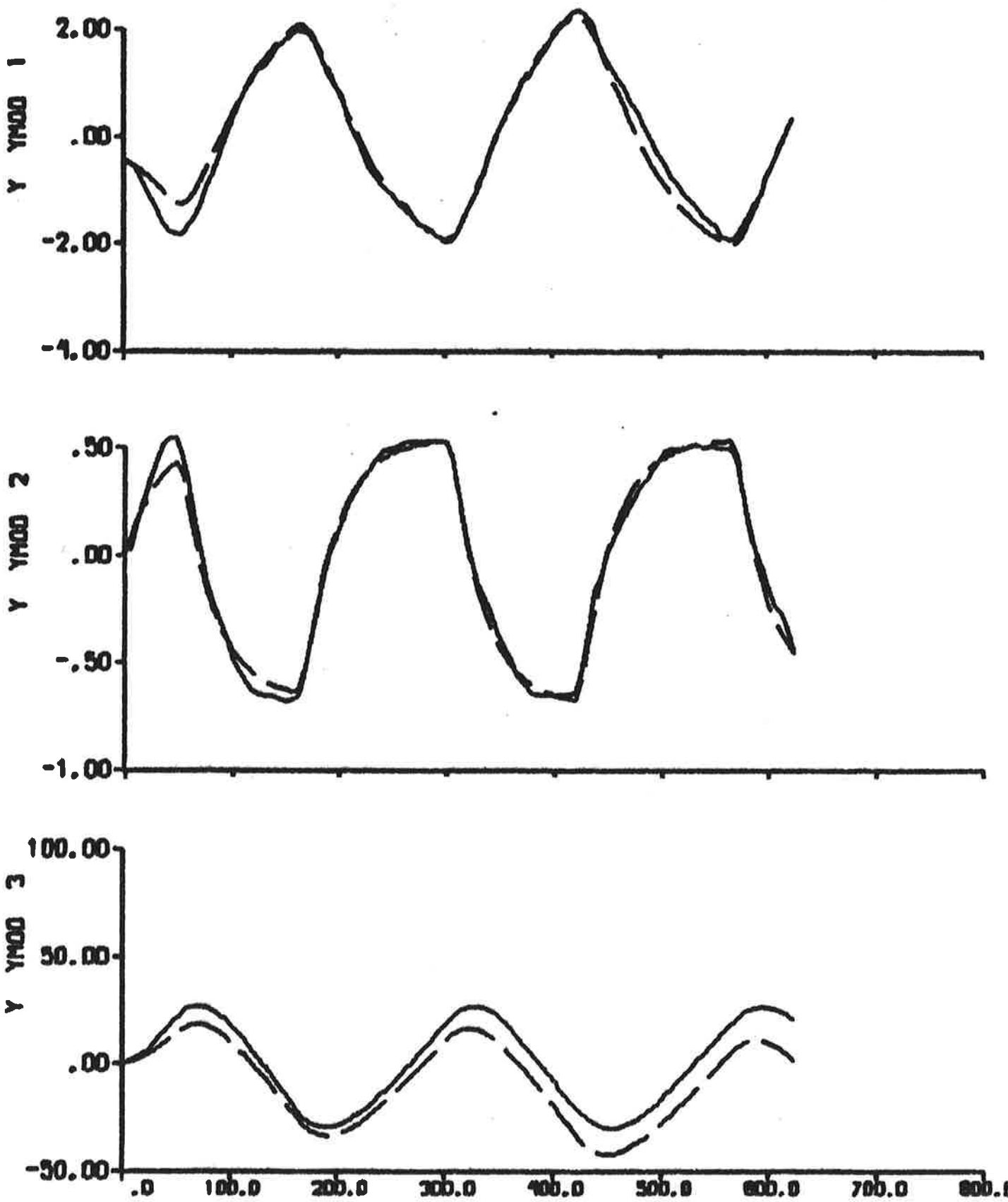

Fig. 4.3 - Result of maximum likelihood identification to data from zig-zag test 1. The dashed lines are model outputs. Cf. Fig. 2.1.

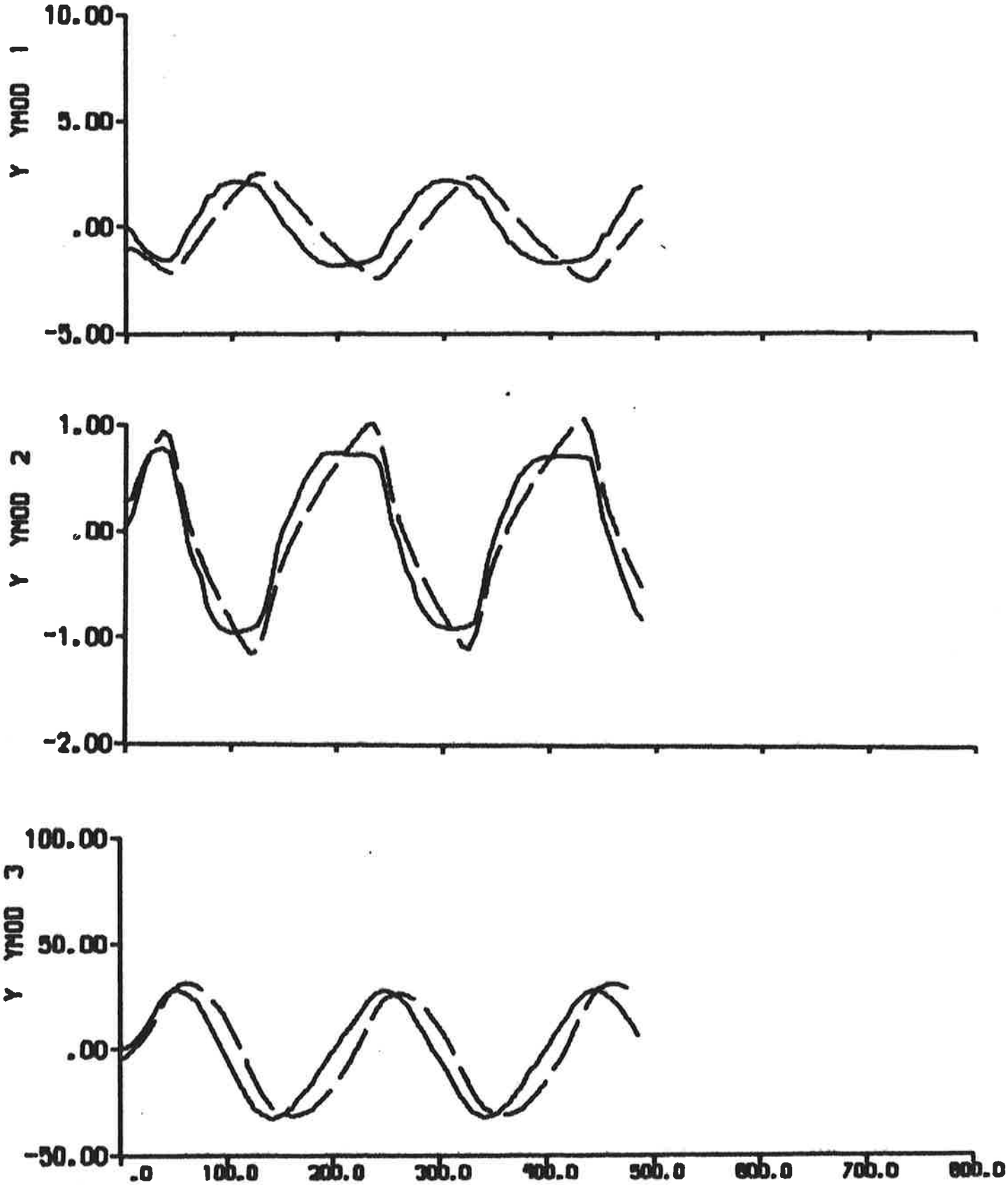

Fig. 4.4 - Result of output error identification to data from zig-zag test 2, when the model is fixed to HyA:s model. The dashed lines are model outputs. Cf. Fig. 2.2.

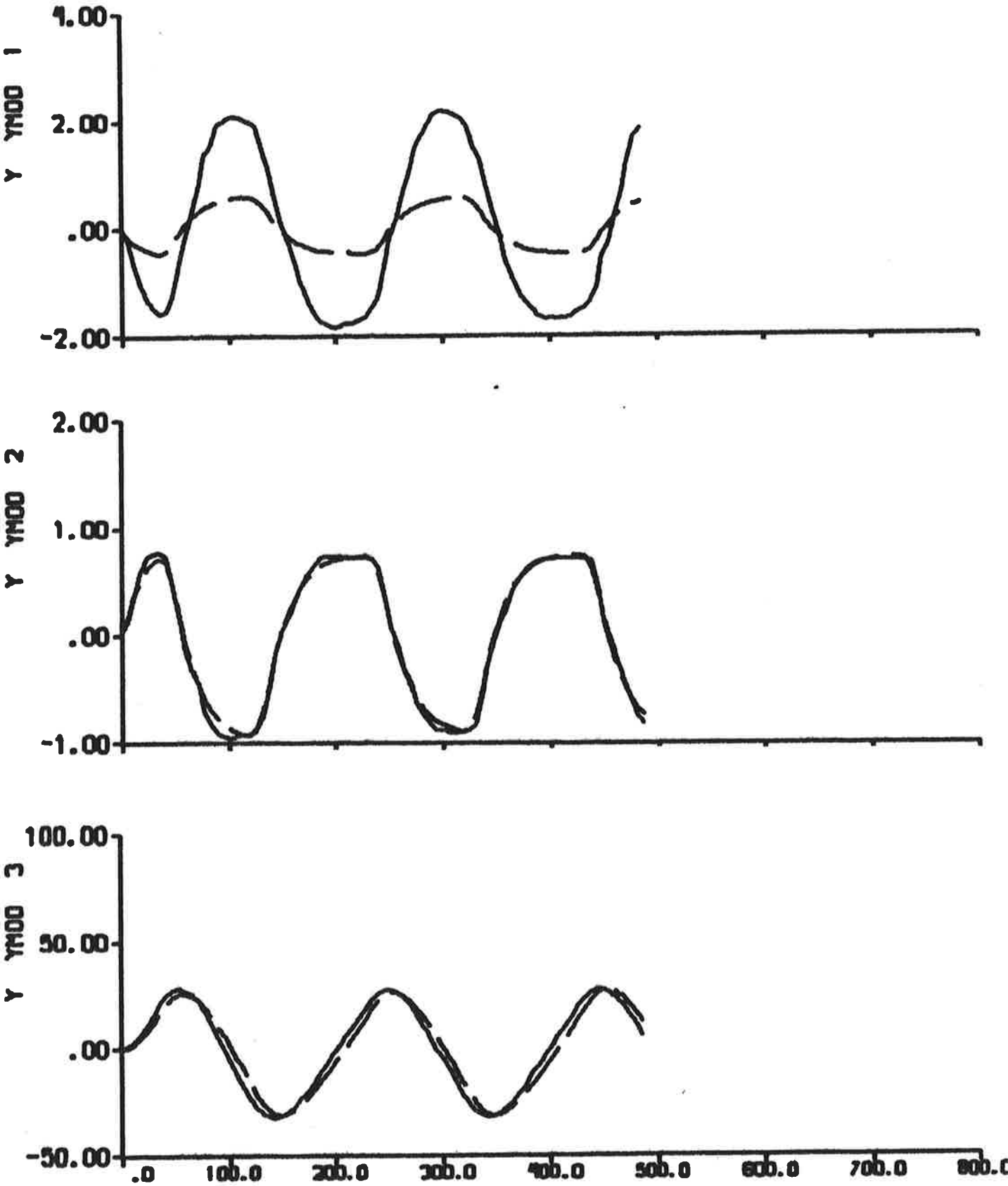

Fig. 4.5 - Result of output error identification to data from zig-zag test 2. The dashed lines are model outputs Cf. Fig. 2.2.

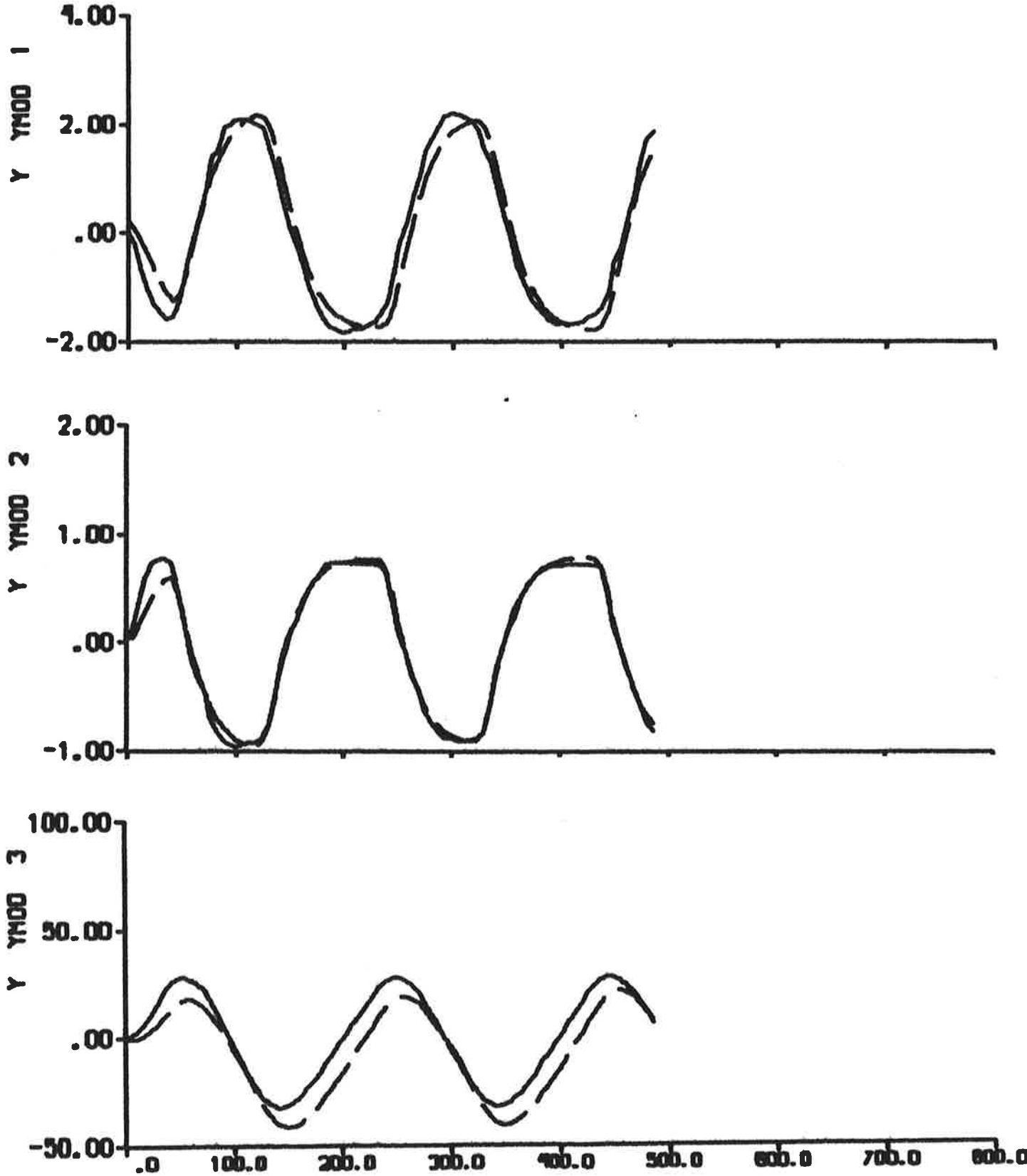

Fig. 4.6 - Result of maximum likelihood identification to data from zig-zag test 2. The dashed lines are model outputs. Cf. Fig. 2.2.

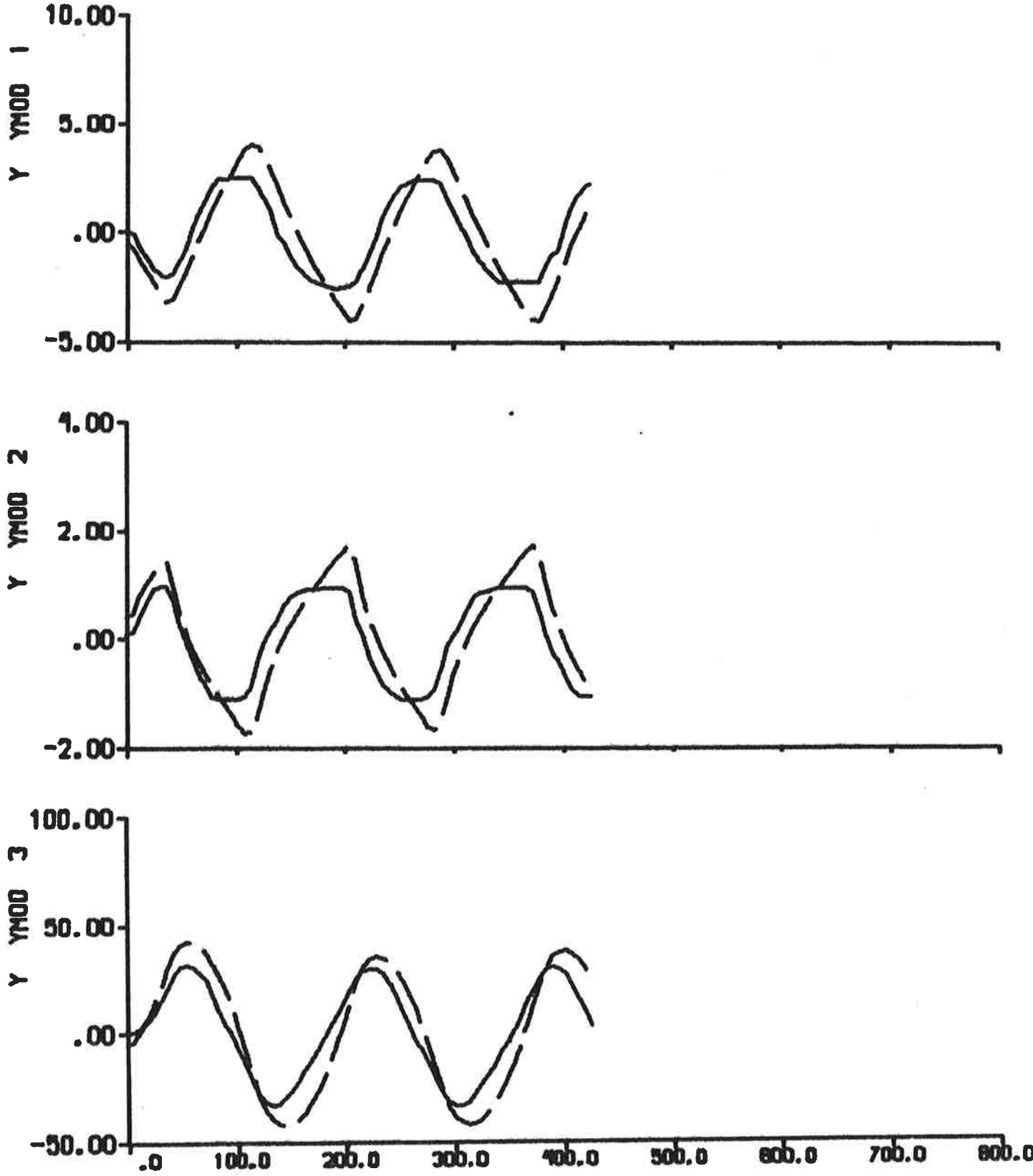

Fig. 4.7 - Result of output error identification to data from zig-zag test 3, when the model is fixed to HyA:s model. The dashed lines are model outputs. Cf. Fig.2.3.

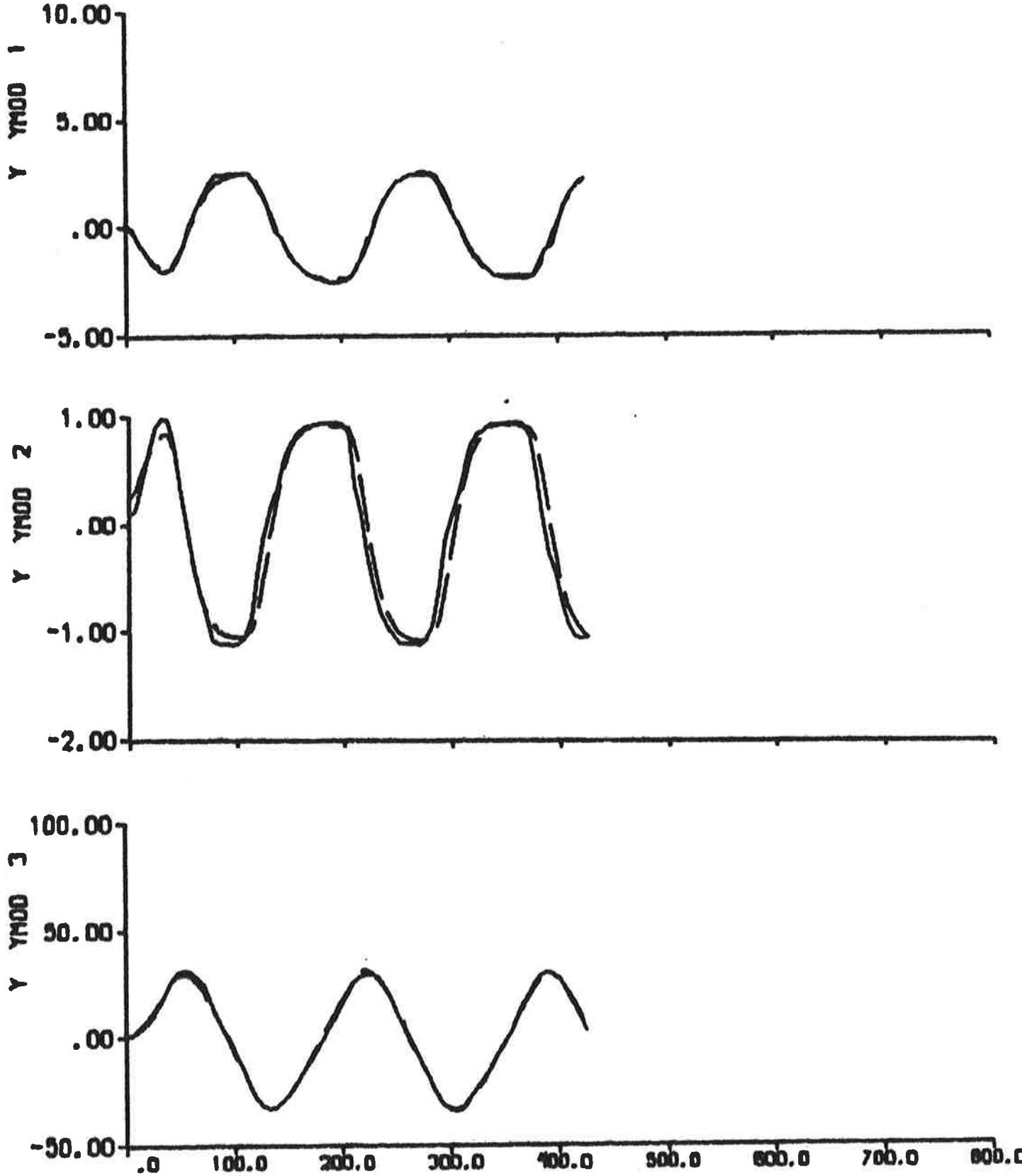

Fig. 4.8 - Result of output error identification to data from zig-zag test 3. The dashed lines are model outputs. Cf. Fig. 2.3.

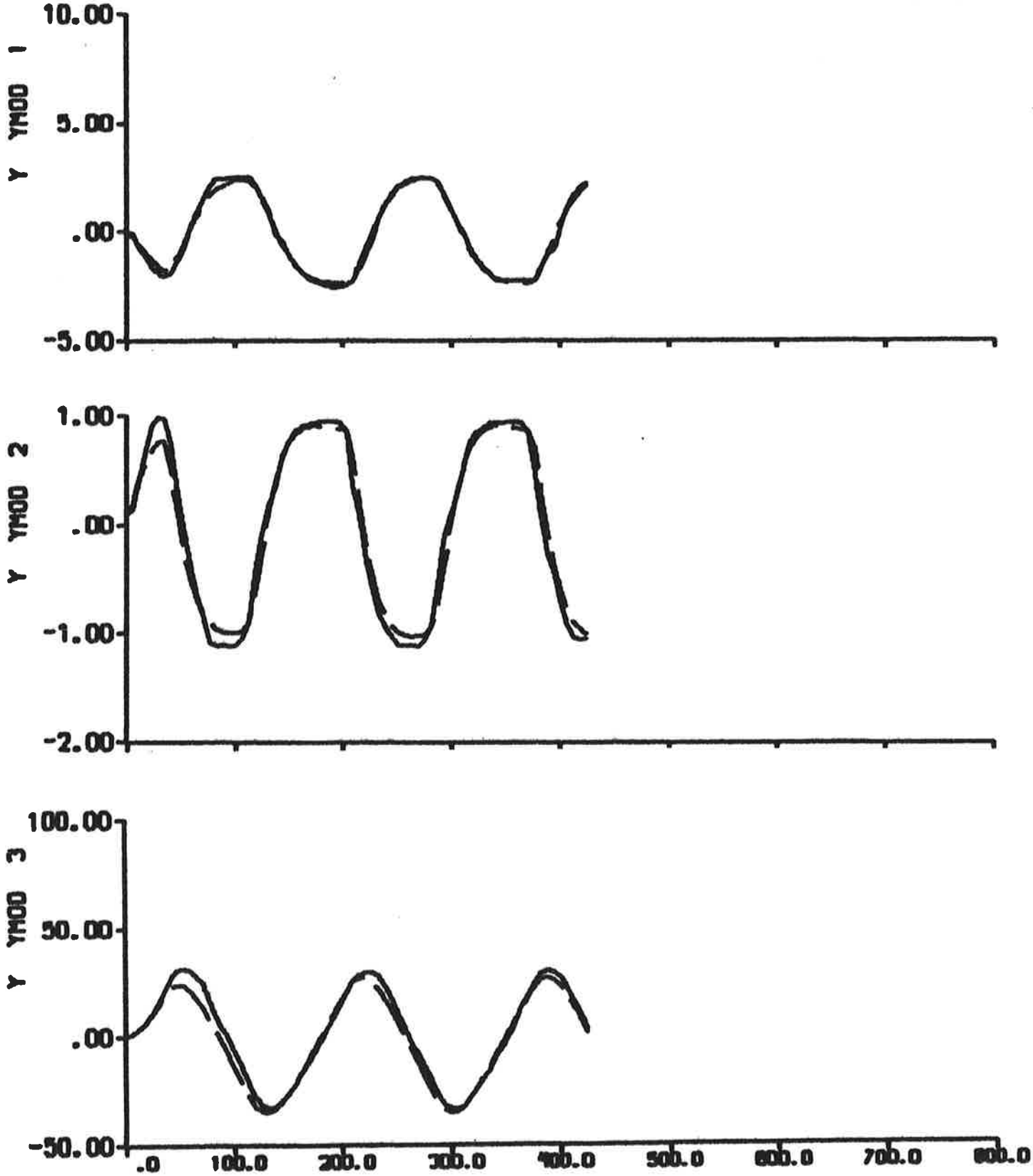

Fig. 4.9 - Result of maximum likelihood identification to data from zig-zag test 3. The dashed lines are model outputs. Cf. Fig. 2.3.

$$K = \begin{pmatrix} 4.7 \cdot 10^{-1} & -1.8 \cdot 10^{-1} & -3.4 \cdot 10^{-3} \\ -1.5 \cdot 10^{-3} & 1.3 \cdot 10^{-2} & 2.4 \cdot 10^{-4} \\ -1.0 \cdot 10^{-2} & 8.4 \cdot 10^{-2} & 1.9 \cdot 10^{-2} \end{pmatrix}$$

$$K = \begin{pmatrix} 3.5 \cdot 10^{-1} & -4.8 \cdot 10^{-1} & -2.5 \cdot 10^{-3} \\ -3.0 \cdot 10^{-3} & 1.4 \cdot 10^{-2} & 0.7 \cdot 10^{-4} \\ -2.3 \cdot 10^{-2} & 8.0 \cdot 10^{-2} & 1.8 \cdot 10^{-2} \end{pmatrix} \qquad (4.1)$$

$$K = \begin{pmatrix} 3.8 \cdot 10^{-1} & -3.5 \cdot 10^{-1} & -6.3 \cdot 10^{-3} \\ -2.5 \cdot 10^{-3} & 1.3 \cdot 10^{-2} & 1.4 \cdot 10^{-4} \\ -2.0 \cdot 10^{-2} & 8.1 \cdot 10^{-2} & 1.8 \cdot 10^{-2} \end{pmatrix}$$

Notice that the filter gains are remarkably similar, although the covariance matrices R_1 and R_2 differ significantly between the different experiments.

The models obtained from the maximum likelihood identifications are better than the models from the output error identifications, if Akaike´s information criterion is considered. It is thus concluded that the model obtained from maximum likelihood identification to data from zig-zag test 1 (Fig. 4.3) is the best one, although N_v' is strongly underestimated. Notice that the hydrodynamic derivatives obtained from the output error method are rather similar to the ones obtained from the maximum likelihood method, when zig-zag test 1 is used.

It was concluded in Åström, Källström, Norrbin and Byström (1975) that a $20^o/20^o$ zig-zag test on a container ship was strongly influenced by nonlinear effects. It is thus reasonable to assume that the difficulties obtained when fitting a linear model to data from the three $20^o/20^o$ zig-zag tests on USS Compass Island are due to nonlinear

contributions. It is then natural to progress by fitting the nonlinear model (3.1) with $\theta_{35} \neq 0$ to the data. The results of such identifications are given in next section.

5. IDENTIFICATION OF NONLINEAR MODELS

The results of fitting the nonlinear model (3.1) when θ_{35} also is estimated to data from the 3 zig-zag tests are given in this section. The analysis performed is quite comparable with the analysis in Section 4.

The results of output error identifications when the linear part of the model is fixed to HyA:s model, output error identifications when the hydrodynamic derivatives also are estimated, and maximum likelihood identifications are shown in Figs. 5.1-5.9. Notice that the nonlinear contributions U4 and U5 of Figs. 5.3 b, 5.6 b and 5.9 b are connected with the simulations of the stochastic models and not with the simulations of the deterministic models. The parameter estimates obtained are summarized in Tables 5.1-5.3.

It is concluded from Figs. 5.1 a, 5.4 a and 5.7 a that the outputs from HyA:s model do not differ much from the measurements. A significant improvement is thus obtained by using the nonlinear model instead of the linear model (cf. Section 4). The effective cross-flow drag coefficient C is estimated to 0.36, 0.53 and 0.70 from the 3 experiments. The value is expected to be of the order of 0.7 for a Mariner class vessel. It is concluded that the best result is obtained when zig-zag test 3 is used. This is not surprising, because the average speed of experiment 3 was 16.5 knots and HyA:s model was determined for 15 knots. The power of the nonlinear model is clearly illustrated by Fig. 5.10, where Figs. 2.3, 4.7 and 5.7 are put together.

		Zig-zag test 1			Zig-zag test 2			Zig-zag test 3		
		Output error (HyA:s model)	Output error	Maximum likeli-hood	Output error (HyA:s model)	Output error	Maximum likeli-hood	Output error (HyA:s model)	Output error	Maximum likeli-hood
Figure		5.1	5.2	5.3	5.4	5.5	5.6	5.7	5.8	5.9
Number of samples N		101	101	101	82	82	82	72	72	72
Number of estimated parameters ν		7	12	17	7	12	17	7	12	17
Loss function V		14.734	0.844	0.004	52.952	0.730	0.087	6.535	2.224	0.356
Akaike´s information criterion AIC		213	-66	-596	315	-26	-191	146	79	-43
Hydrodynamic derivatives ('prime' system, mass unit $\rho L^3/2$)	Y_v' (θ_5)	-0.01160*	-0.00981	-0.00892	-0.01160*	-0.04899	-0.04886	-0.01160*	-0.02554	-0.01487
	$Y_r'-m'$ (θ_6)	-0.00526*	-0.00732	-0.00817	-0.00526*	-0.01980	-0.02090	-0.00526*	-0.01267	-0.00875
	N_v' (θ_7)	-0.00291*	-0.00043	-0.00075	-0.00291*	0.00346	-0.00010	-0.00291*	-0.00071	-0.00123
	$N_r'-m'x_G'$ (θ_8)	-0.00184*	-0.00103	-0.00100	-0.00184*	0.00114	-0.00022	-0.00184*	-0.00042	-0.00062
	Y_δ' (θ_{11})	0.00278*	0.00233	0.00240	0.00278*	0.00122	0.00169	0.00278*	0.00154	0.00178
	N_δ' $(-\theta_{11}\theta_{12})$	-0.00133*	-0.00112**	-0.00115**	-0.00133*	-0.00059**	-0.00081**	-0.00133*	-0.00074**	-0.00085**
Cross-flow drag	C (θ_{35})	0.36	0.16	0.35	0.53	0.26	0.46	0.70	0.62	0.79
Biases	θ_{13} [-]	$1.5\cdot10^{-4}$	$1.1\cdot10^{-4}$	$1.9\cdot10^{-7}$	$1.2\cdot10^{-4}$	$9.2\cdot10^{-5}$	$6.2\cdot10^{-5}$	$-2.2\cdot10^{-5}$	$-1.4\cdot10^{-4}$	$-6.1\cdot10^{-5}$
	θ_{14} [-]	$-2.6\cdot10^{-5}$	$-3.0\cdot10^{-5}$	$-4.7\cdot10^{-5}$	$-4.8\cdot10^{-5}$	$-2.9\cdot10^{-5}$	$-3.6\cdot10^{-5}$	$-6.0\cdot10^{-5}$	$-2.8\cdot10^{-5}$	$-3.8\cdot10^{-5}$
Initial state	θ_{25} [knots]	-0.02	-0.87	-0.48	-0.70	0.07	0.21	-0.03	0.07	-0.04
	θ_{26} [deg/s]	0.042	0.067	0.019	0.332	0.250	0.047	0.223	0.126	0.047
	θ_{27} [deg]	-0.27	1.98	0.51	0.69	-2.61	-1.21	1.94	0.77	0.29
Time delay	T_D $(T-T\lvert\sin\theta_{34}\rvert)$ [s]	0.0	0.1	1.6	0.0	1.4	5.7	3.0	2.2	1.0

* = fixed value ** = θ_{12} fixed to 0.48

Table 5.1 - Parameter values from identifications of nonlinear models. The corresponding hydrodynamic derivatives in the 'bis' system are obtained by dividing with m' = 0.00798

		Zig-zag test 1		Zig-zag test 2		Zig-zag test 3	
	HyA:s model	Output error	Maximum likeli-hood	Output error	Maximum likeli-hood	Output error	Maximum likeli-hood
K'	-3.90	-1.73	-4.31	-1.92	-4.67	-11.79	9.39
K_1'	-1.65	-1.37	-1.42	-	-1.00	-0.90	-1.04
K_v'	2.01	1.53	4.22	0.80	2.03	5.91	-5.41
K_{1v}'	0.21	0.17	0.18	-	0.12	0.12	0.13
T_1'	5.70	2.62	7.09	complex poles	4.51	14.84	-13.54
T_2'	0.37	0.71	0.64		0.33	0.51	0.60
T_3'	0.89	1.47	1.50	0.38	0.32	0.58	0.90
T_{3v}'	0.22	0.21	0.19	0.11	0.09	0.15	0.20

Table 5.2 - Normalized ('prime' system) transfer function parameters (cf. (3.7),(3.8) and (3.9)) computed from the models in Table 5.1.

	Zig-zag test 1	Zig-zag test 2	Zig-zag test 3
$R_1(1,1)$ $(\lvert\theta_{18}\rvert)$ [s]	$4.7 \cdot 10^{-5}$	$4.6 \cdot 10^{-6}$	$7.2 \cdot 10^{-5}$
$R_1(1,2)$ $(\sqrt{\lvert\theta_{18}\rvert\lvert\theta_{19}\rvert} \cdot \sin\theta_{20})$ [s]	$-9.1 \cdot 10^{-6}$	$-1.1 \cdot 10^{-7}$	$6.2 \cdot 10^{-6}$
$R_1(2,2)$ $(\lvert\theta_{19}\rvert)$ [s]	$2.5 \cdot 10^{-6}$	$4.5 \cdot 10^{-6}$	$5.9 \cdot 10^{-7}$
$R_2(1,1)$ $(\lvert\theta_{21}\rvert)$ [knots]^2	$5.7 \cdot 10^{-9}$	$3.4 \cdot 10^{-8}$	$9.2 \cdot 10^{-2}$
$R_2(2,2)$ $(\lvert\theta_{23}\rvert)$ [deg/s]^2	$1.1 \cdot 10^{-3}$	$2.5 \cdot 10^{-2}$	$9.2 \cdot 10^{-4}$

Table 5.3 - Parameter values of the covariance matrices obtained from maximum likelihood identifications.

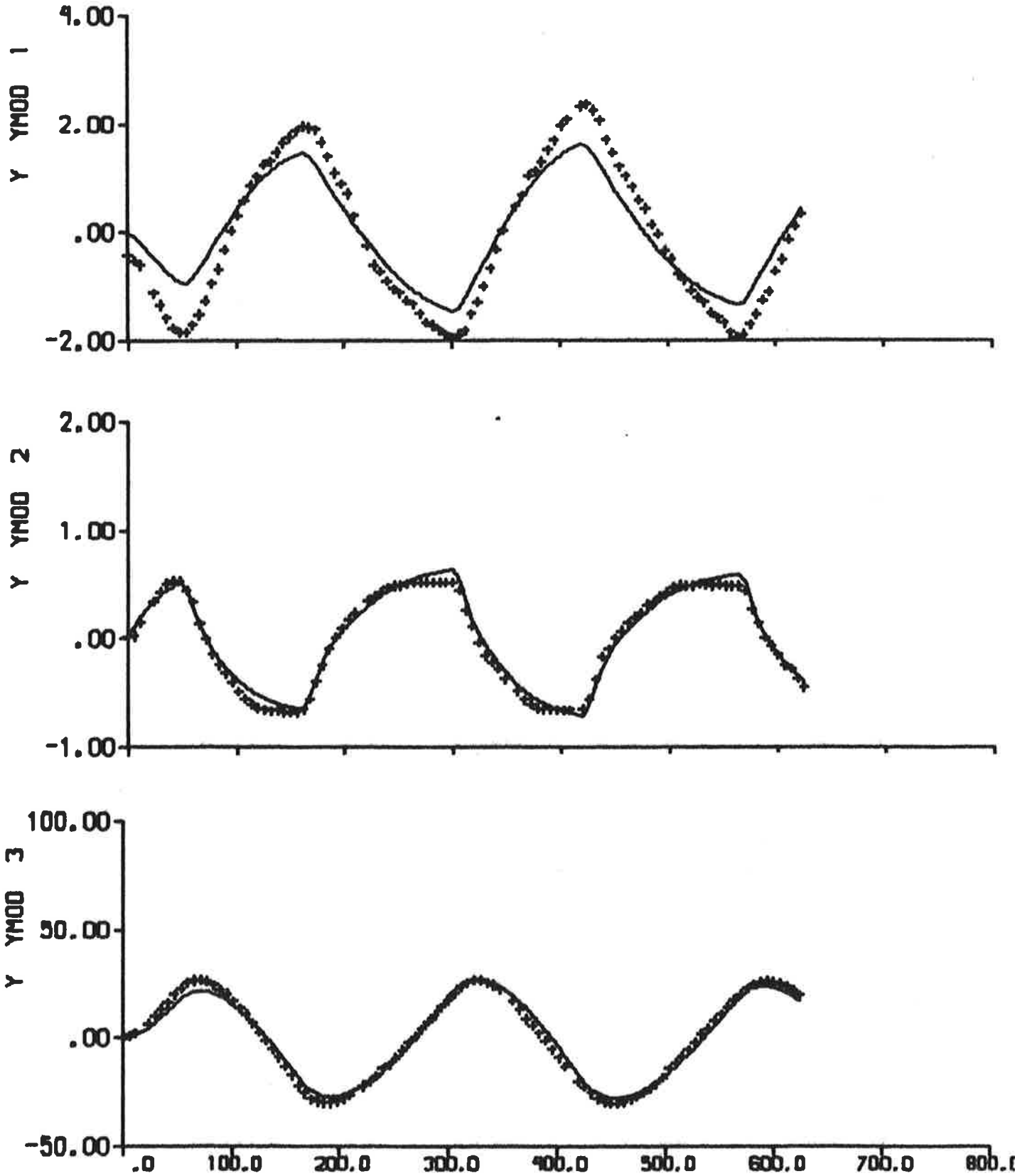

Fig. 5.1 a - Result of output error identification to data from zig-zag test 1, when the linear part of the model is fixed to HyA:s model. The continuous lines are model outputs. Cf. Fig. 2.1.

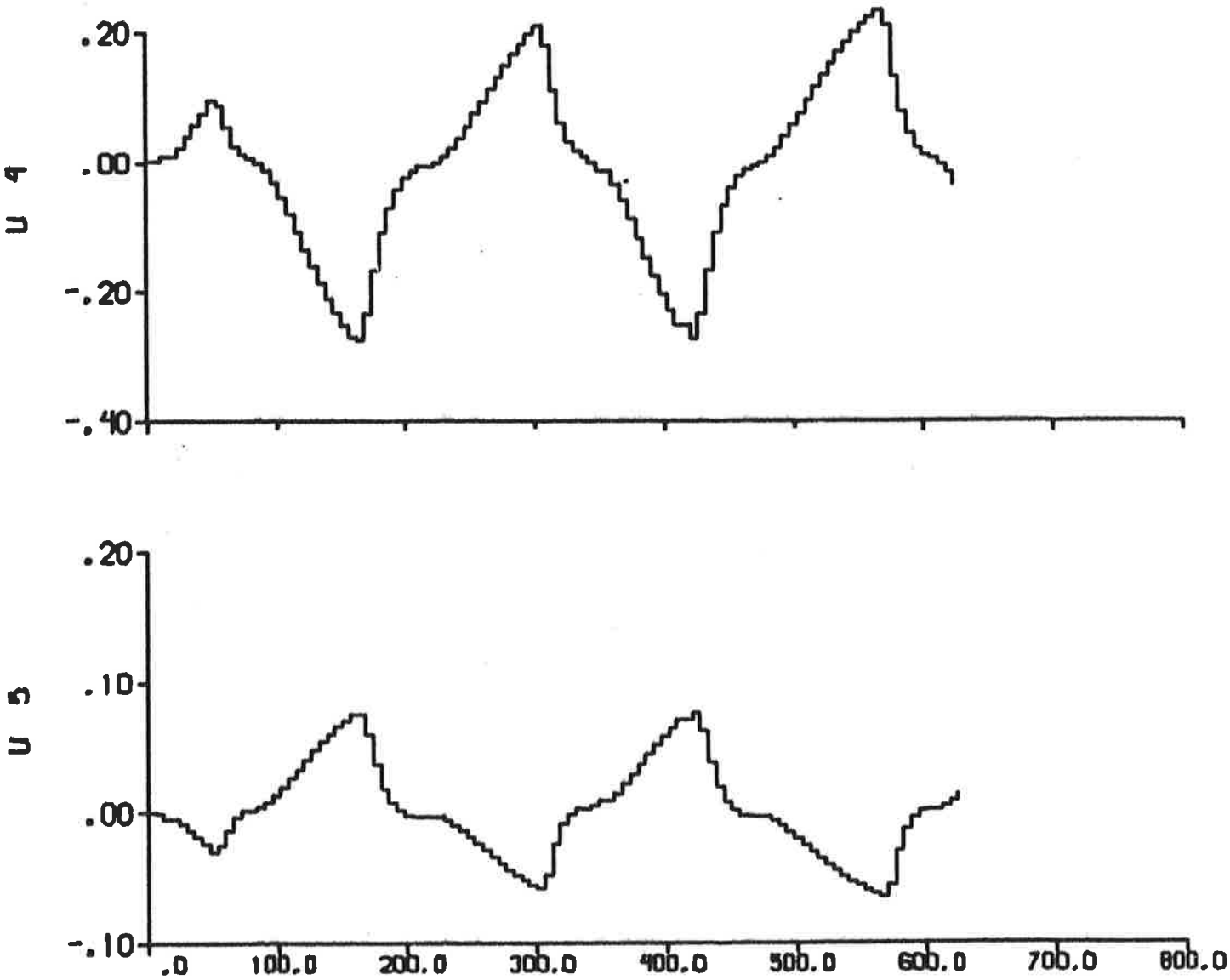

Fig. 5.1 b - Additional inputs U4 = f_Y/m' and U5 = f_N/m' describing the nonlinear contributions.

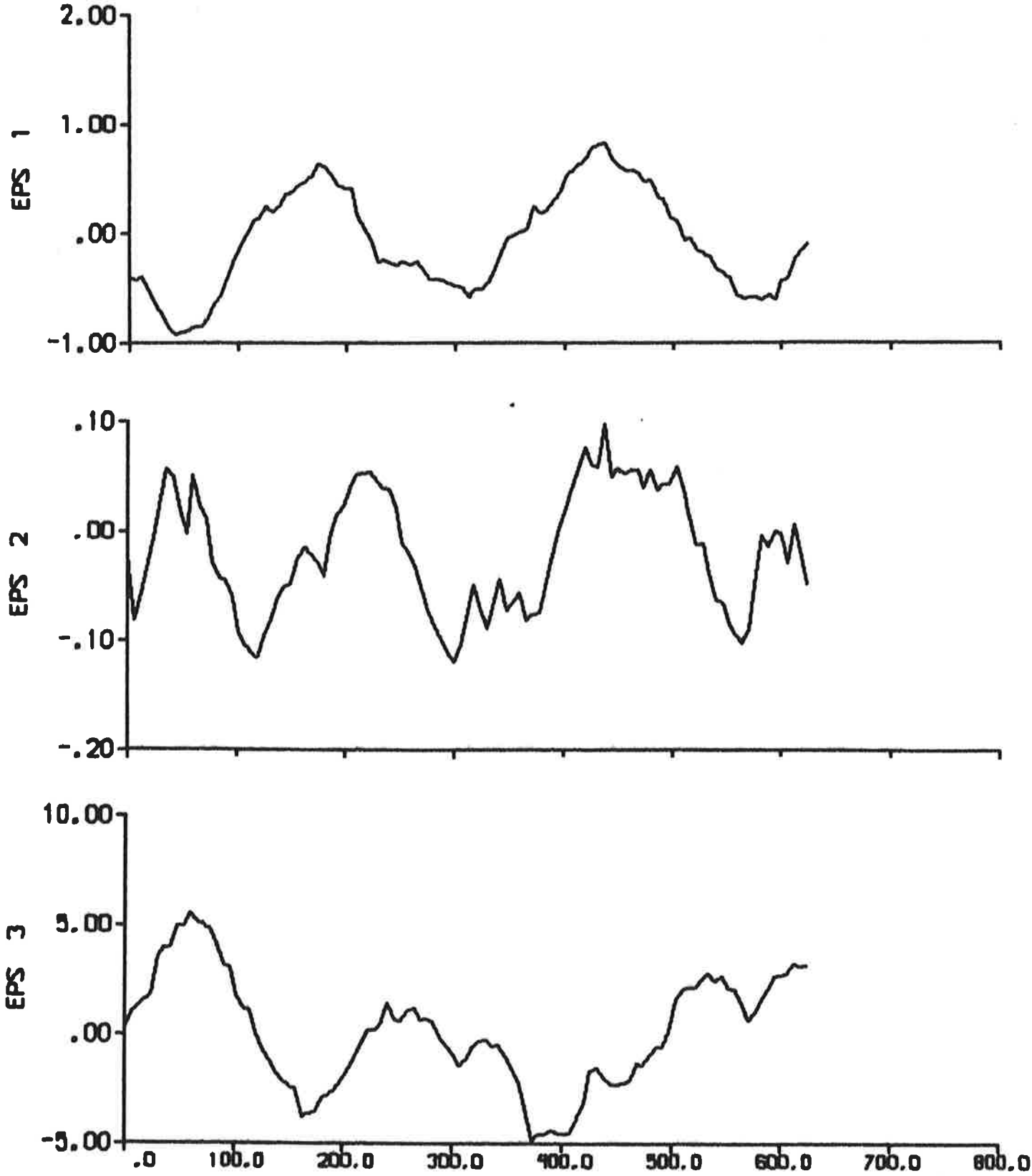

Fig. 5.1 c - Residuals

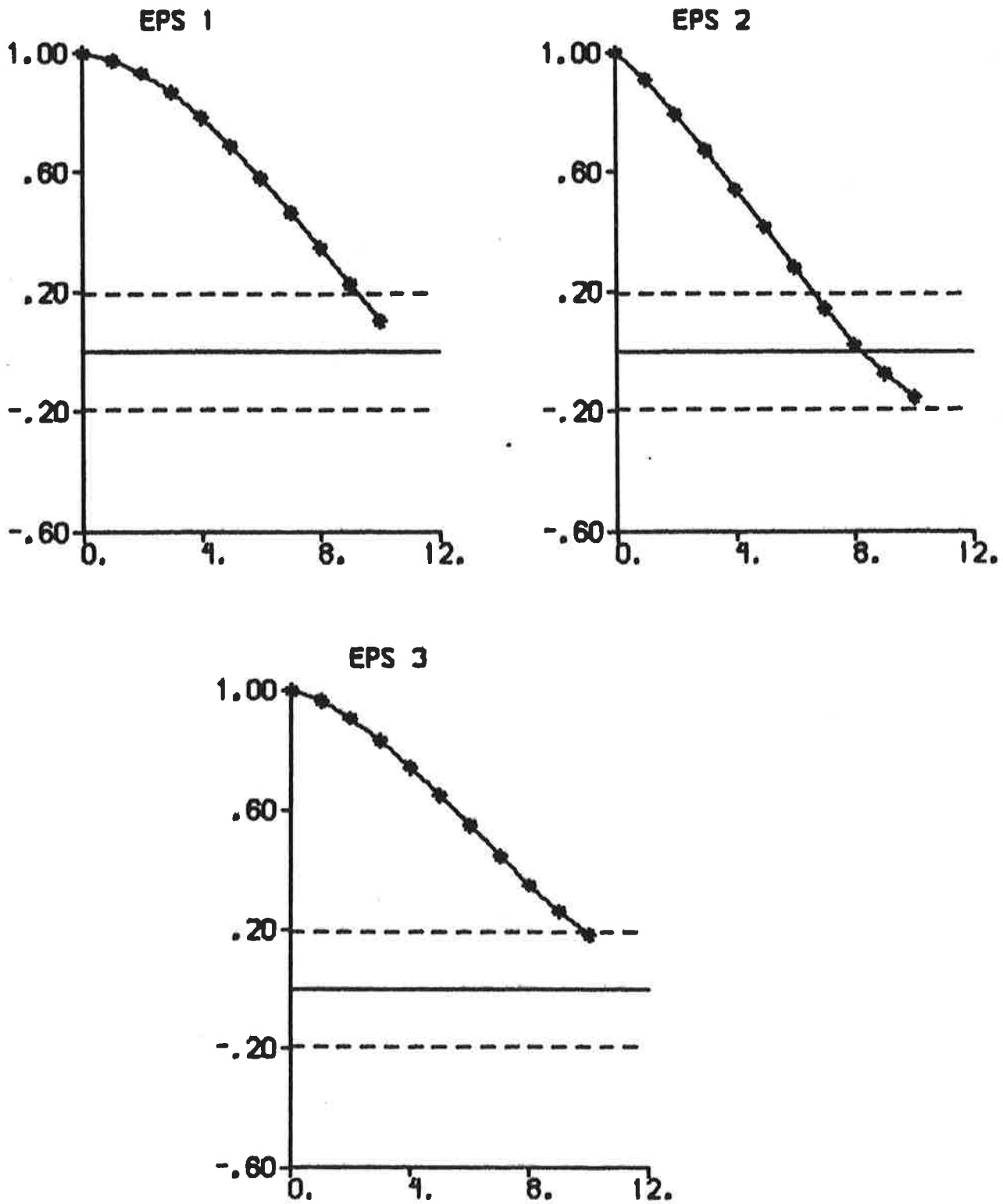

Fig. 5.1 d - Autocorrelation functions of residuals. The dashed lines are ±2σ limits.

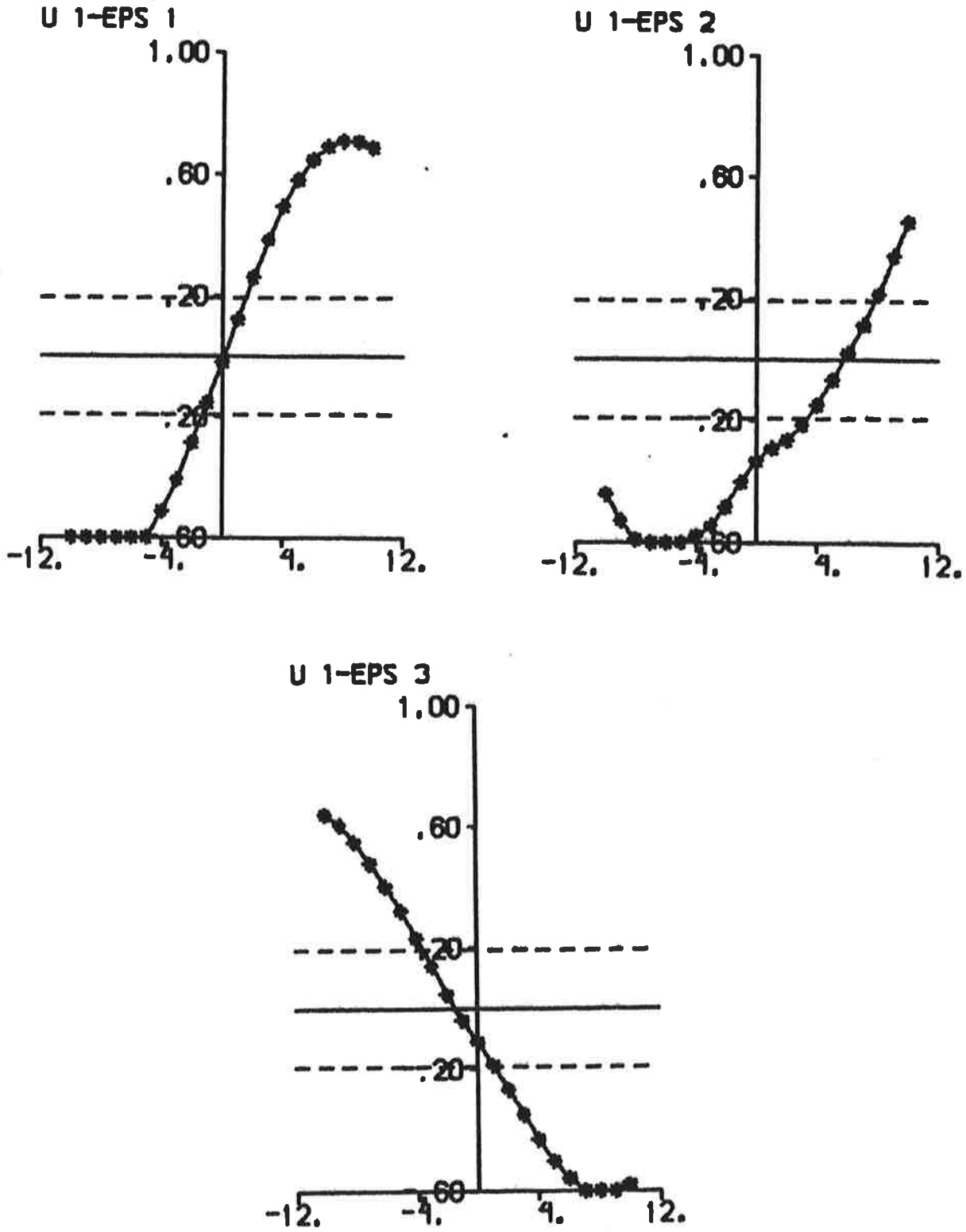

Fig. 5.1 e - Cross correlation functions between rudder input and residuals. The dashed lines are ±2σ limits.

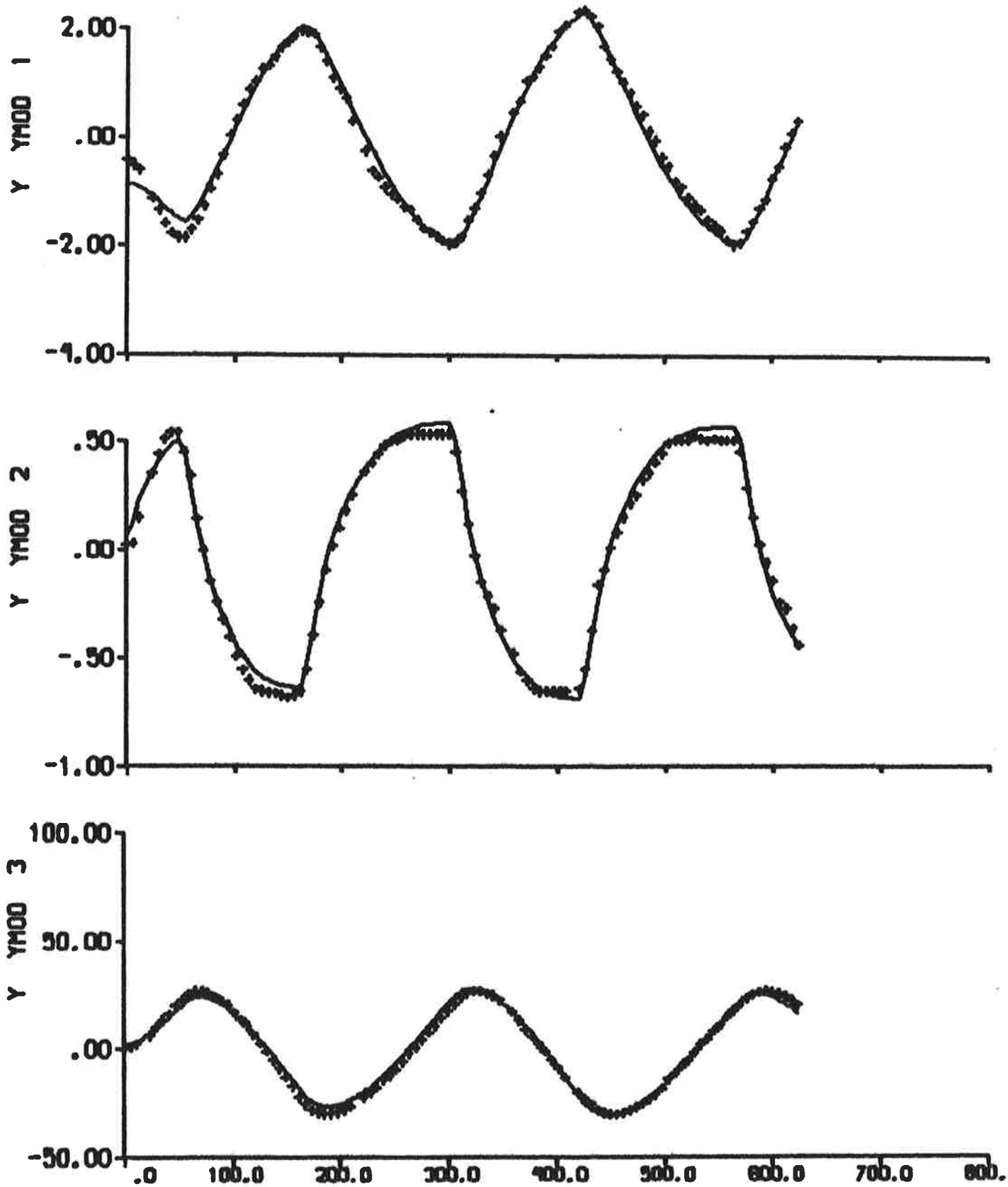

Fig. 5.2 a - Result of output error identification to data from zig-zag test 1. The continuous lines are model outputs. Cf. Fig. 2.1.

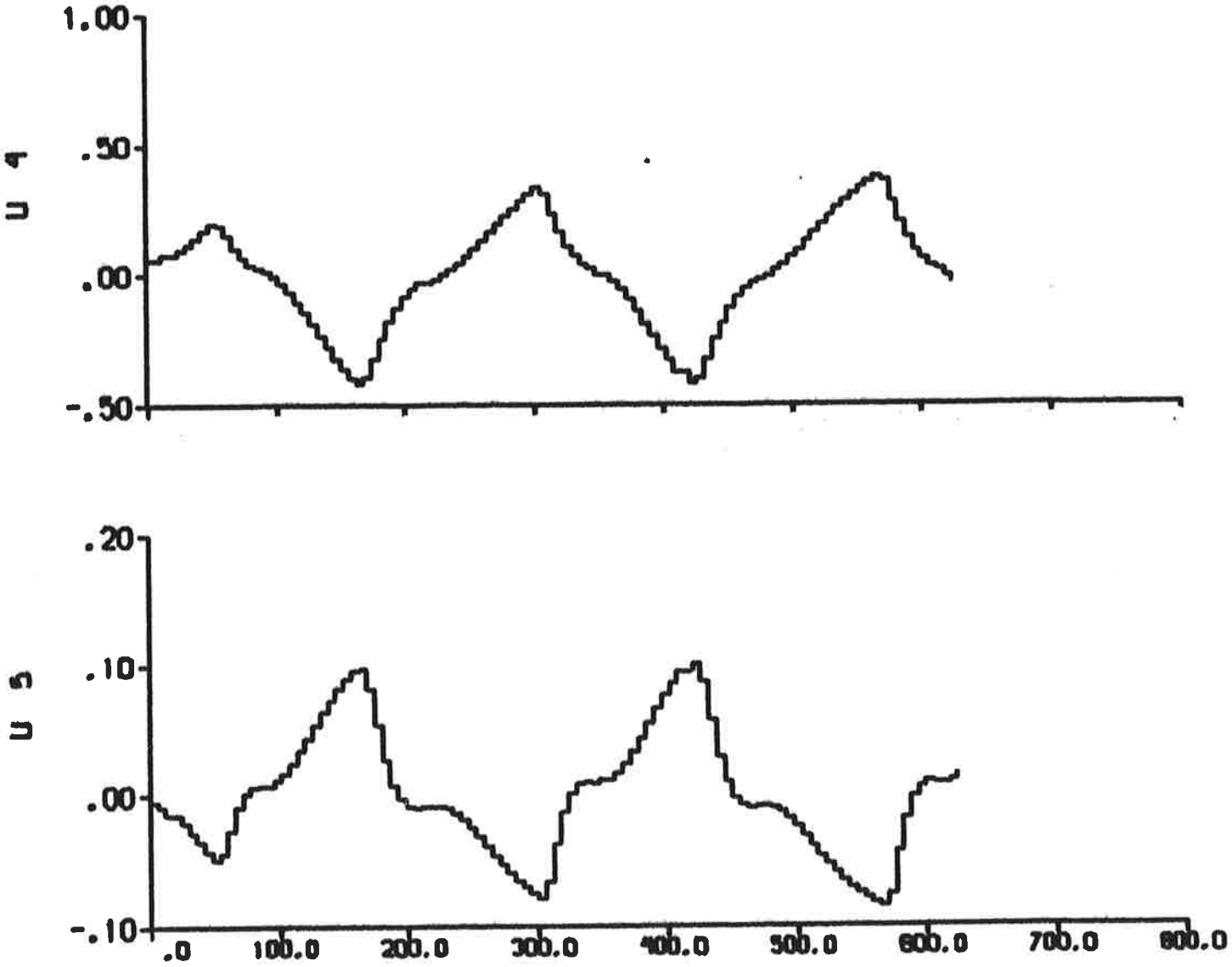

Fig. 5.2 b - Additional inputs U4 = f_Y/m' and U5 = f_N/m' describing the nonlinear contributions.

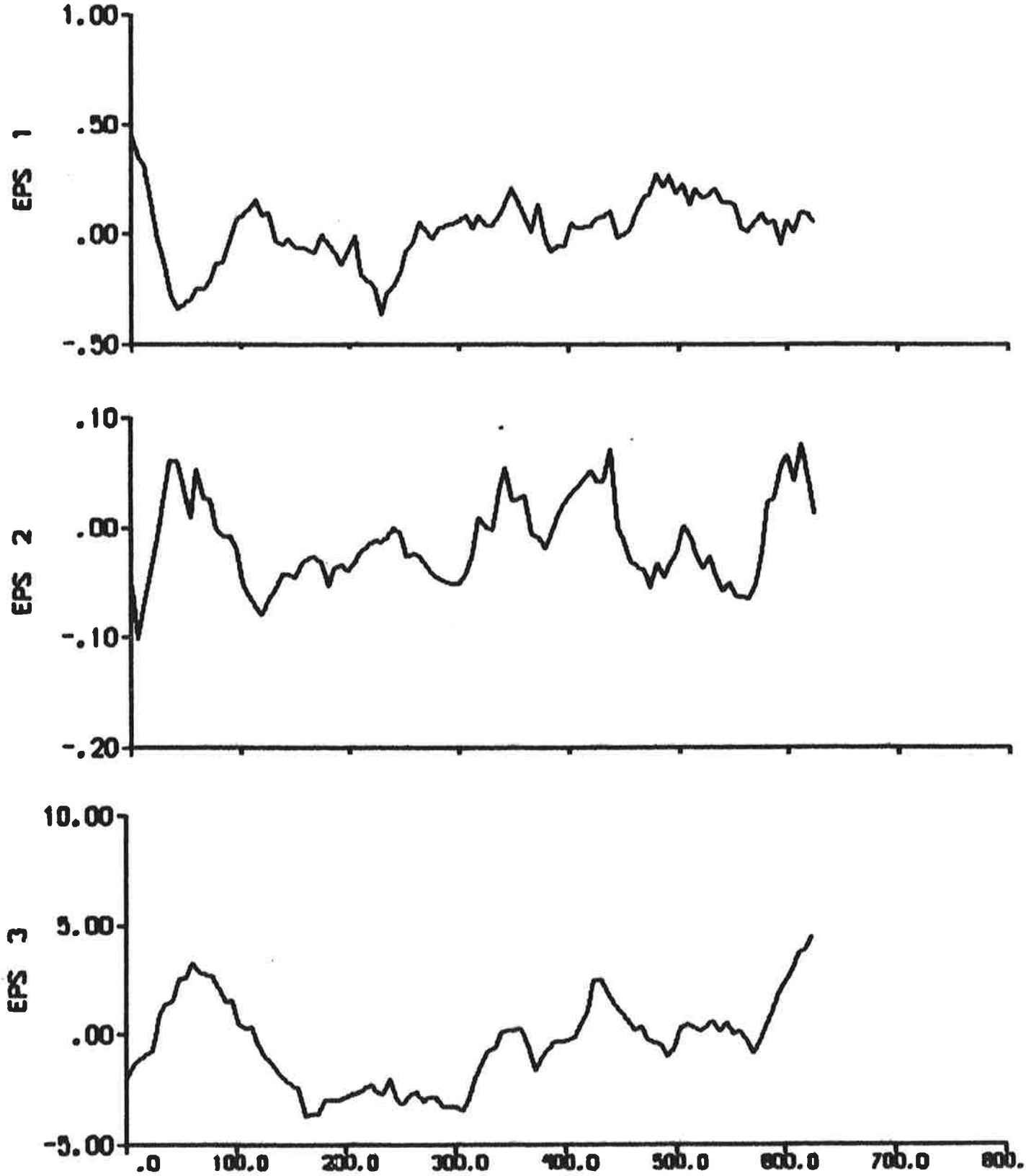

Fig. 5.2 c - Residuals.

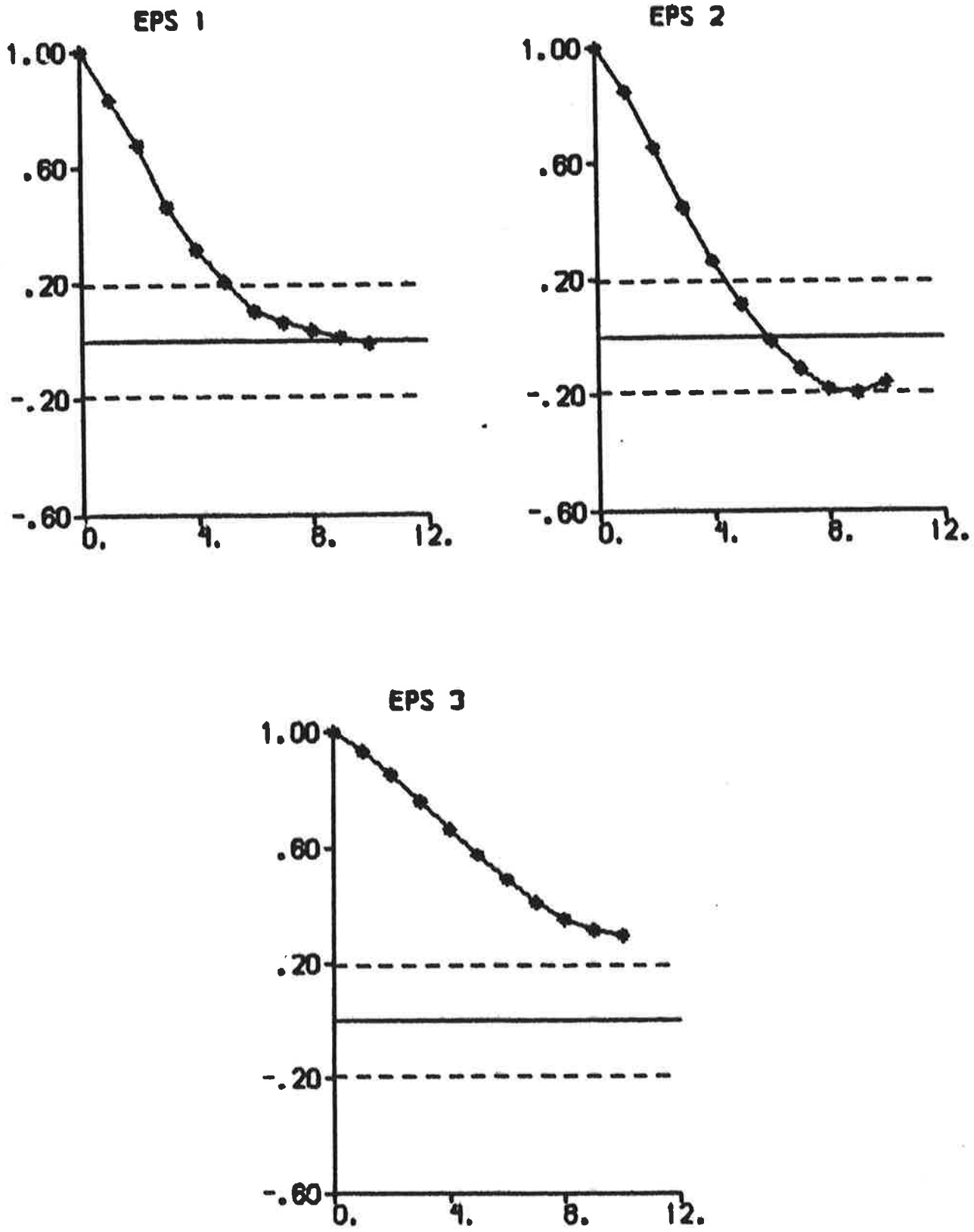

Fig. 5.2 d - Autocorrelation functions of residuals. The dashed lines are ±2σ limits.

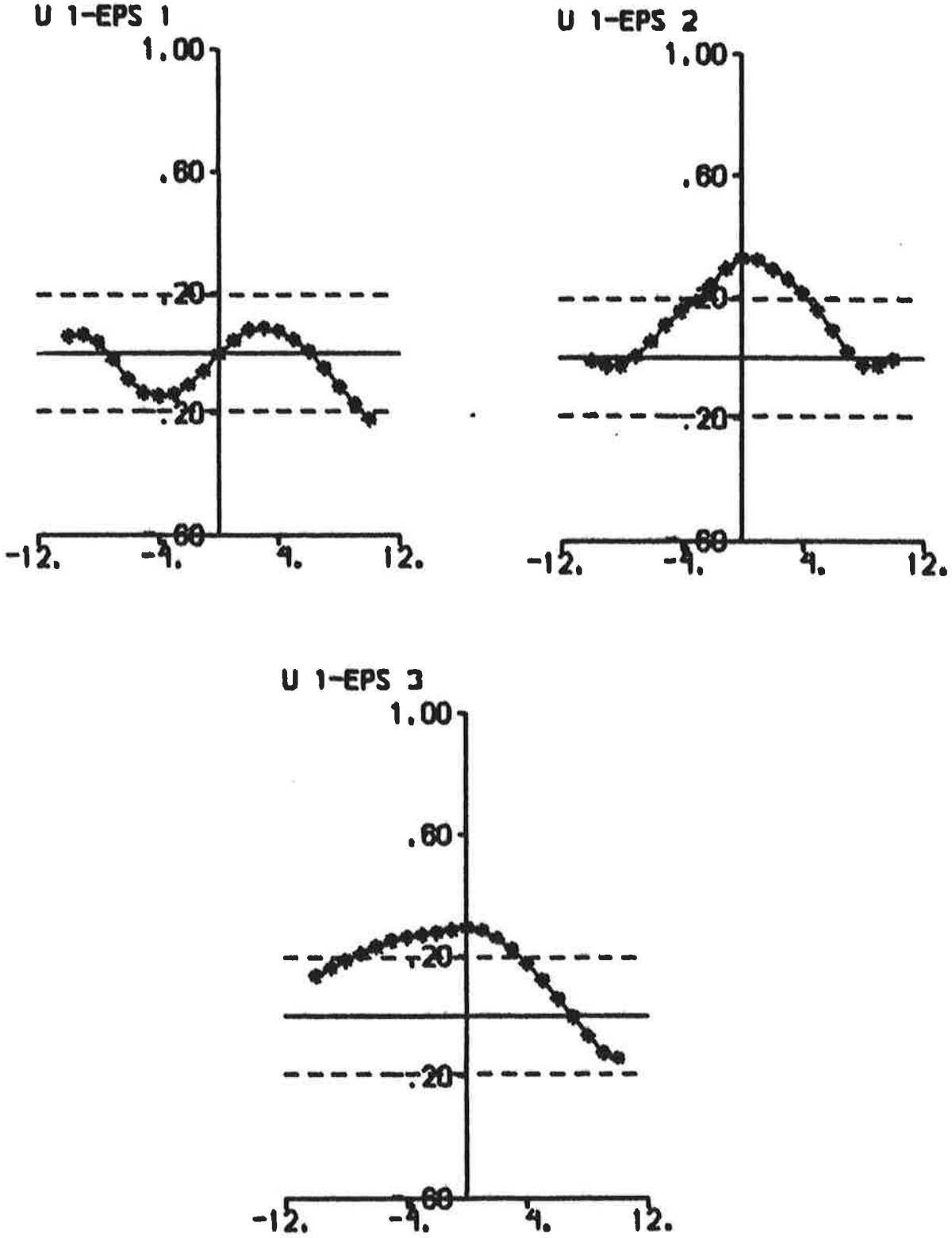

Fig. 5.2 e - Cross correlation functions between rudder input and residuals. The dashed lines are ±2σ limits.

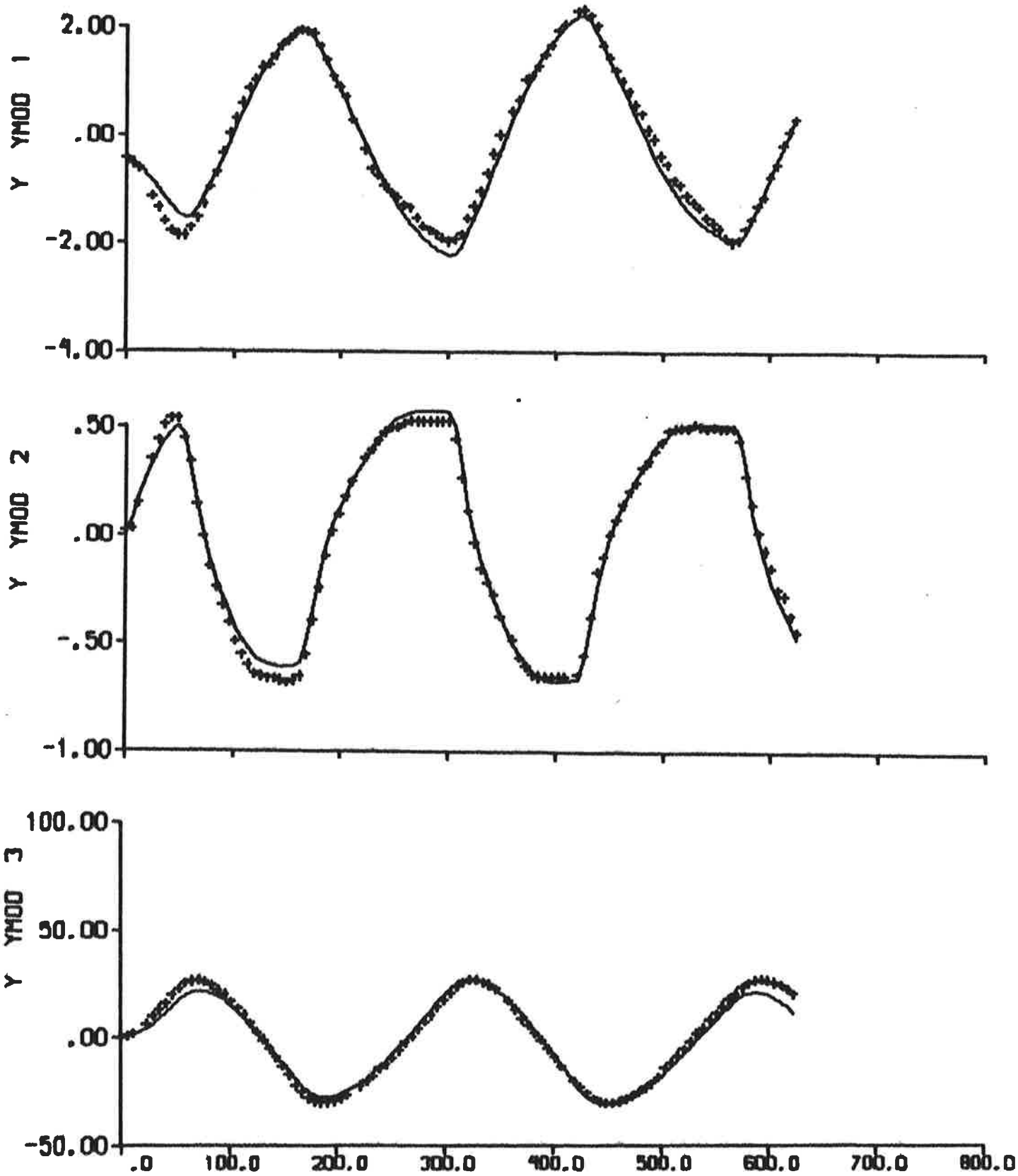

Fig. 5.3 a - Result of maximum likelihood identification to data from zig-zag test 1. The continuous lines are model outputs. Cf. Fig. 2.1.

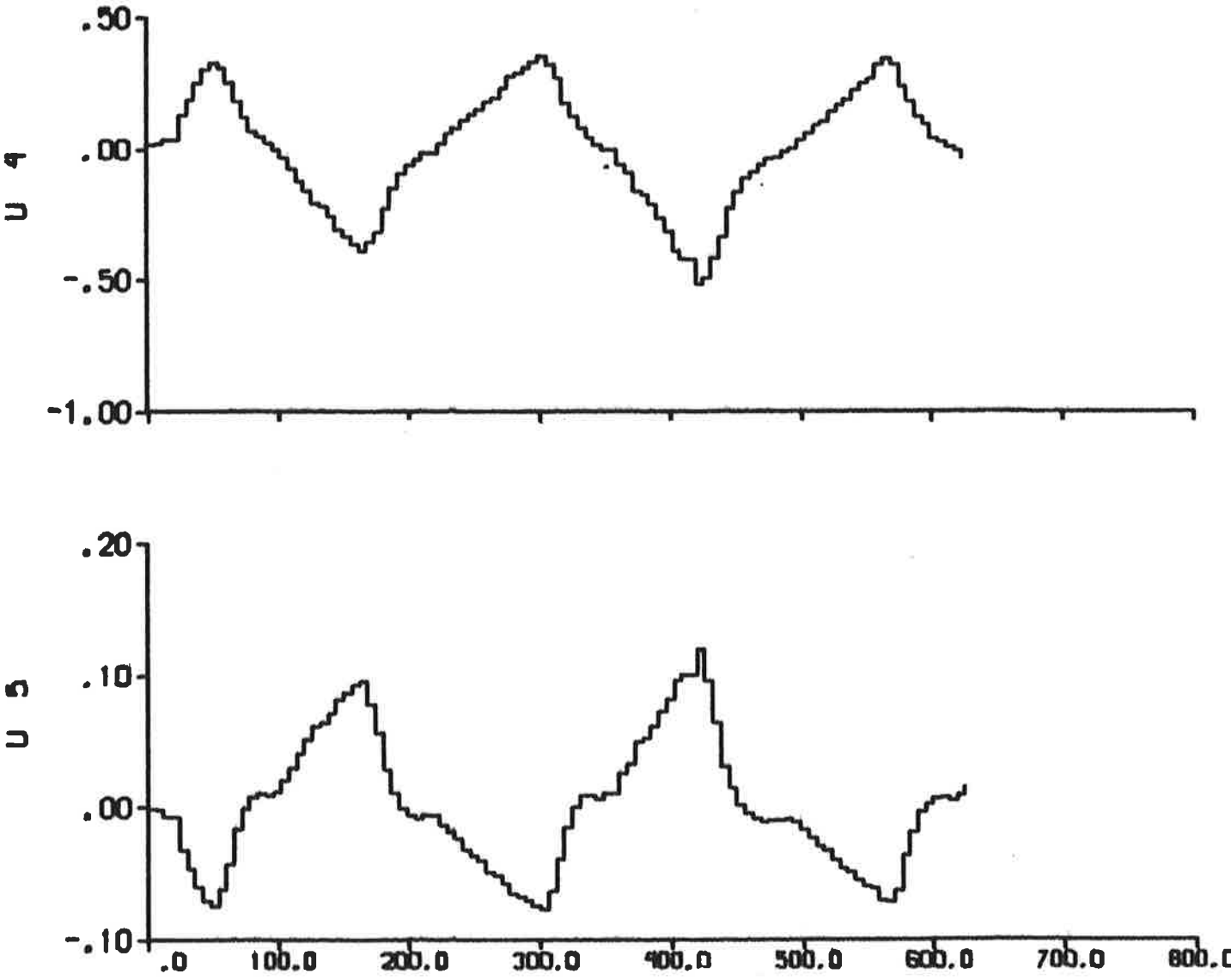

Fig. 5.3 b - Additional inputs U4 = f_Y/m' and U5 = f_N/m' describing the nonlinear contributions.

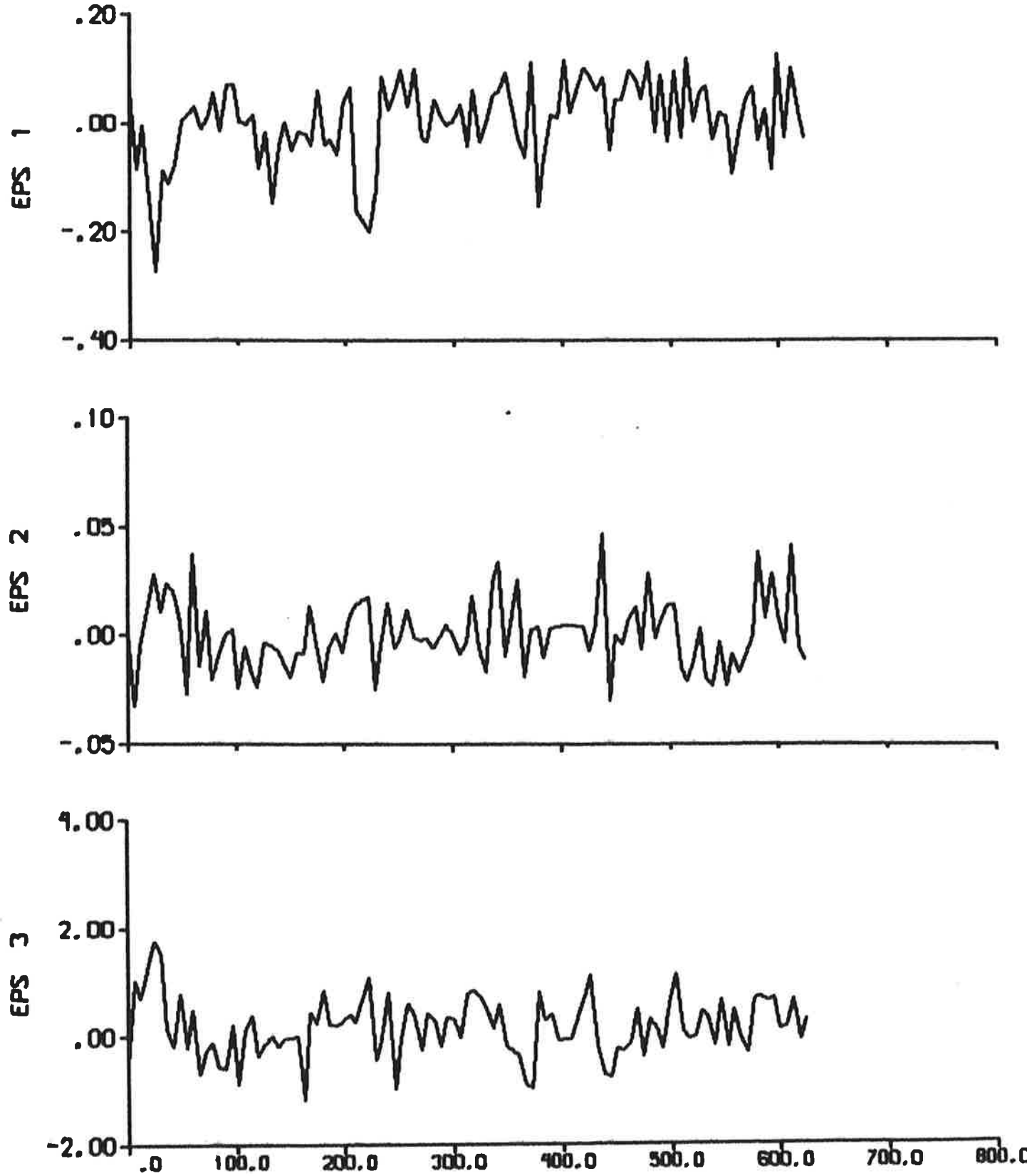

Fig. 5.3 c - Residuals.

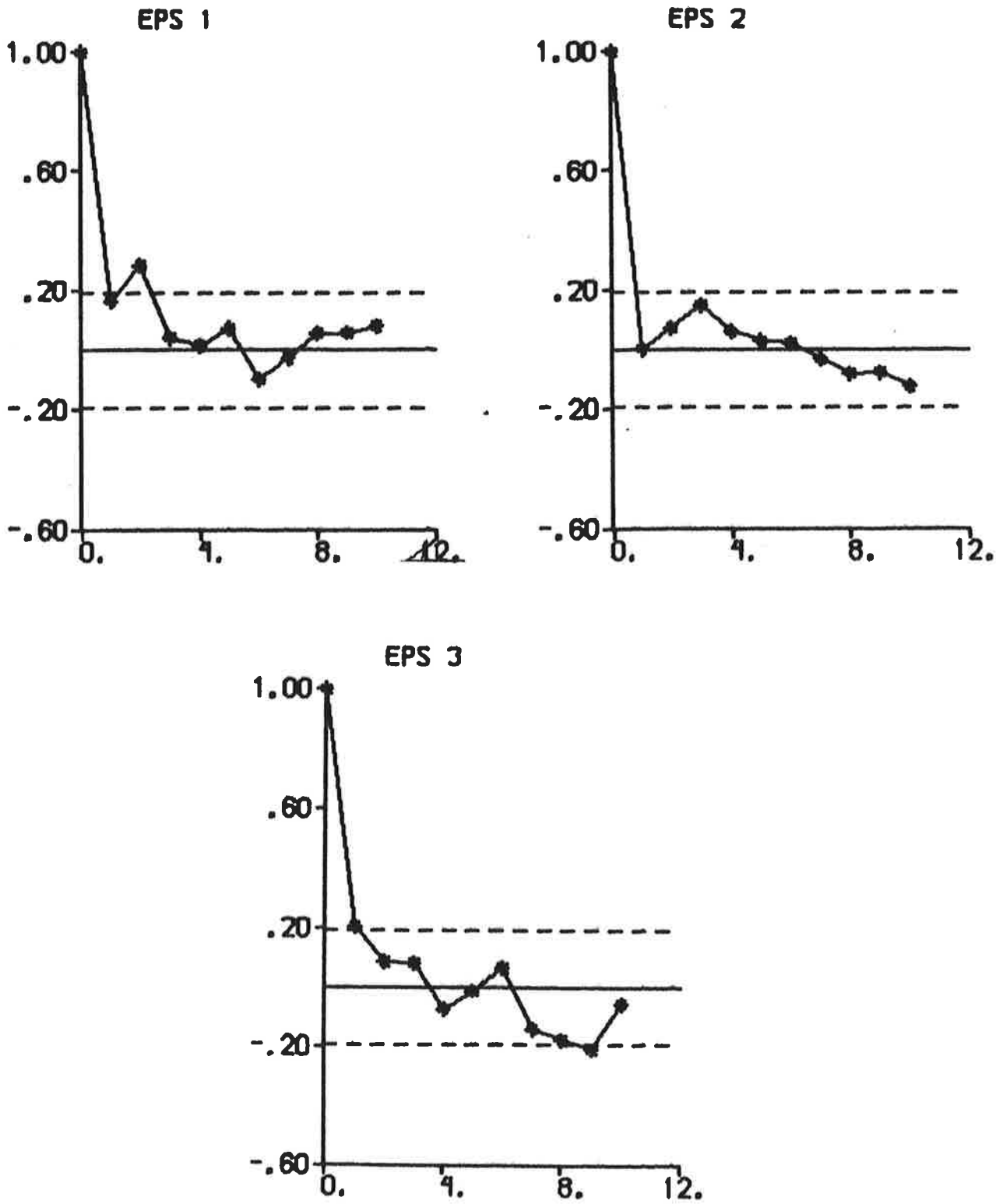

Fig. 5.3 d - Autocorrelation functions of residuals. The dashed lines are ±2σ limits.

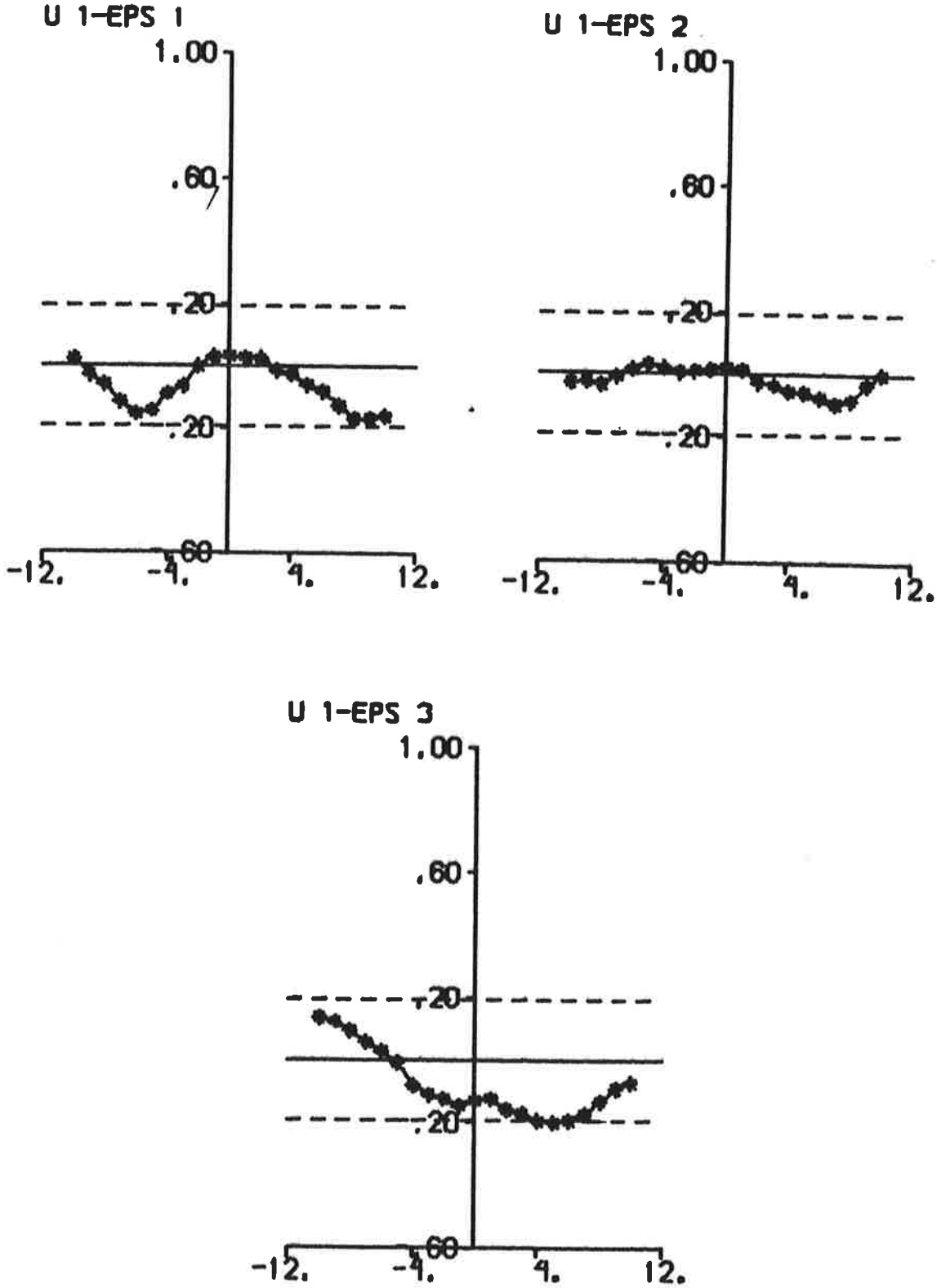

Fig. 5.3 e - Cross correlation functions between rudder input and residuals. The dashed lines are ±2σ limits.

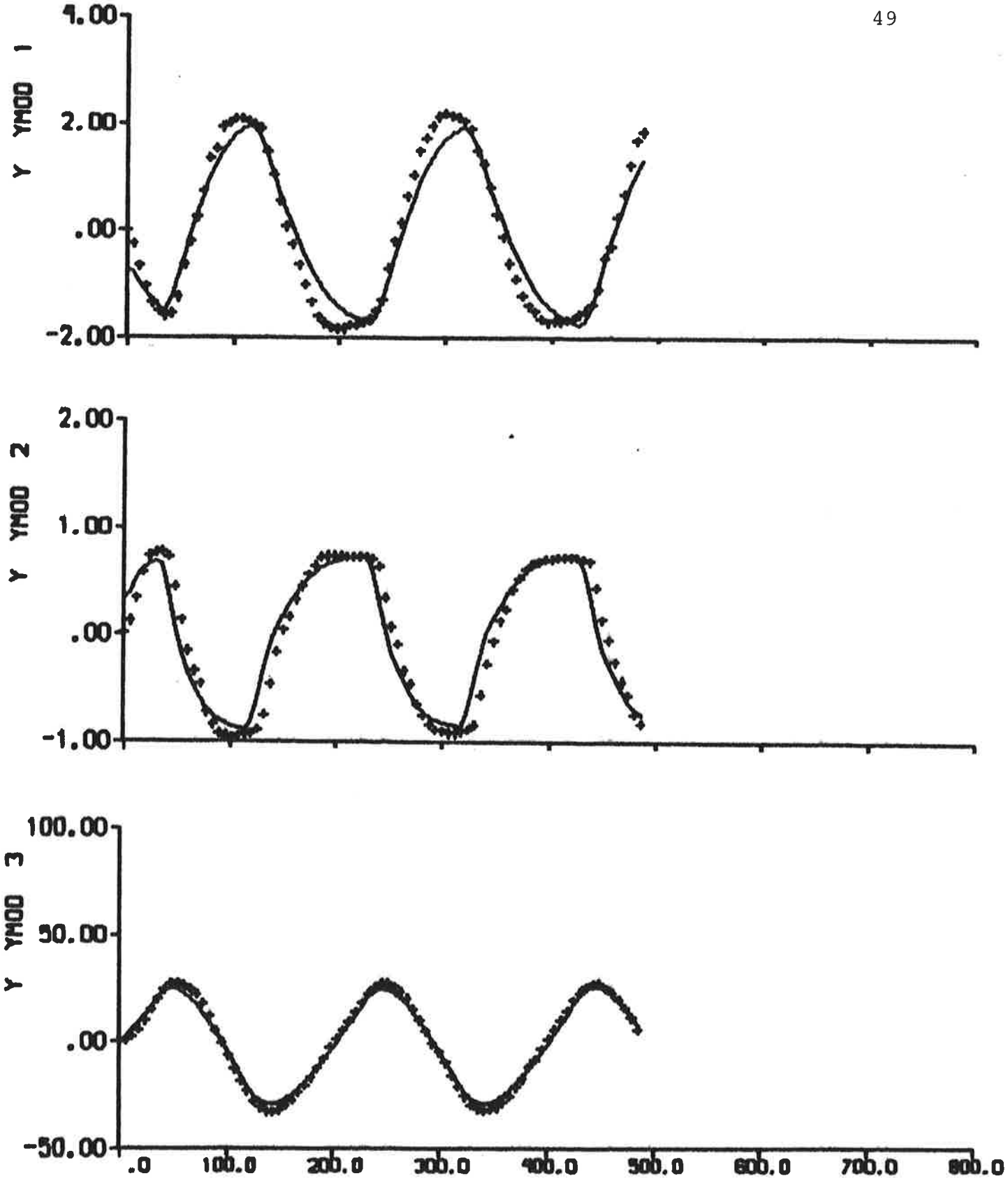

Fig. 5.4 a - Result of output error identification to data from zig-zag test 2, when the linear part of the model is fixed to HyA:s model. The continuous lines are model outputs. Cf. Fig. 2.2.

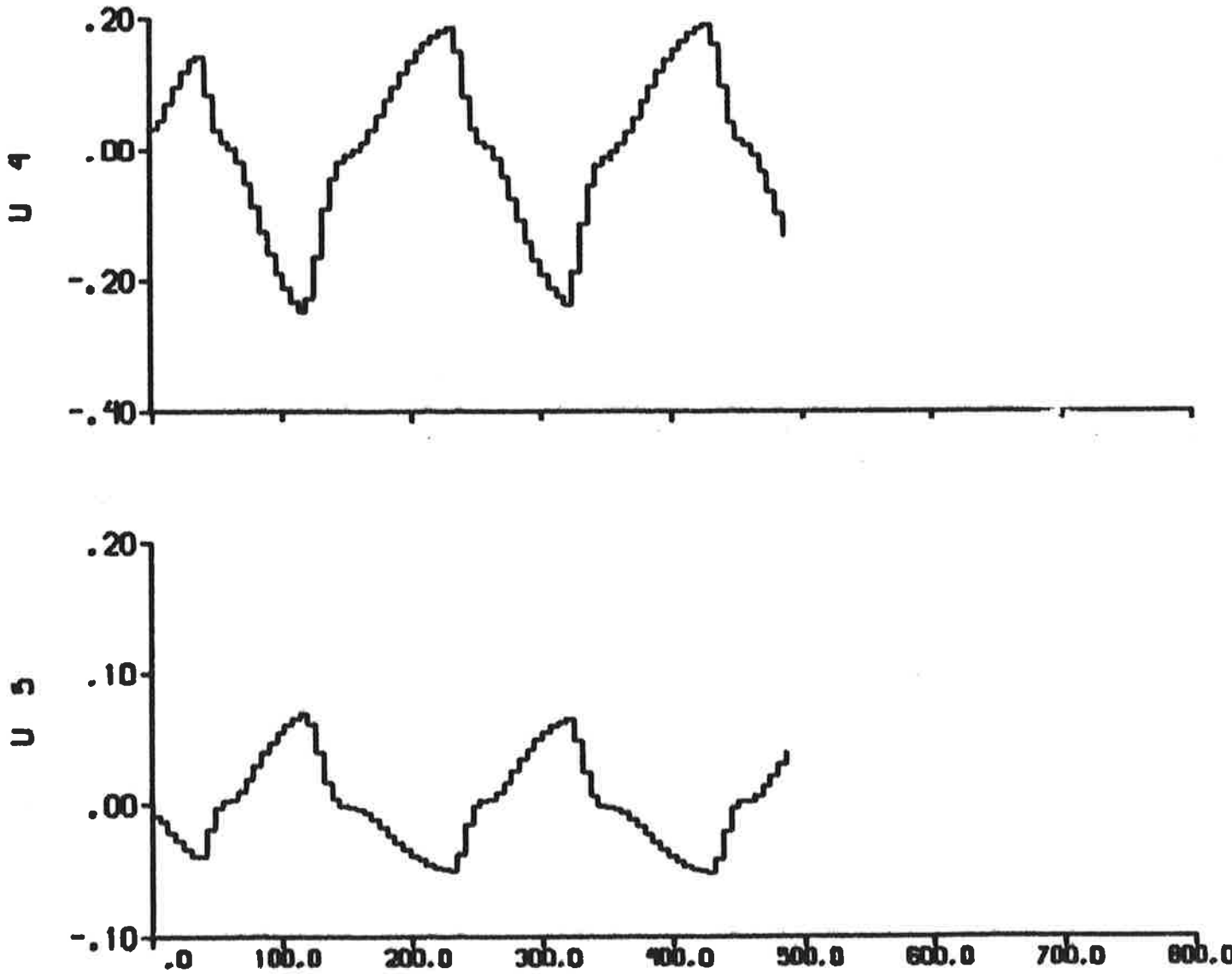

Fig. 5.4 b - Additional inputs U4 = f_Y/m' and U5 = f_N/m' describing the nonlinear contributions.

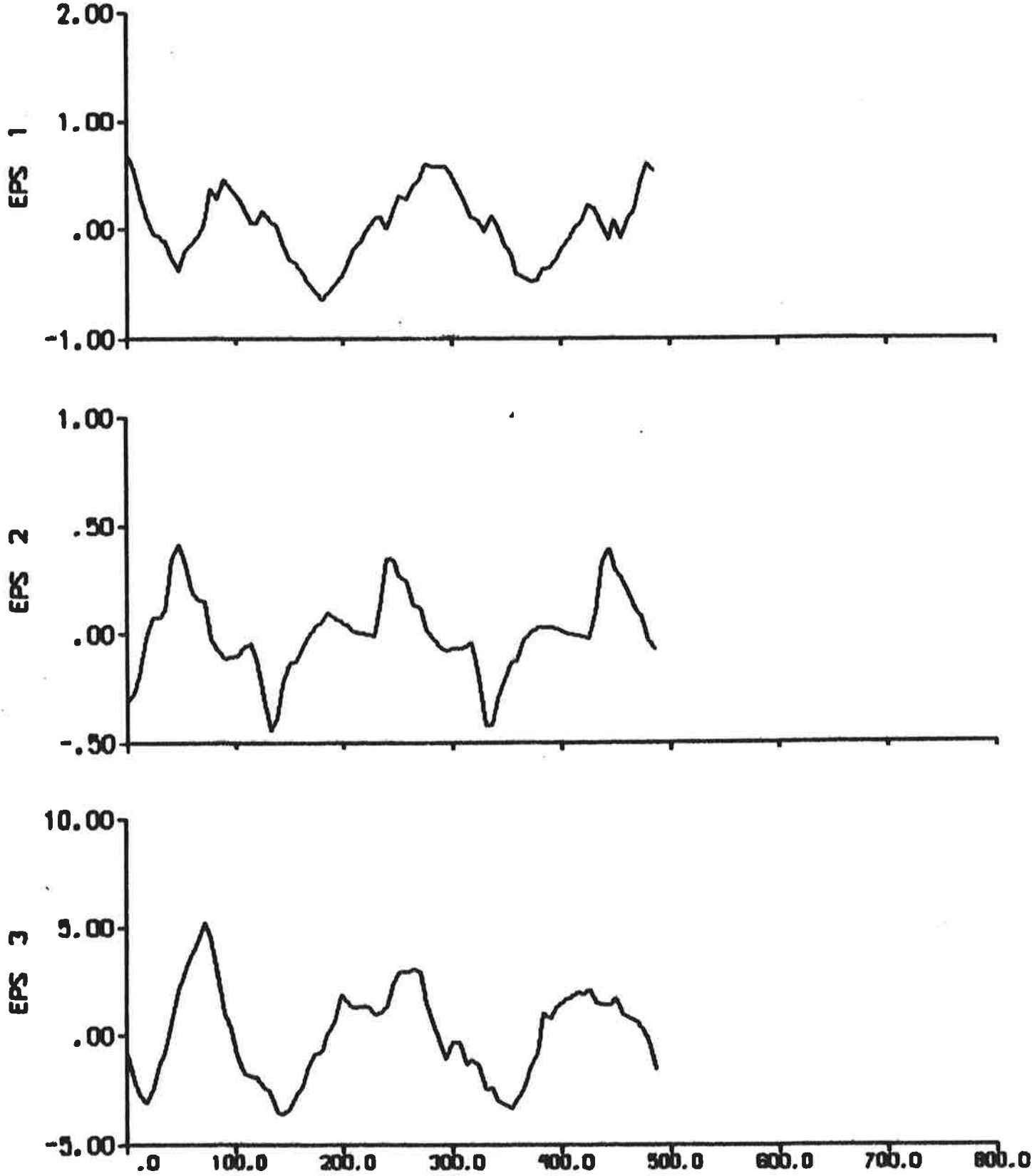

Fig. 5.4 c - Residuals.

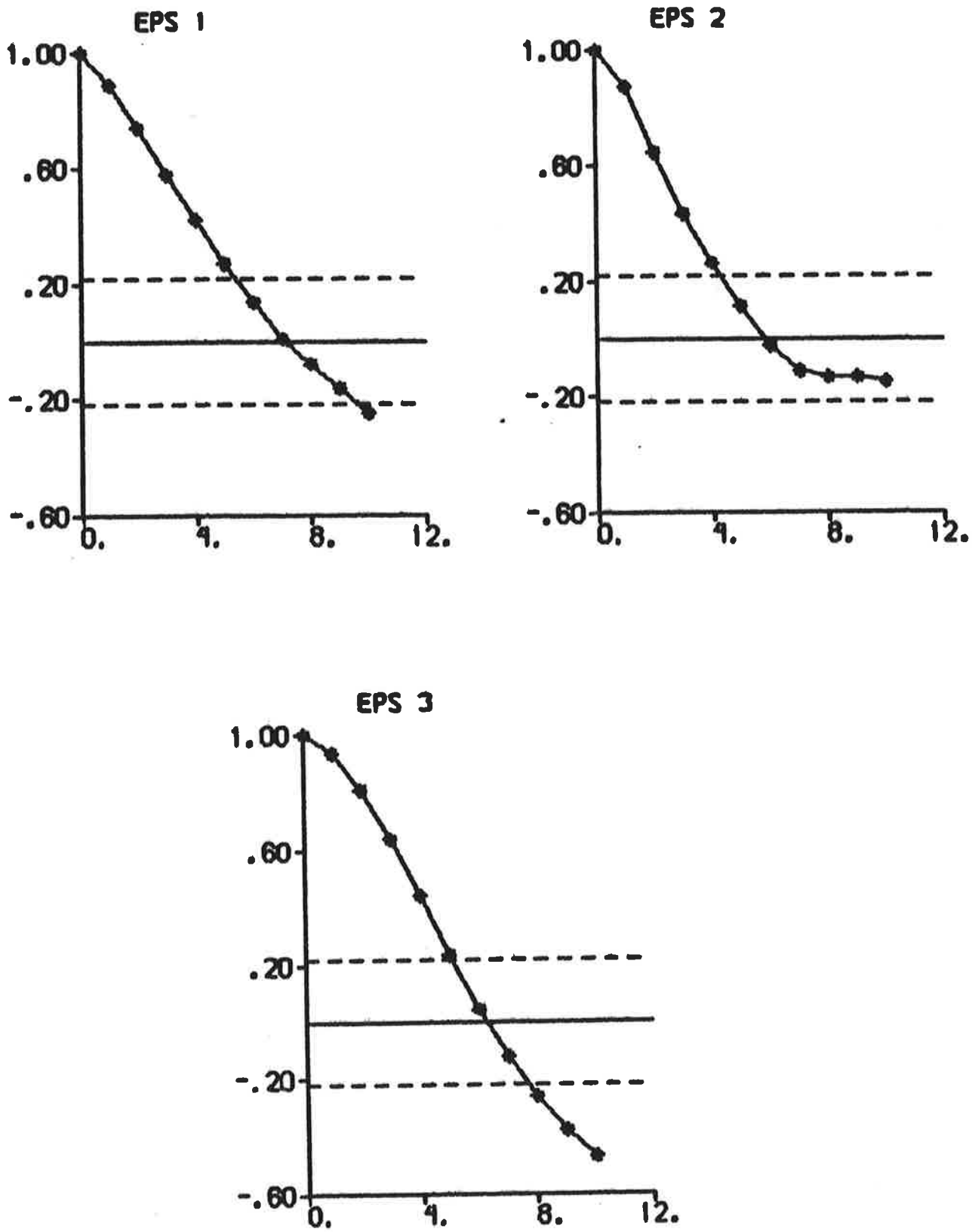

Fig. 5.4 d - Autocorrelation functions of residuals.
The dashed lines are ±2σ limits.

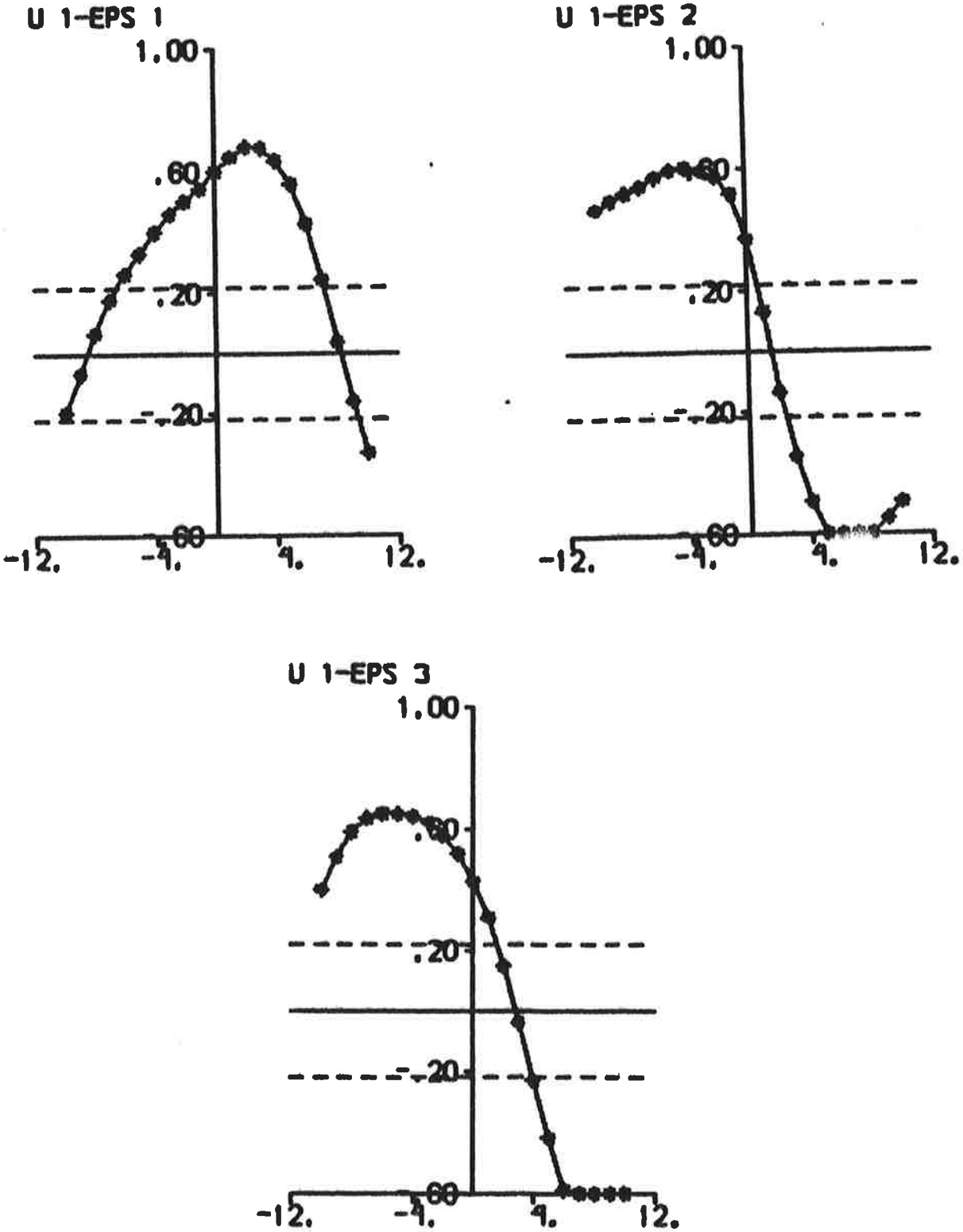

Fig. 5.4 e - Cross correlation functions between rudder input and residuals. The dashed lines are ±2σ limits.

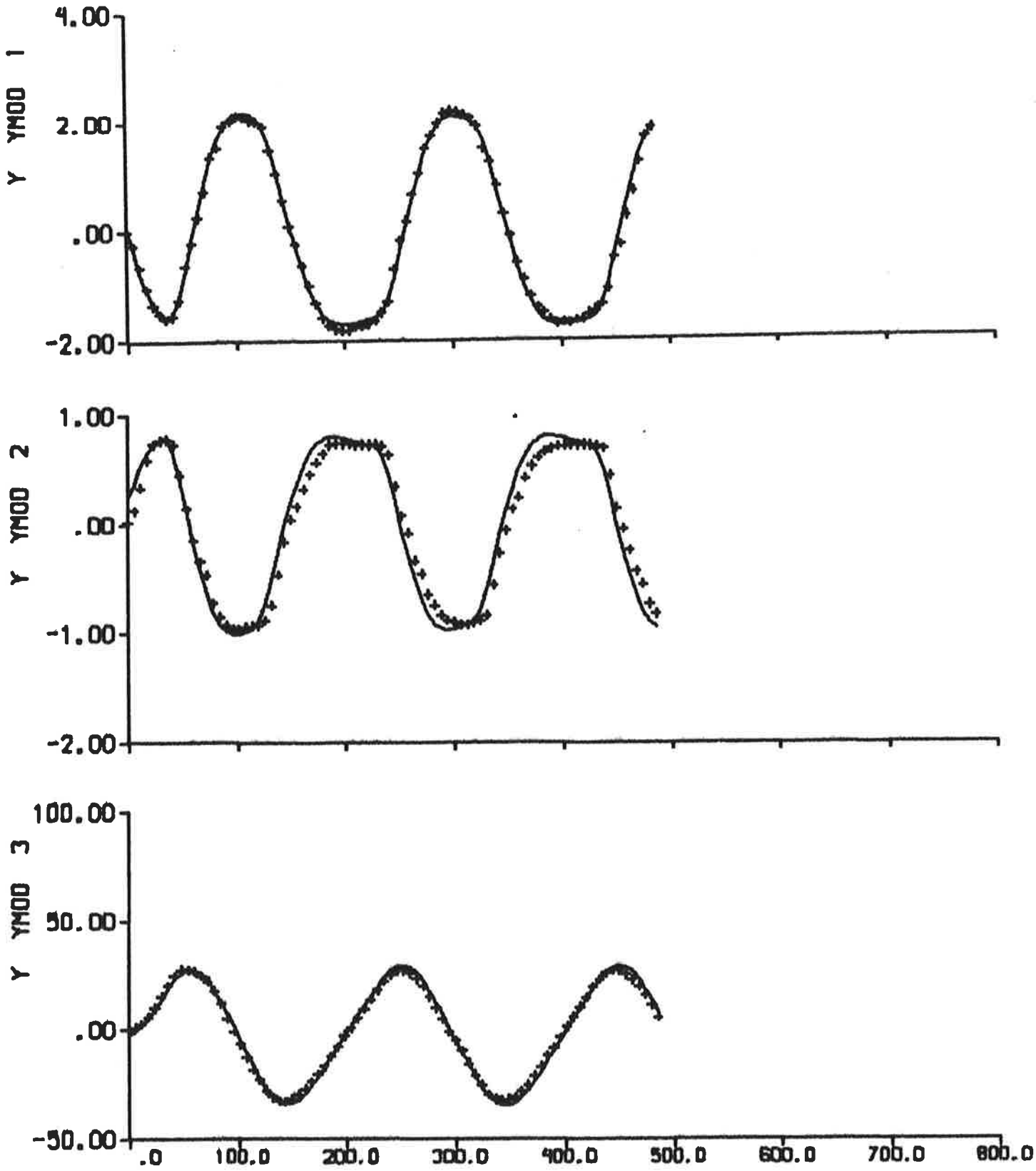

Fig. 5.5 a - Result of output error identification to data from zig-zag test 2. The continuous lines are model outputs. Cf. Fig. 2.2.

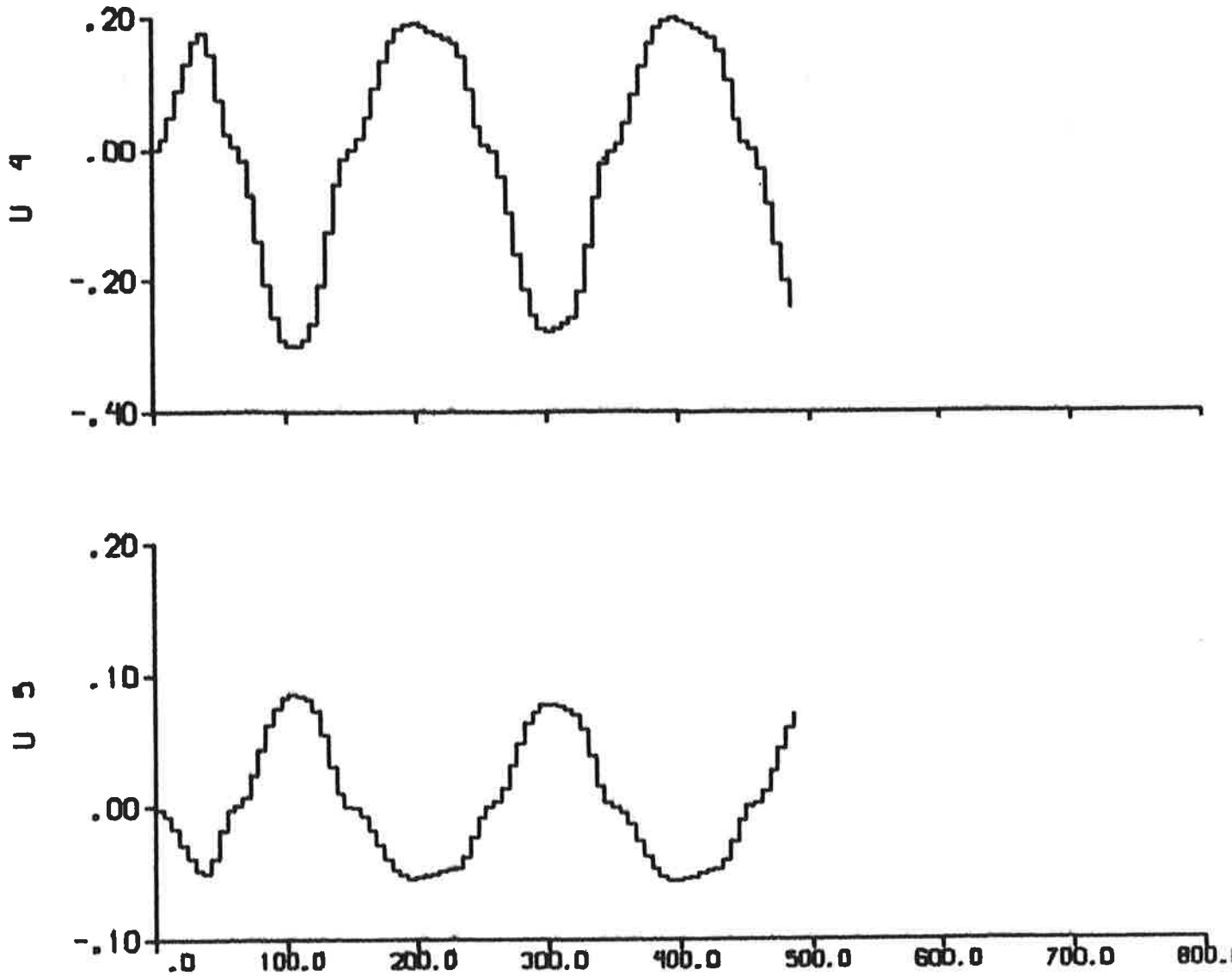

Fig. 5.5 b - Additional inputs $U4 = f_Y/m'$ and $U5 = f_N/m'$ describing the nonlinear contributions.

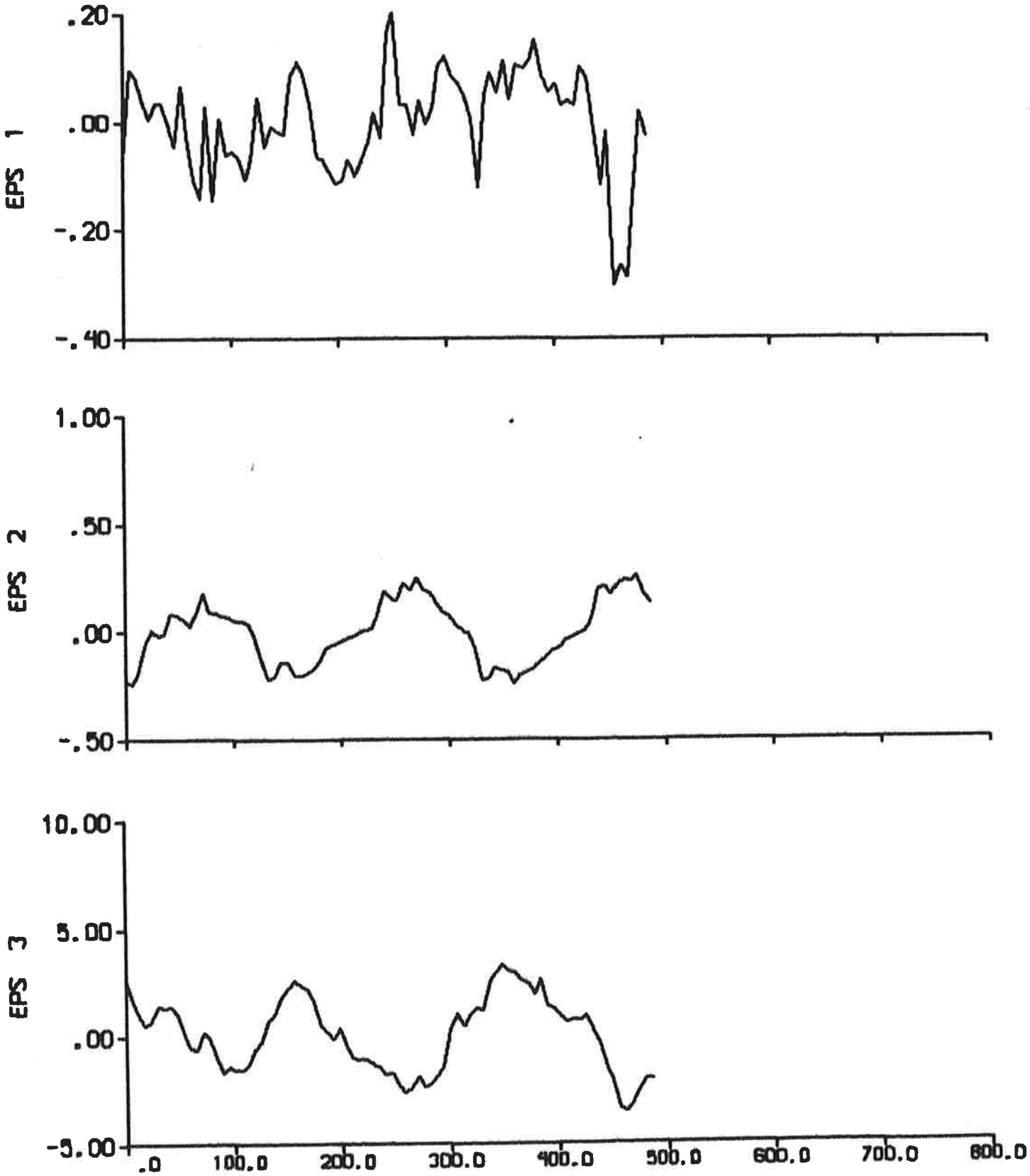

Fig. 5.5 c - Residuals.

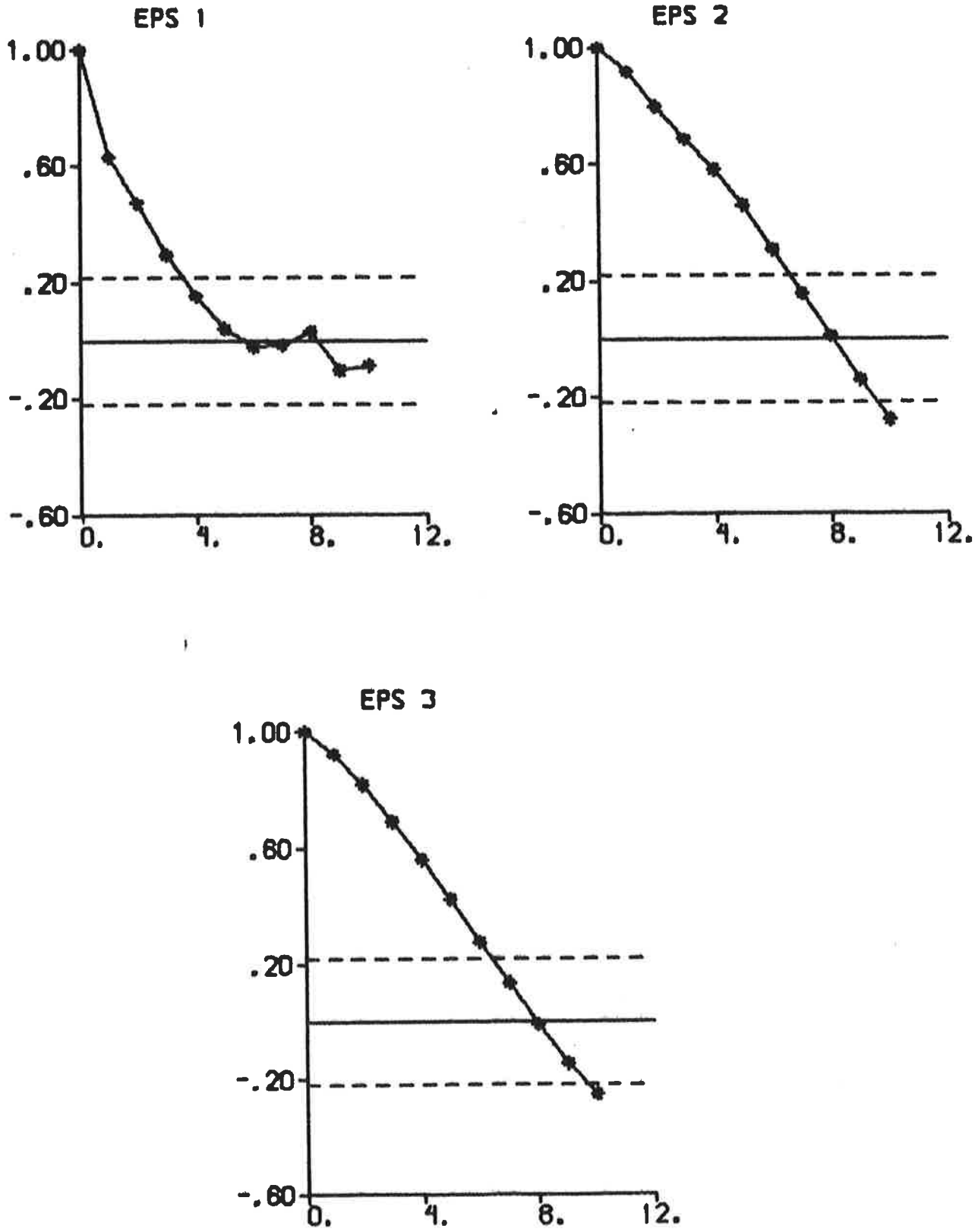

Fig. 5.5 d - Autocorrelation functions of residuals.
The dashed lines are ±2σ limits.

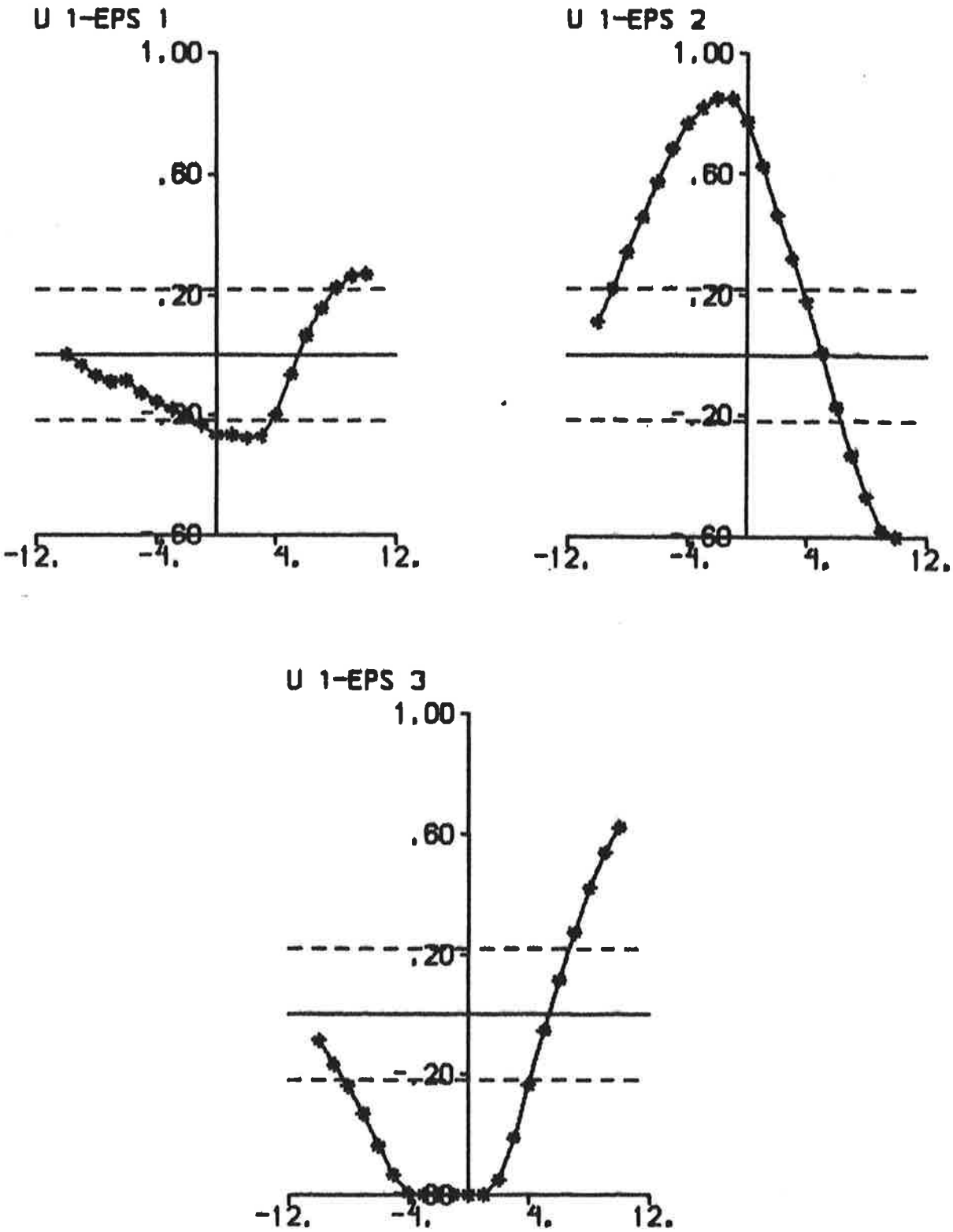

Fig. 5.5 e - Cross correlation functions between rudder input and residuals. The dashed lines are ±2σ limits.

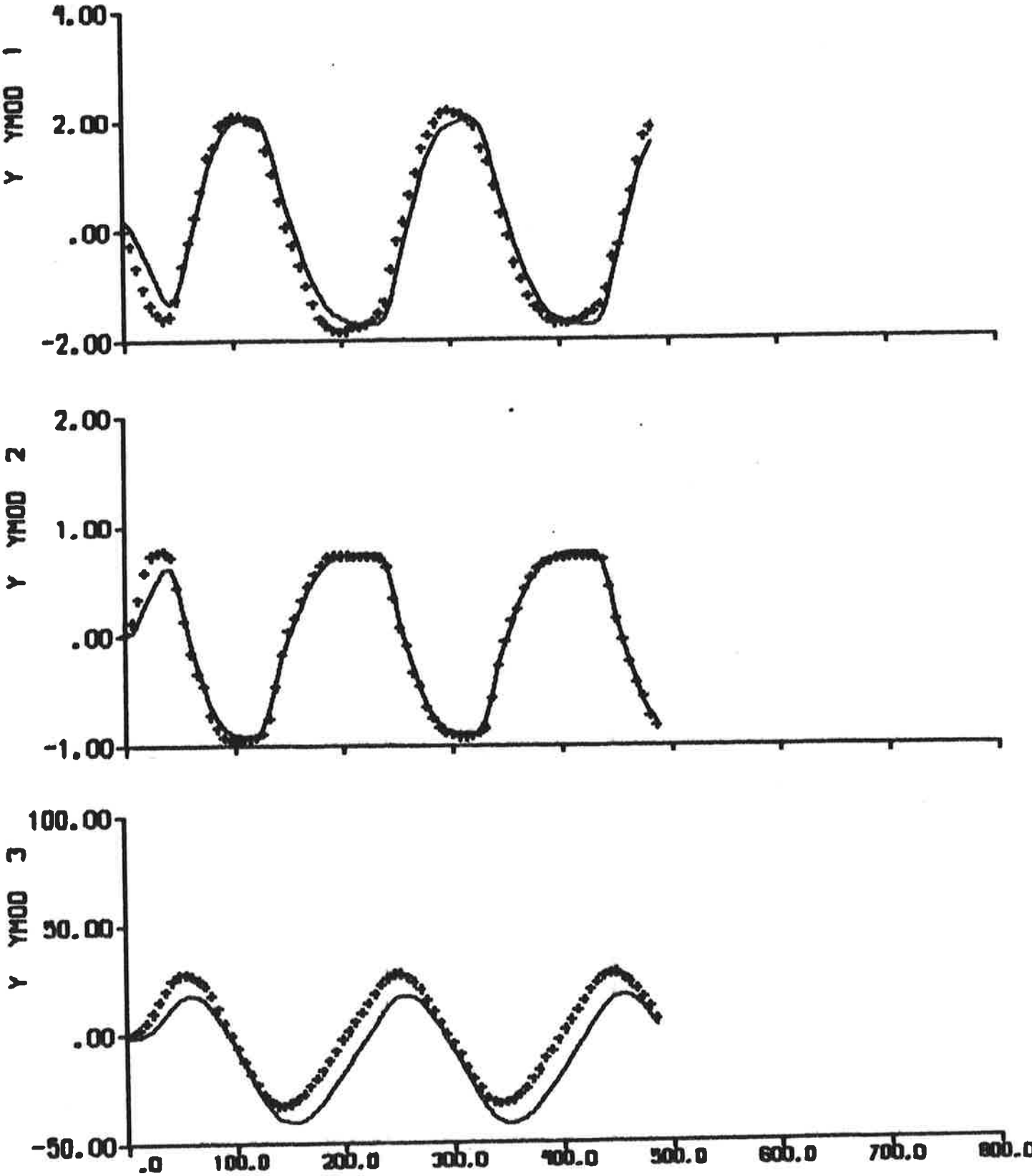

Fig. 5.6 a - Result of maximum likelihood identification to data from zig-zag test 2. The continuous lines are model outputs. Cf. Fig. 2.2.

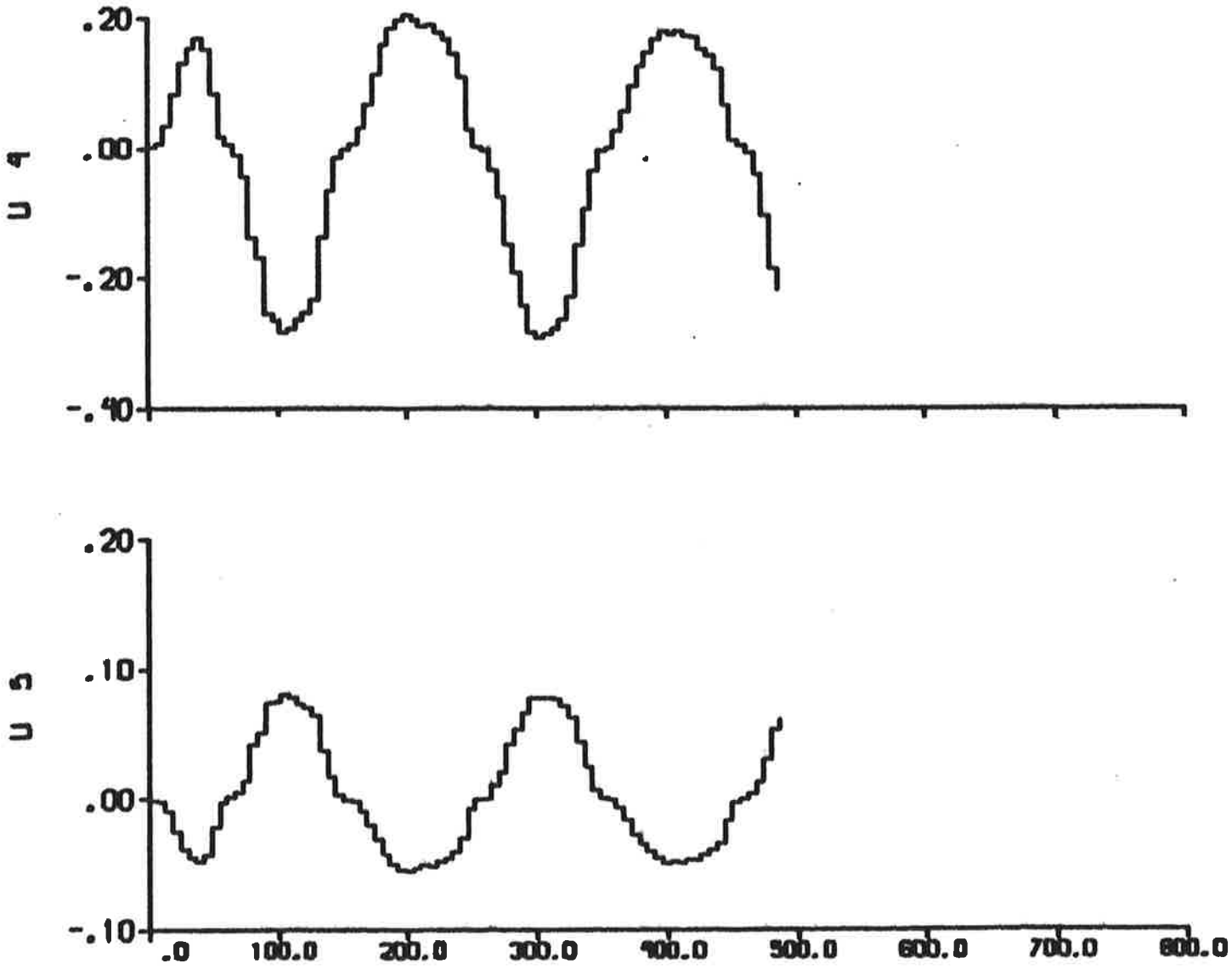

Fig. 5.6 b - Additional inputs U4= f_Y/m' and U5 = f_N/m' describing the nonlinear contributions.

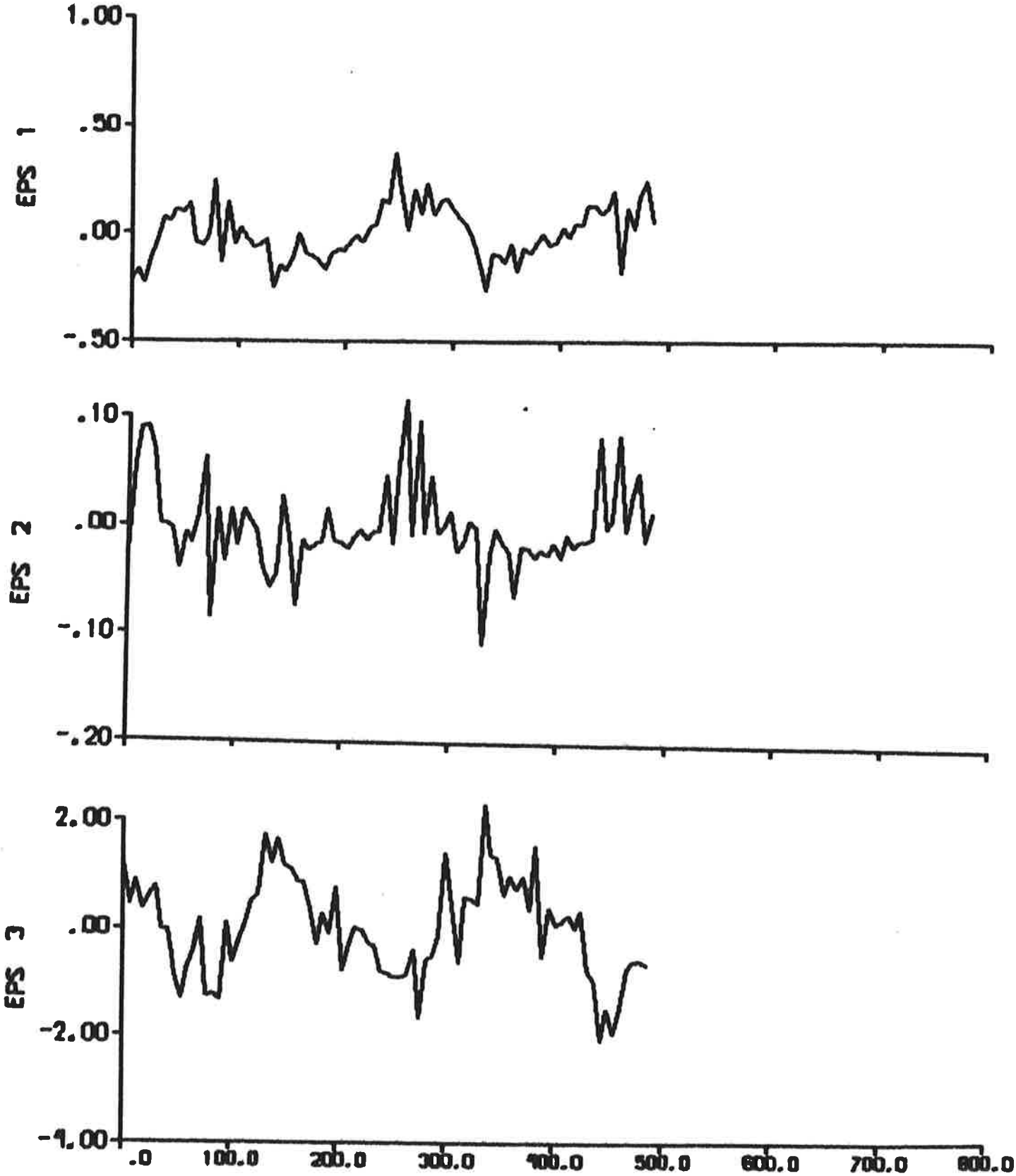

Fig. 5.6 c - Residuals.

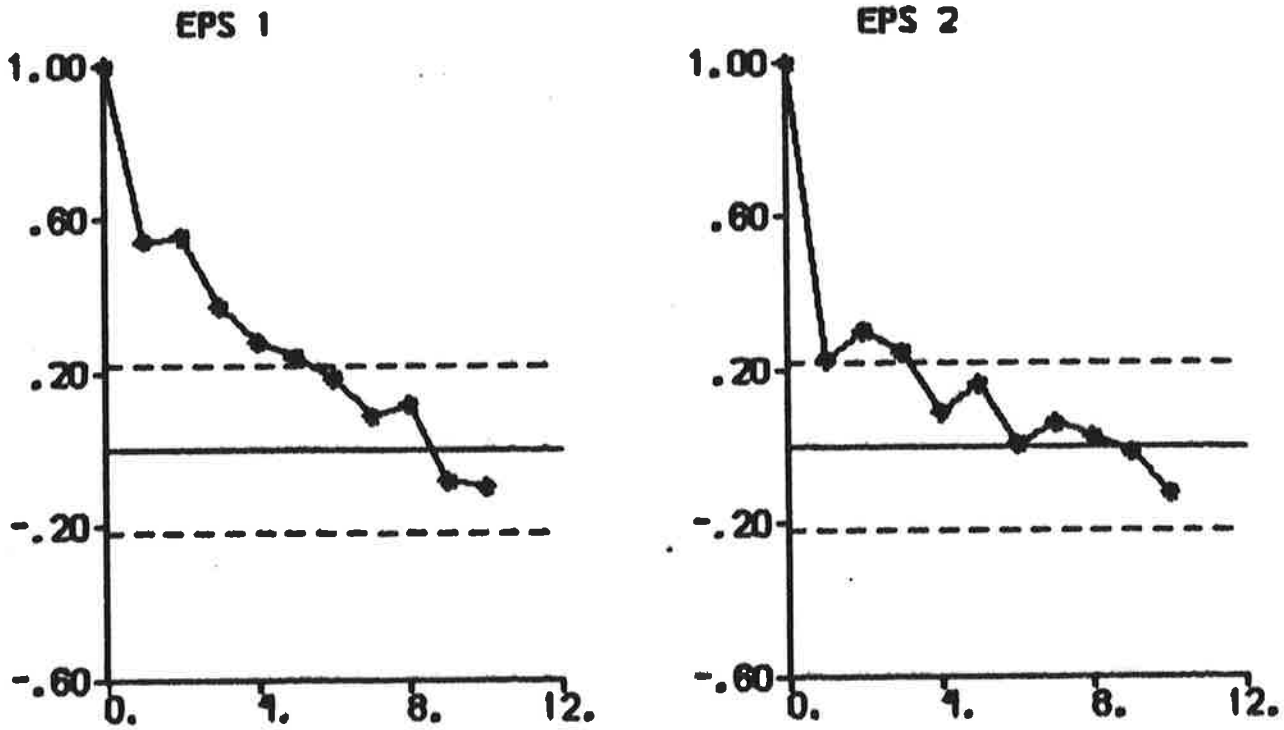

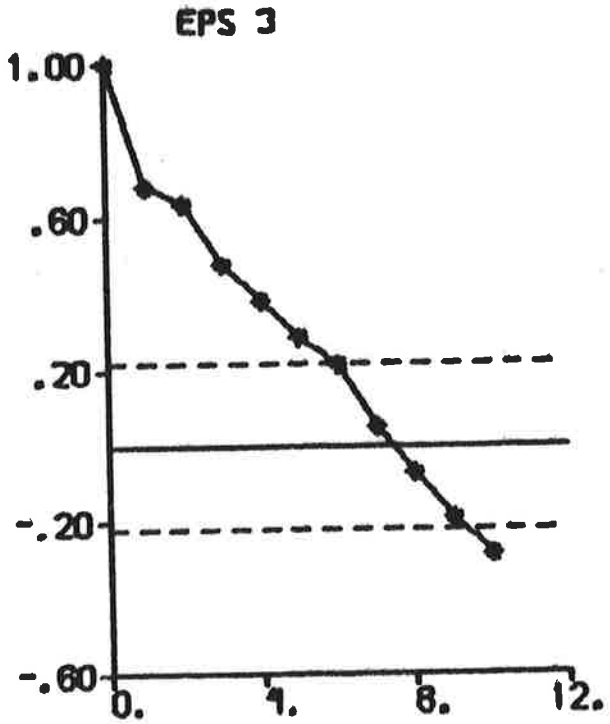

Fig. 5.6 d - Autocorrelation functions of residuals.
The dashed lines are ±2σ limits.

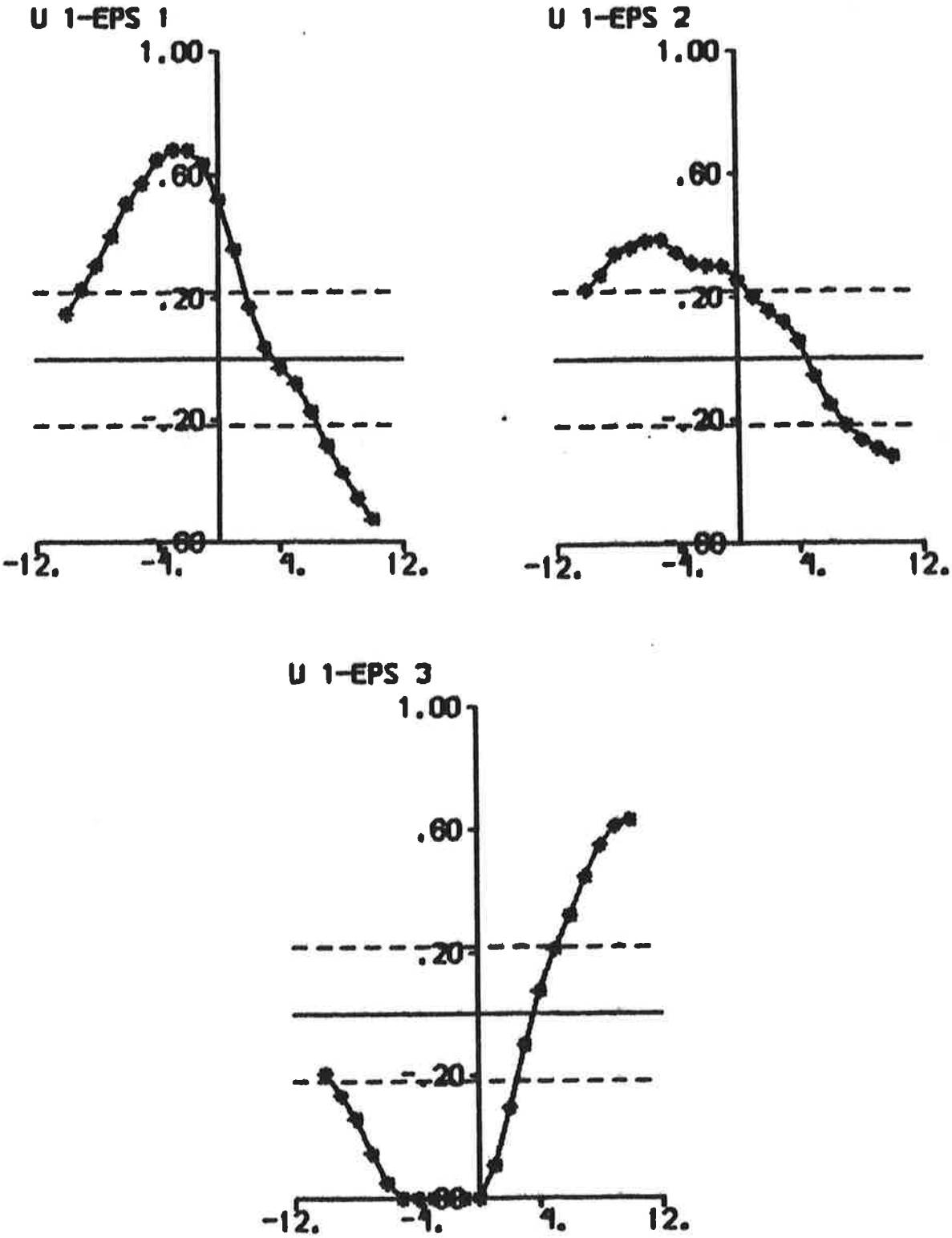

Fig. 5.6 e - Cross correlation functions between rudder input and residuals. The dashed lines are ±2σ limits.

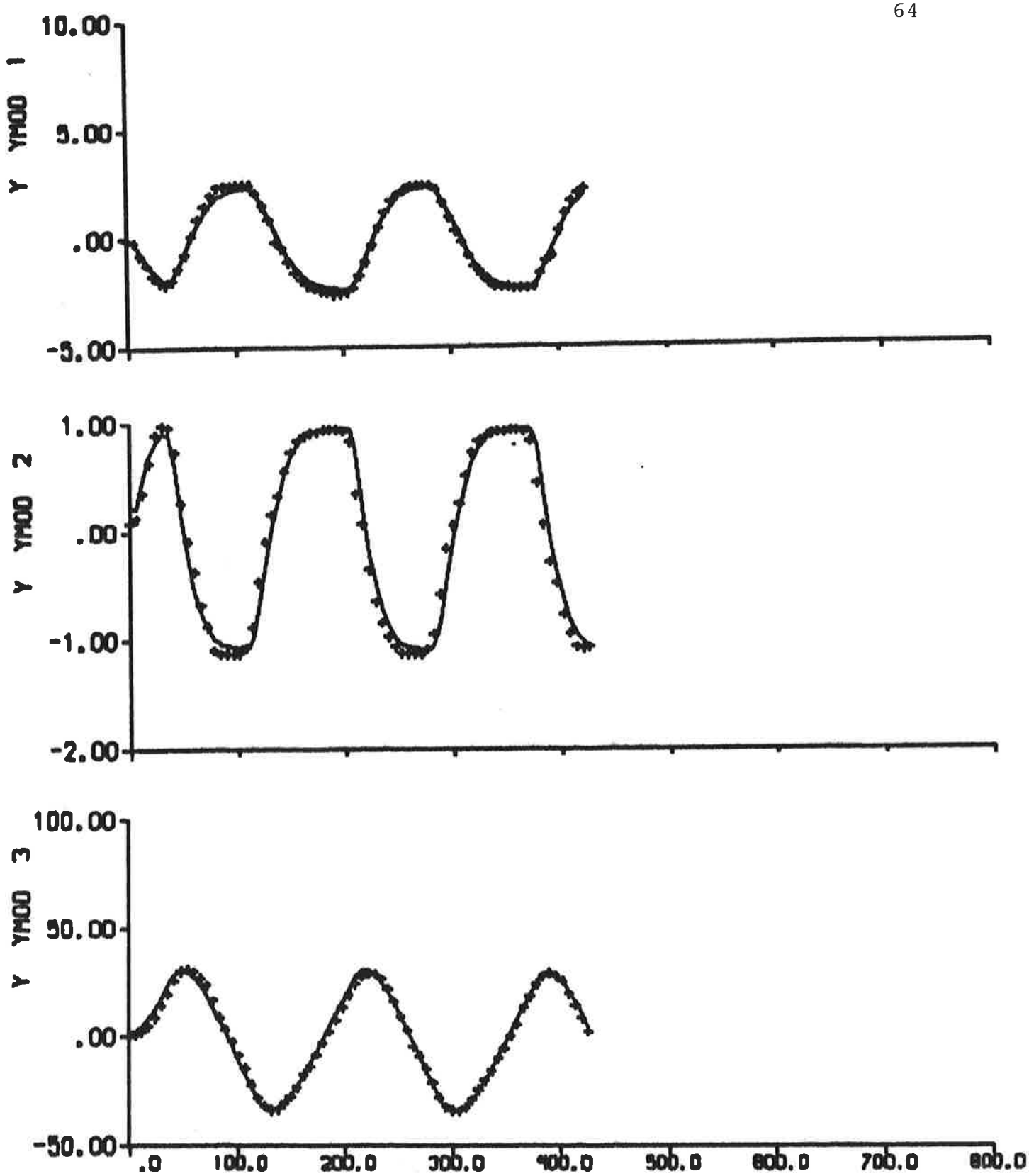

Fig. 5.7 a - Result of output error identification to data from zig-zag test 3, when the linear part of the model is fixed to HyA:s model. The continuous lines are model outputs. Cf. Fig. 2.3.

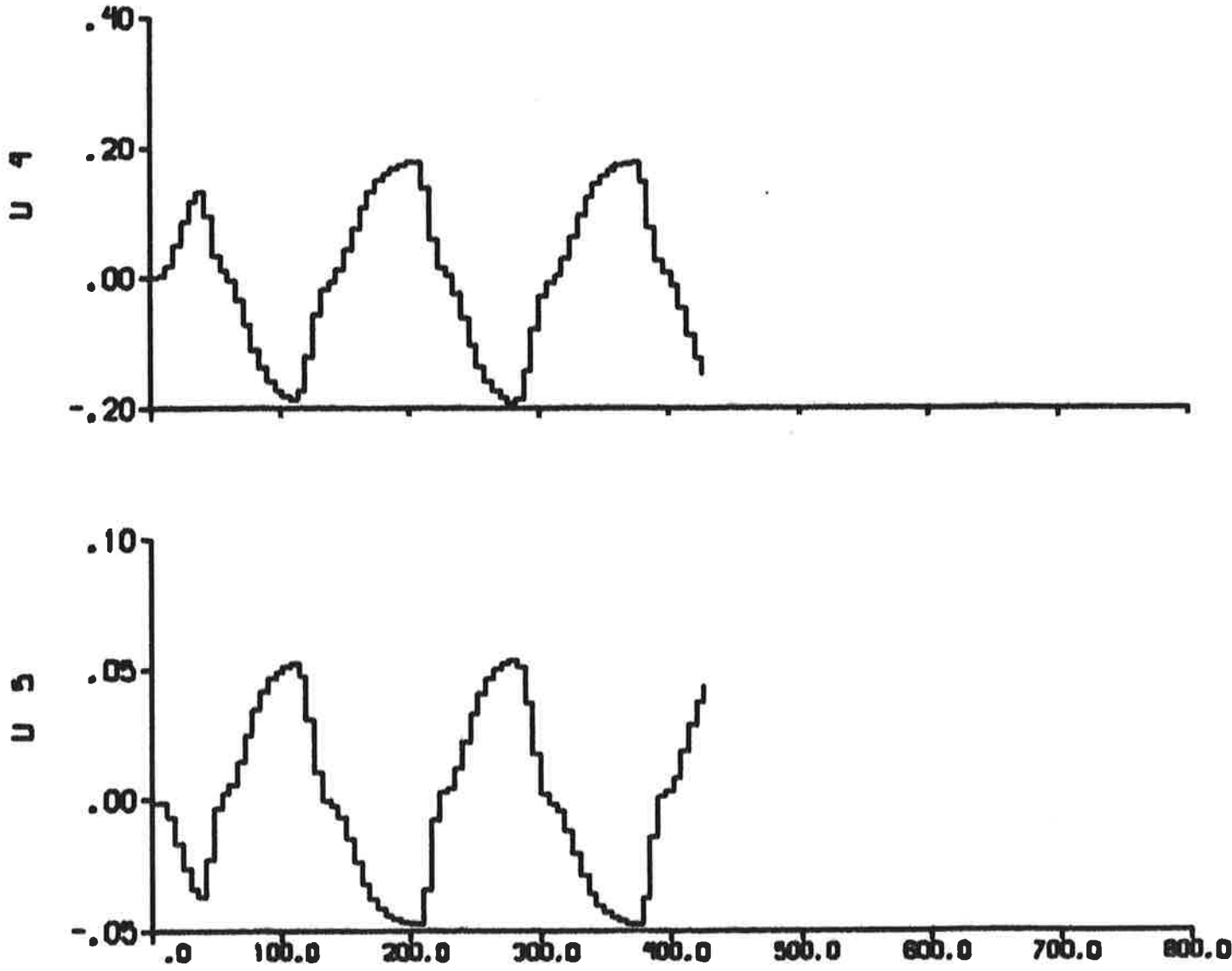

Fig. 5.7 b - Additional inputs U4= f_Y/m' and U5 = f_N/m' describing the nonlinear contributions.

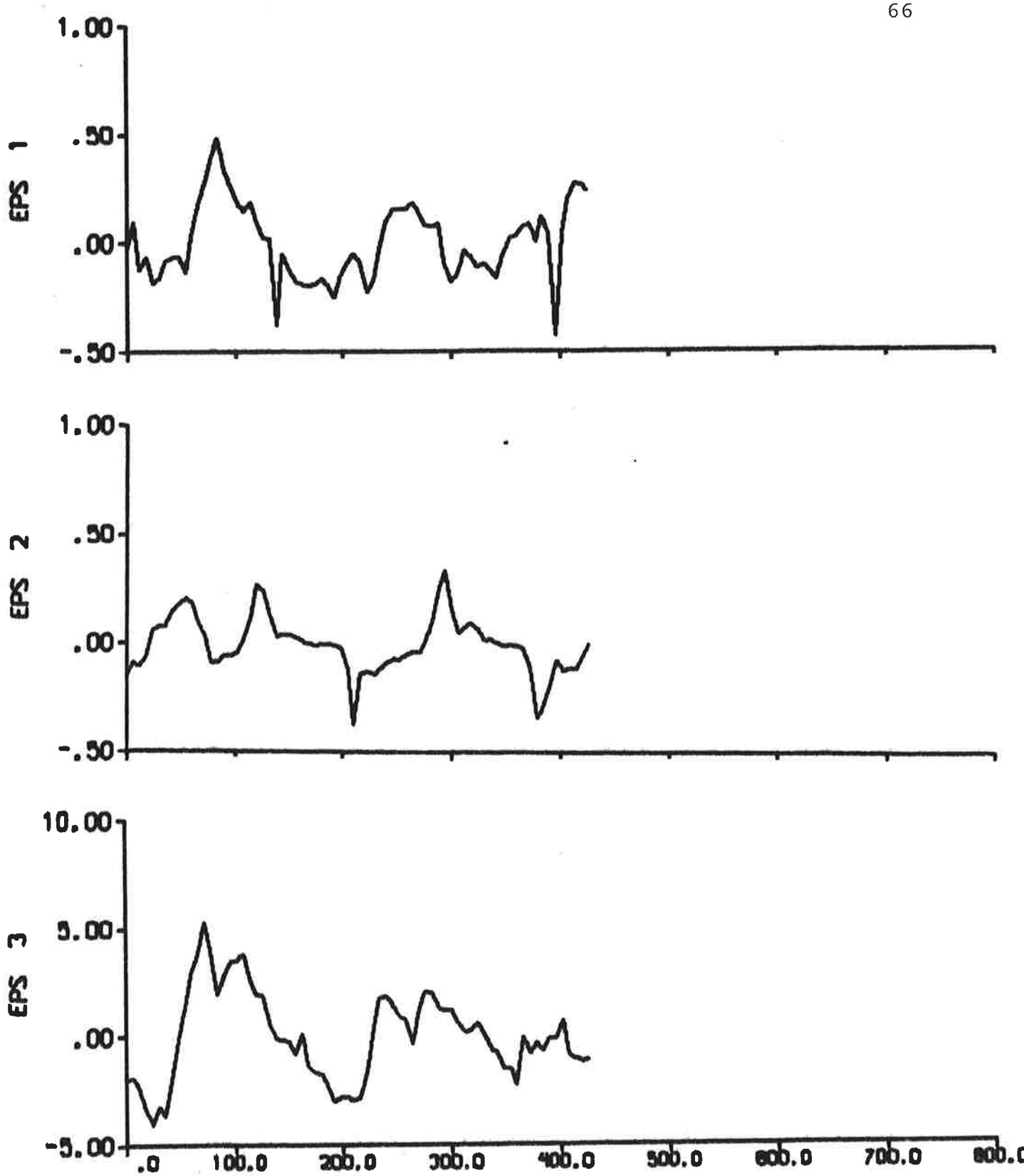

Fig. 5.7 c - Residuals.

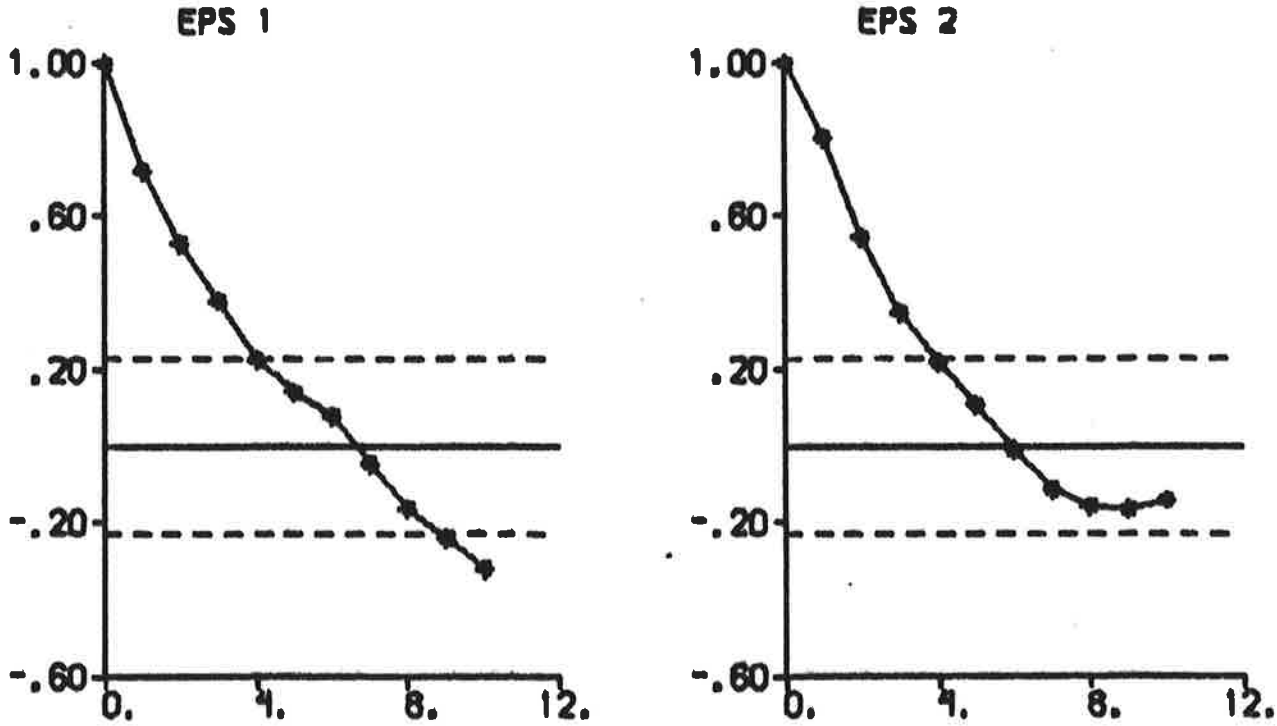

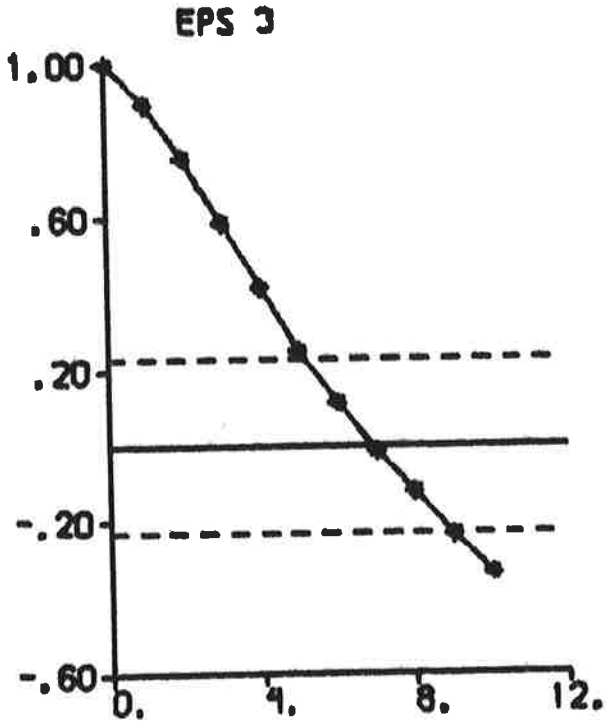

Fig. 5.7 d - Autocorrelation functions of residuals.
The dashed lines are ±2σ limits.

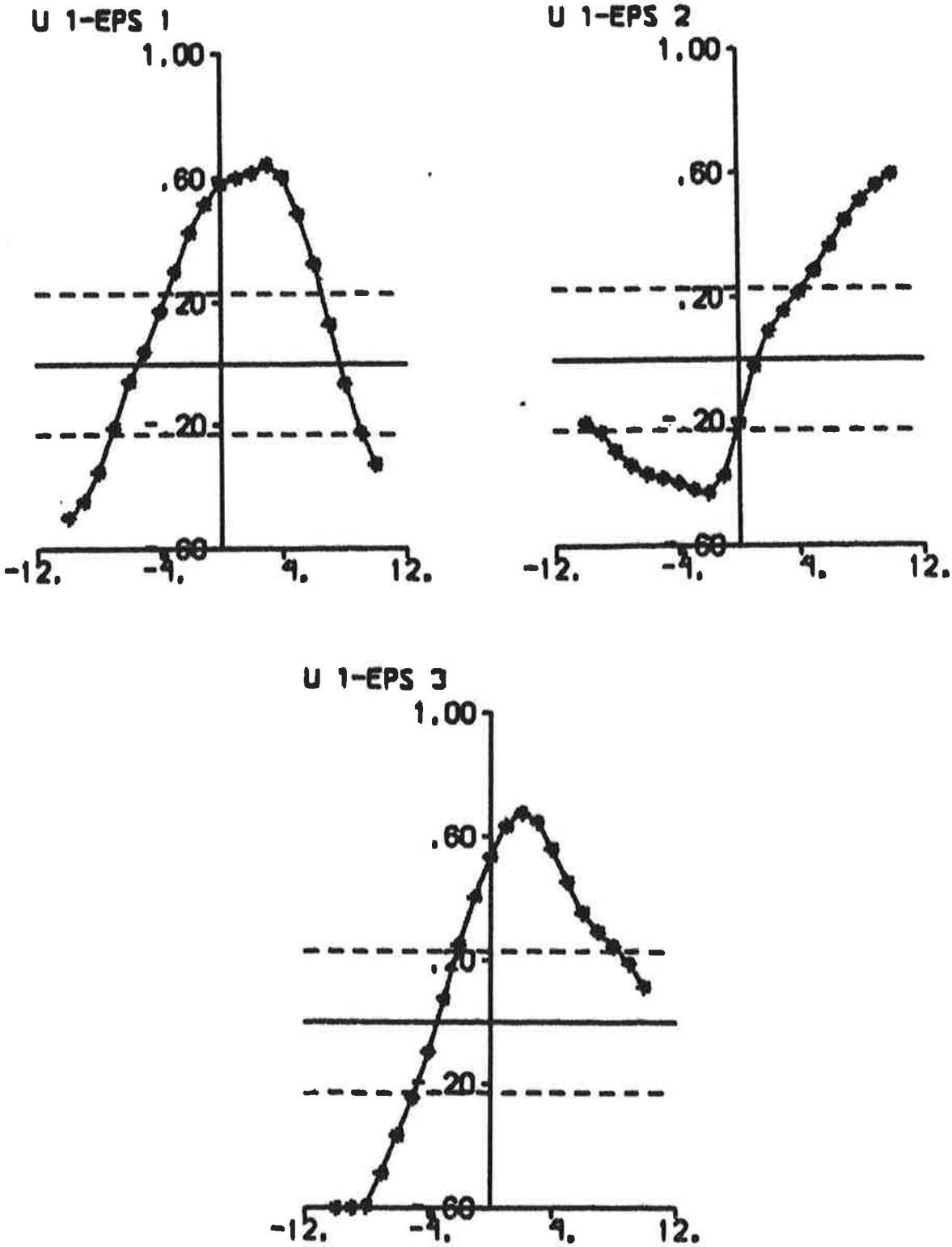

Fig. 5.7 e - Cross correlation functions between rudder input and residuals. The dashed lines are ±2σ limits.

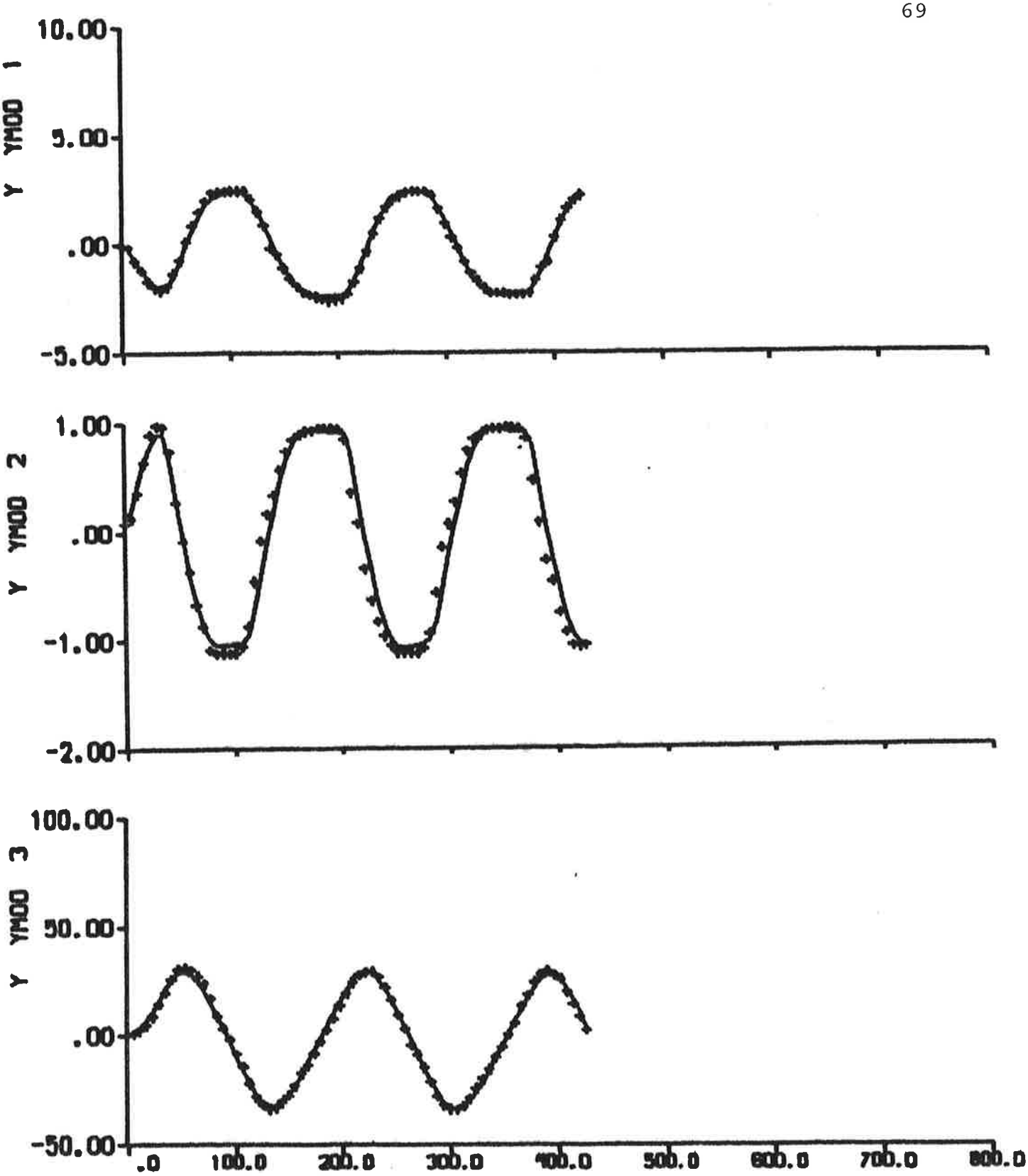

Fig. 5.8 a - Result of output error identification to data from zig-zag test 3. The continuous lines are model outputs. Cf. Fig. 2.3.

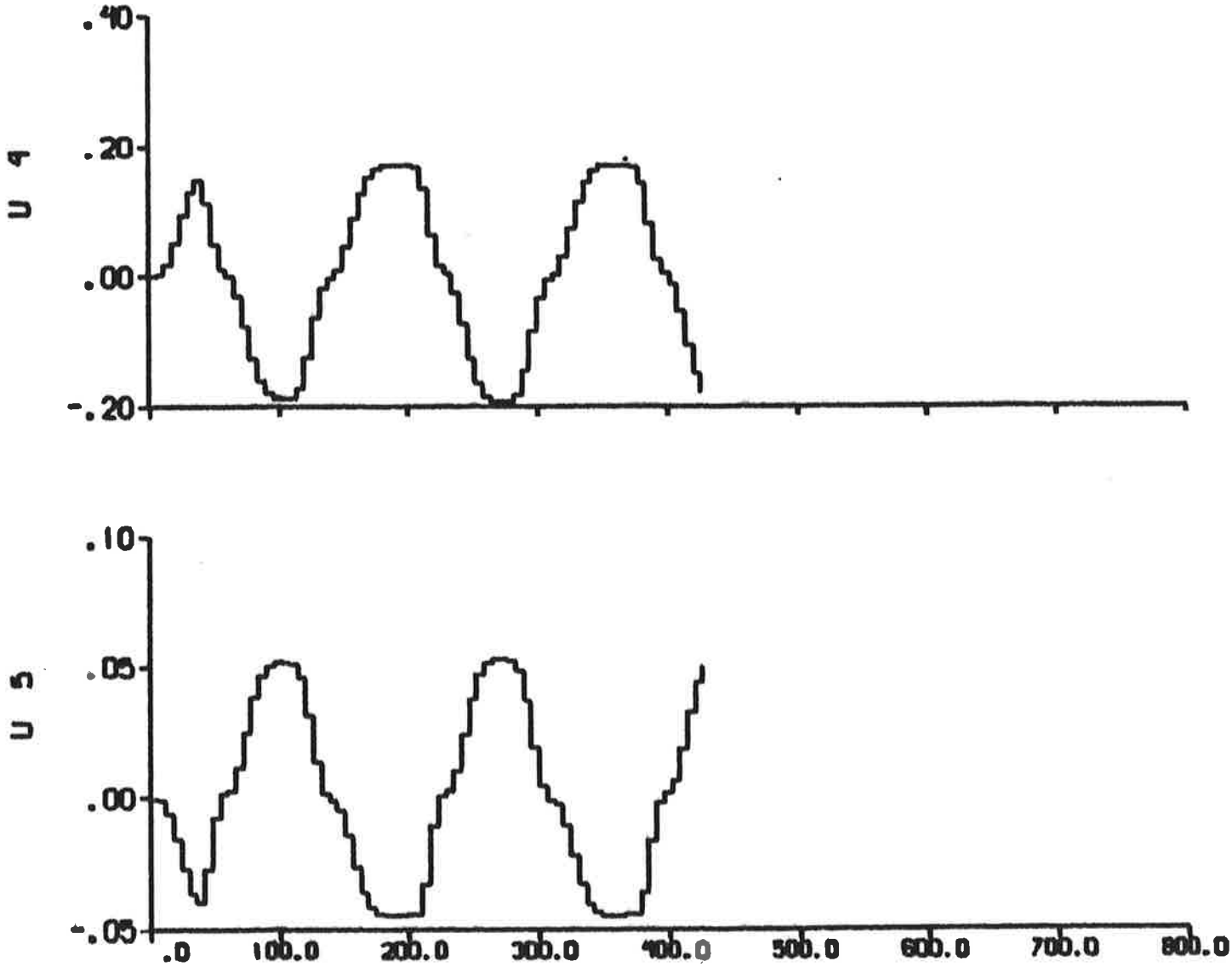

Fig. 5.8 b - Additional inputs U4 = f_Y/m' and U5 = f_N/m' describing the nonlinear contributions.

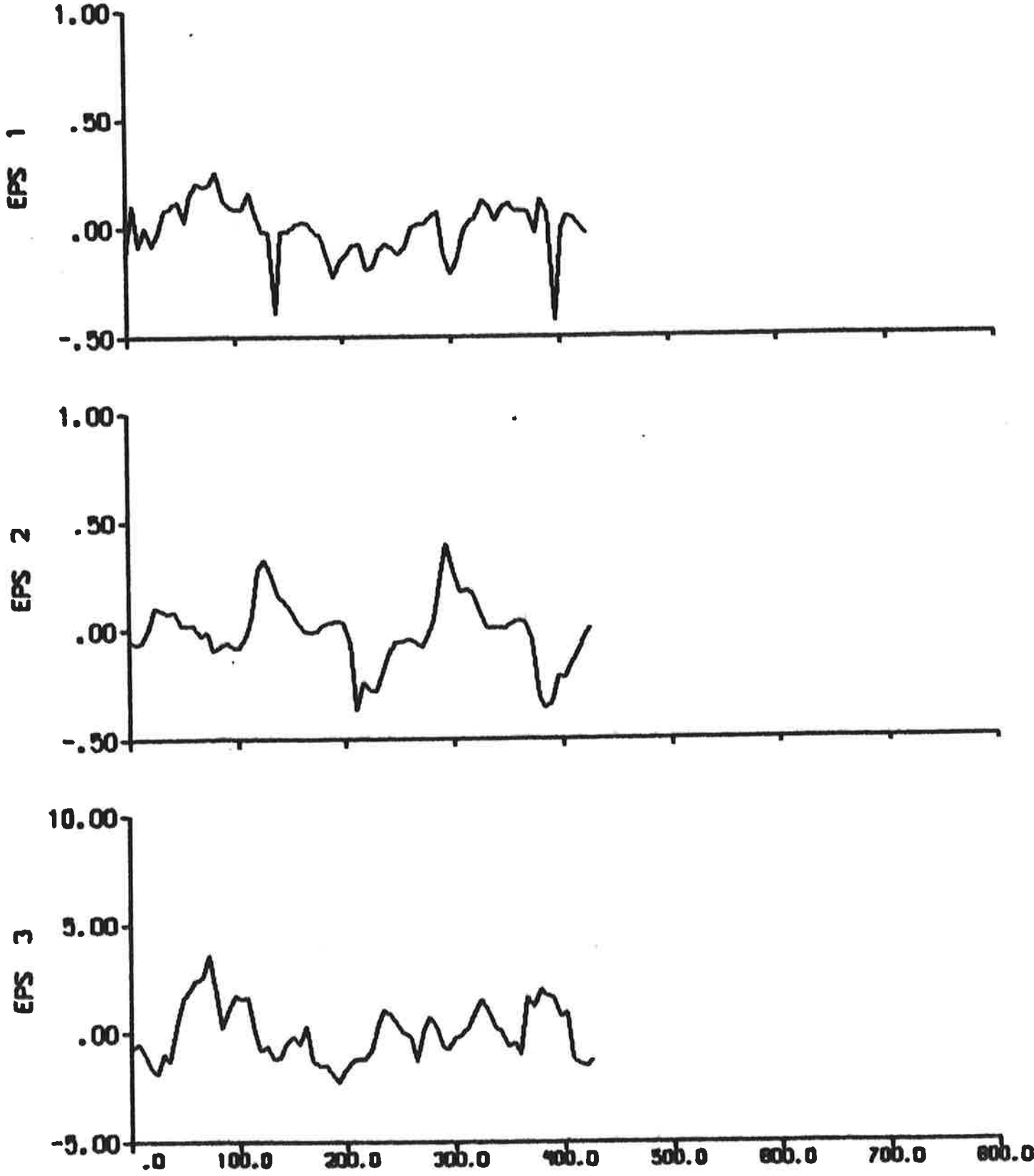

Fig. 5.8 c - Residuals.

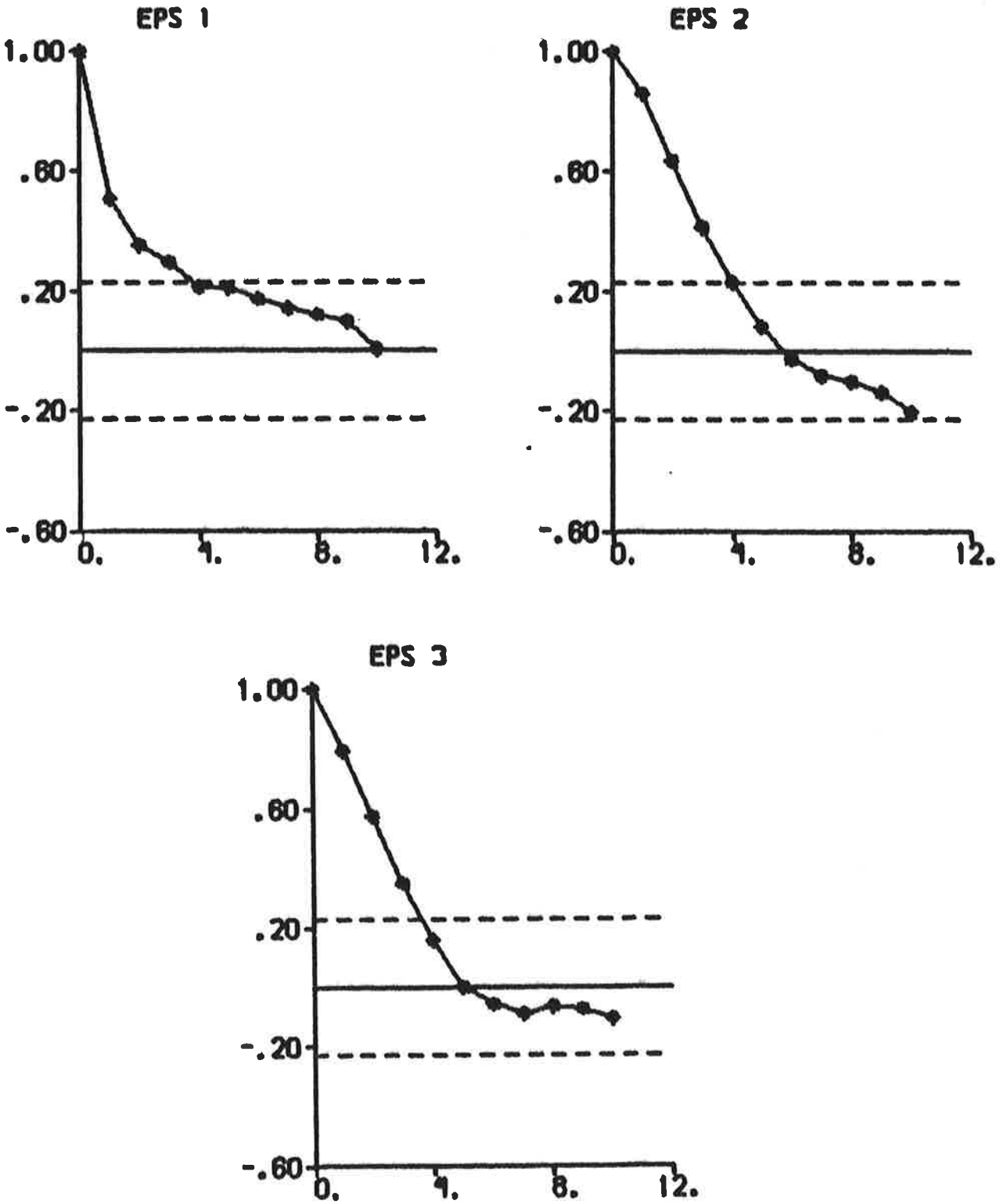

Fig. 5.8 d - Autocorrelation functions of residuals.
The dashed lines are ±2σ limits.

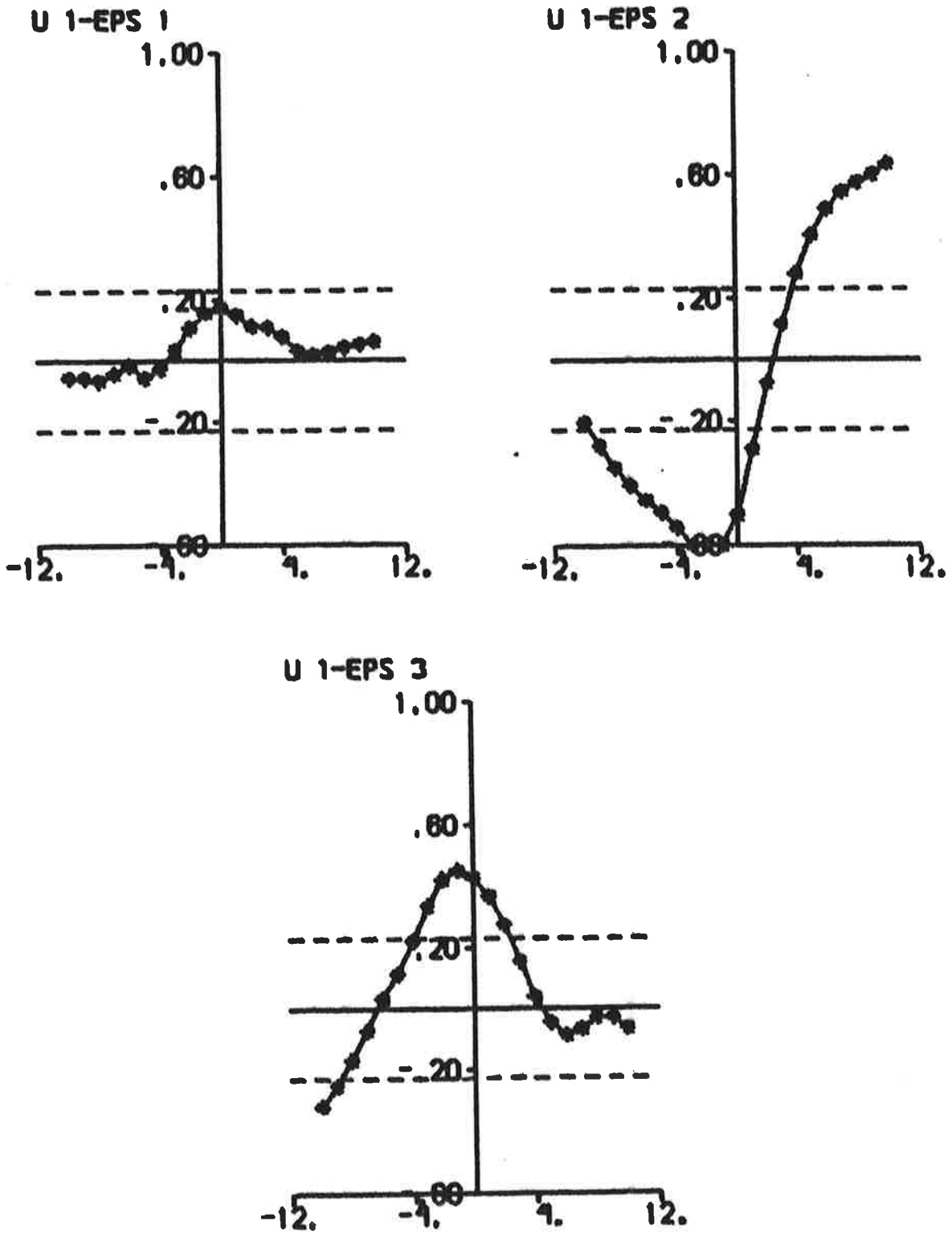

Fig. 5.8 e - Cross correlation functions between rudder input and residuals. The dashed lines are ±2σ limits.

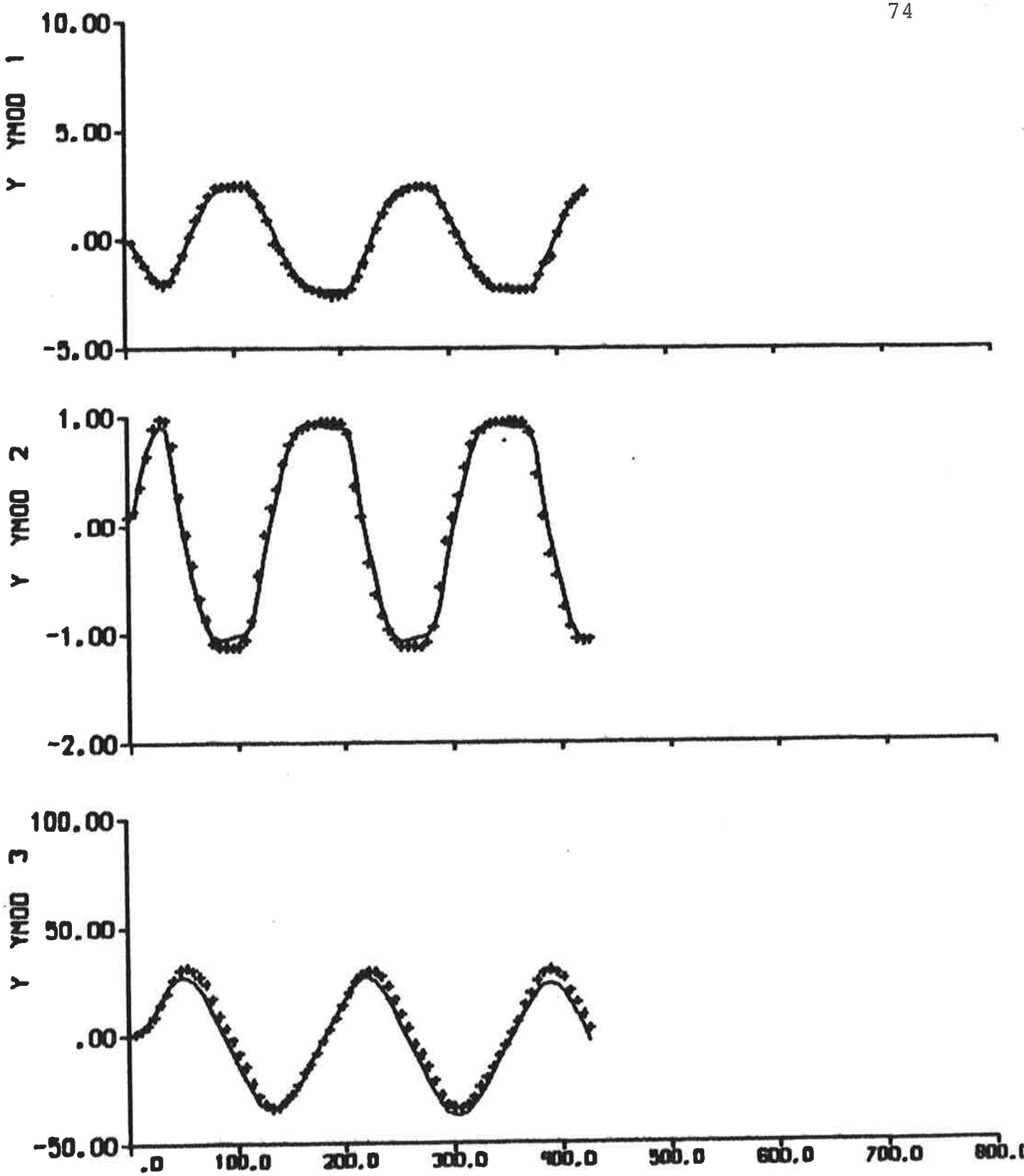

Fig. 5.9 a - Result of maximum likelihood identification to data from zig-zag test 3. The continuous lines are model outputs. Cf. Fig. 2.3.

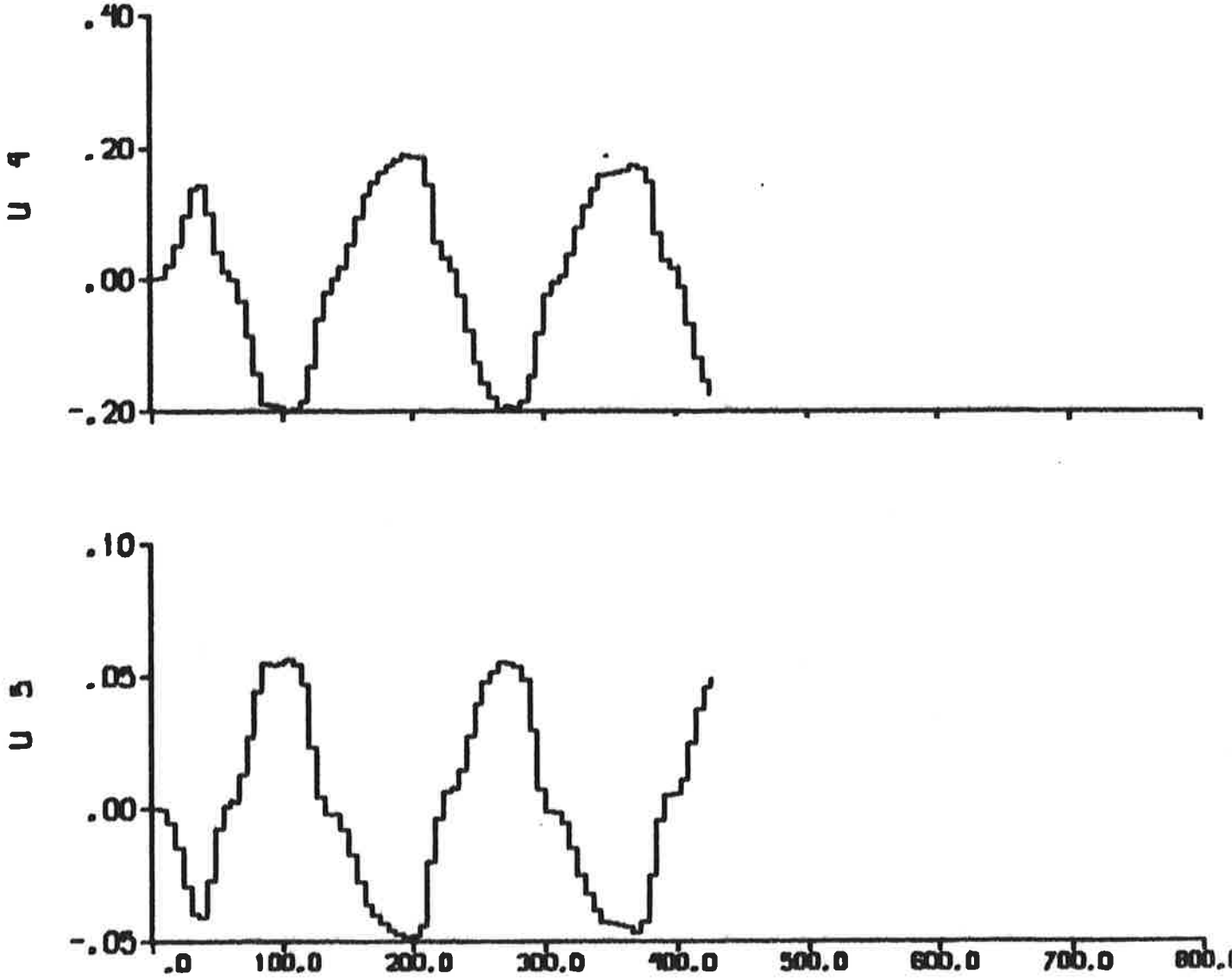

Fig. 5.9 b - Additional inputs U4 = f_Y/m' and U5 = f_N/m' describing the nonlinear contributions.

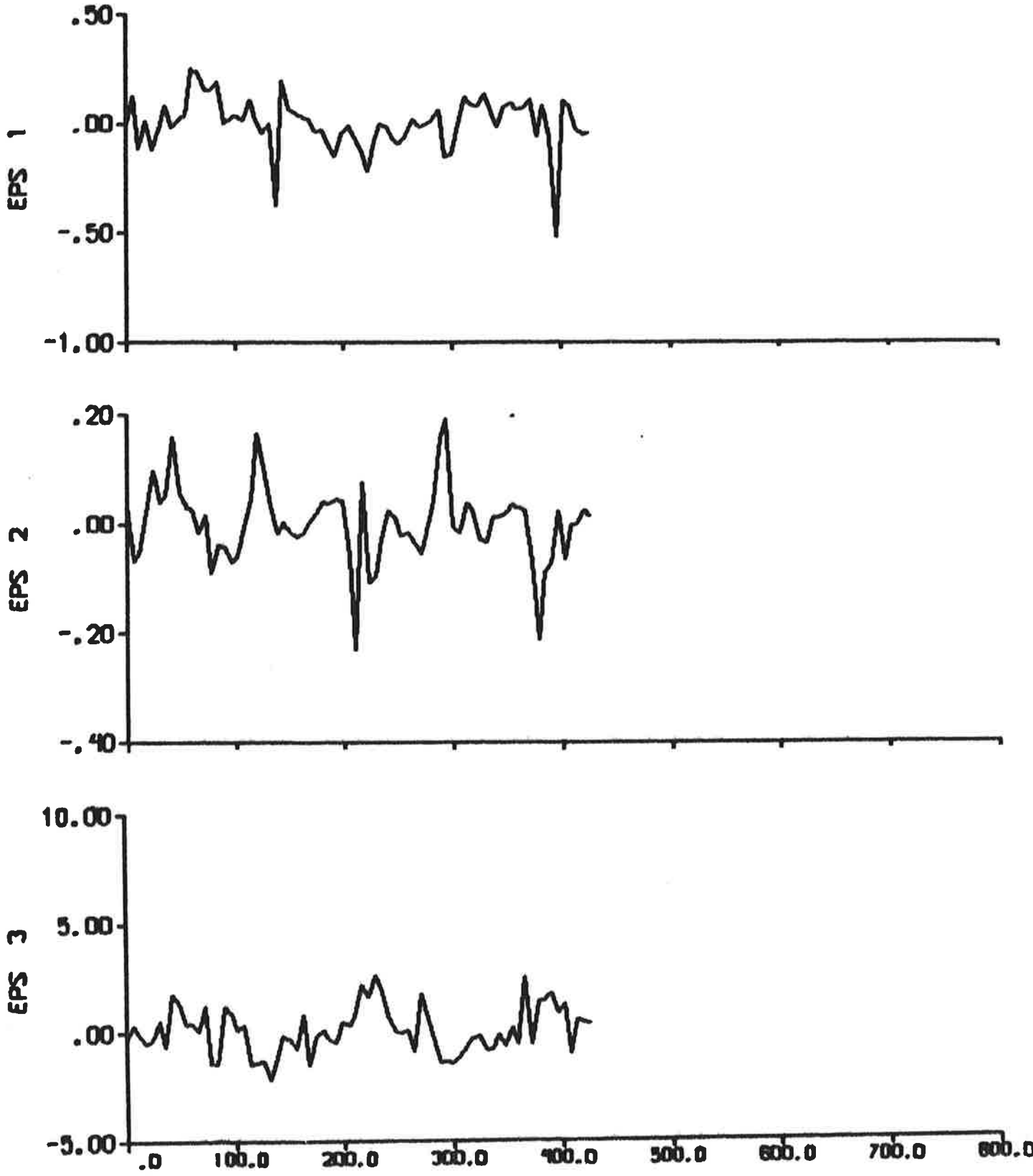

Fig. 5.9 c - Residuals.

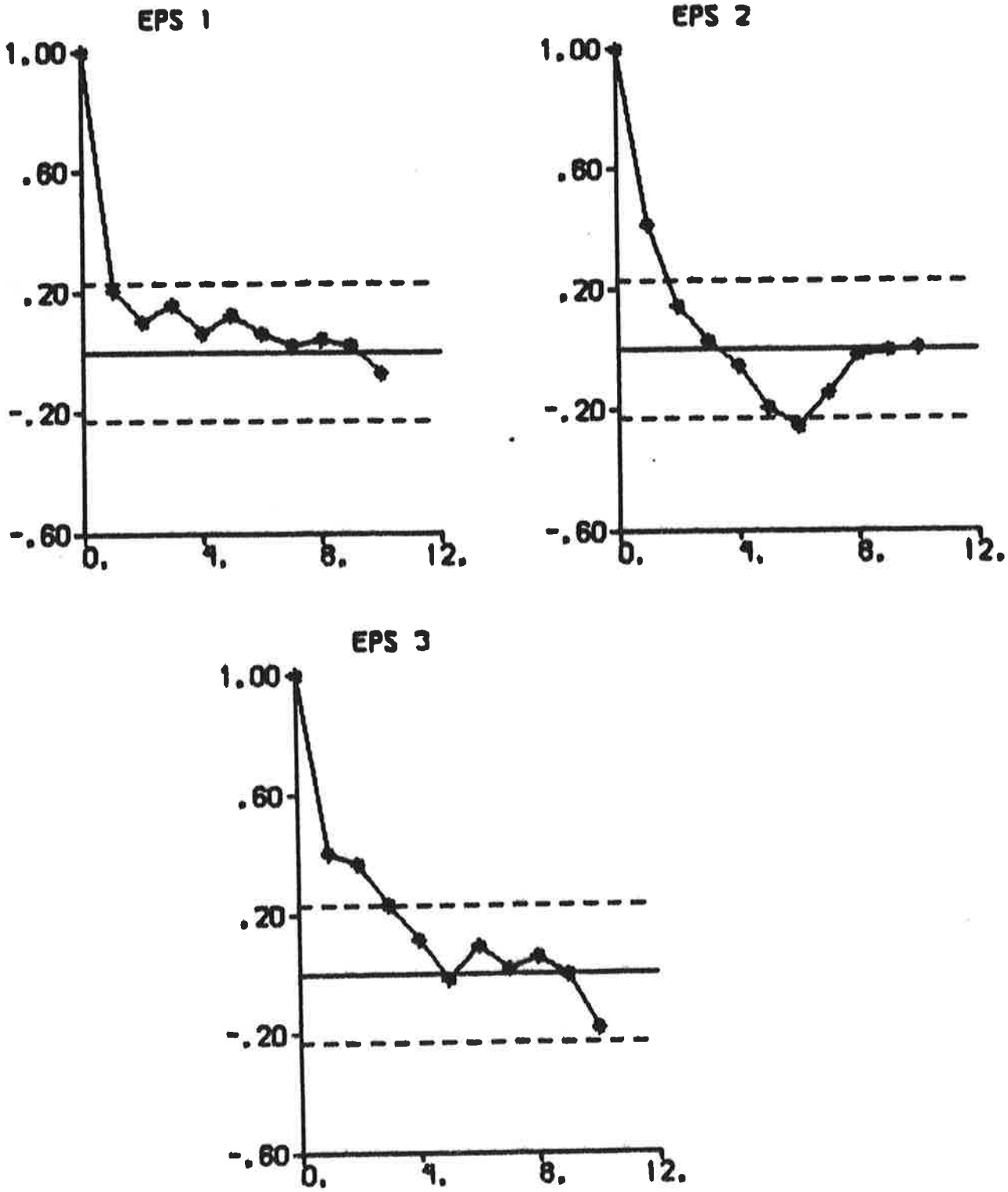

Fig. 5.9 d - Autocorrelation functions of residuals.
The dashed lines are ±2σ limits.

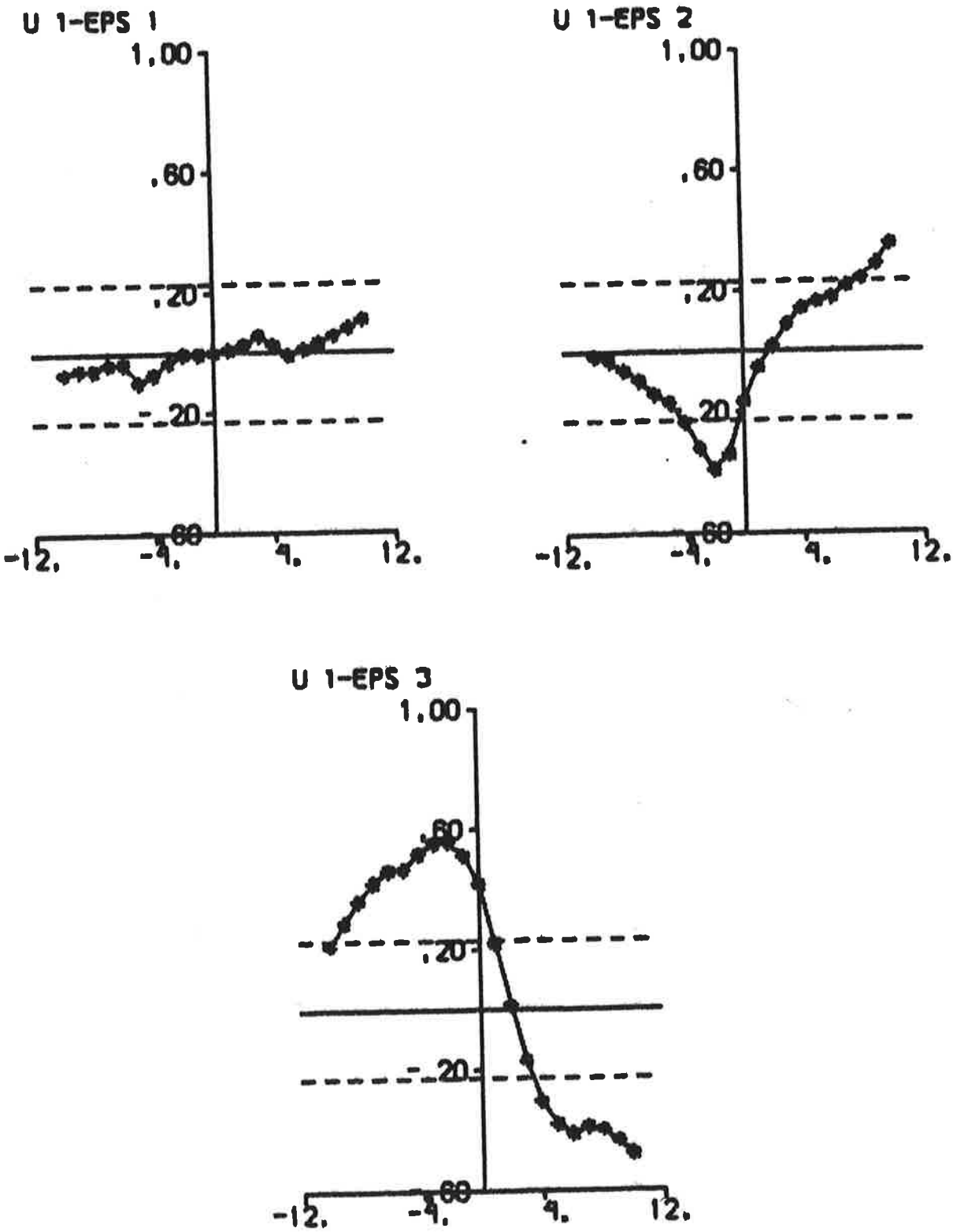

Fig. 5.9 e - Cross correlation functions between rudder input and residuals. The dashed lines are ±2σ limits.

The parameters obtained from the output error identifications and the maximum likelihood identifications are reasonable, except the ones obtained when the output error method is applied to data from zig-zag test 2. The consistency between model outputs and measurements is very good in all cases. Based on parameter estimates obtained, analysis of residuals, and Akaike´s information criterion it is concluded that the models obtained from maximum likelihood identifications are distinctly better than the ones obtained from output error identifications.

The parameters of the covariance matrices estimated with the maximum likelihood method are shown in Table 5.3. The corresponding stationary filter gains (cf. (3.4)) obtained from zig-zag test 1,2 and 3 are:

$$K = \begin{pmatrix} 4.9 \cdot 10^{-1} & -1.7 \cdot 10^{-1} & -3.0 \cdot 10^{-3} \\ -1.4 \cdot 10^{-3} & 1.2 \cdot 10^{-2} & 2.1 \cdot 10^{-4} \\ -0.8 \cdot 10^{-2} & 7.9 \cdot 10^{-2} & 1.9 \cdot 10^{-2} \end{pmatrix}$$

$$K = \begin{pmatrix} 4.0 \cdot 10^{-1} & -4.3 \cdot 10^{-1} & -6.6 \cdot 10^{-3} \\ -4.1 \cdot 10^{-3} & 1.2 \cdot 10^{-2} & 1.8 \cdot 10^{-4} \\ -2.6 \cdot 10^{-2} & 7.3 \cdot 10^{-2} & 1.9 \cdot 10^{-2} \end{pmatrix} \qquad (5.1)$$

$$K = \begin{pmatrix} 2.7 \cdot 10^{-1} & 0.3 \cdot 10^{-1} & -9.8 \cdot 10^{-3} \\ -0.6 \cdot 10^{-3} & 1.3 \cdot 10^{-2} & 1.4 \cdot 10^{-4} \\ -0.1 \cdot 10^{-2} & 8.6 \cdot 10^{-2} & 1.8 \cdot 10^{-2} \end{pmatrix}$$

As in Section 4 it is concluded that the filter gains are remarkably similar, although the covariance matrices R_1 and R_2 differ significantly between the different experiments. Cf. also (4.1).

If the parameter values obtained from the 3 maximum likelihood identifications are compared and the residuals are analysed, it is concluded that the models from zig-zag tests 1 and 3 are distinctly better than the model from zig-zag test 2.

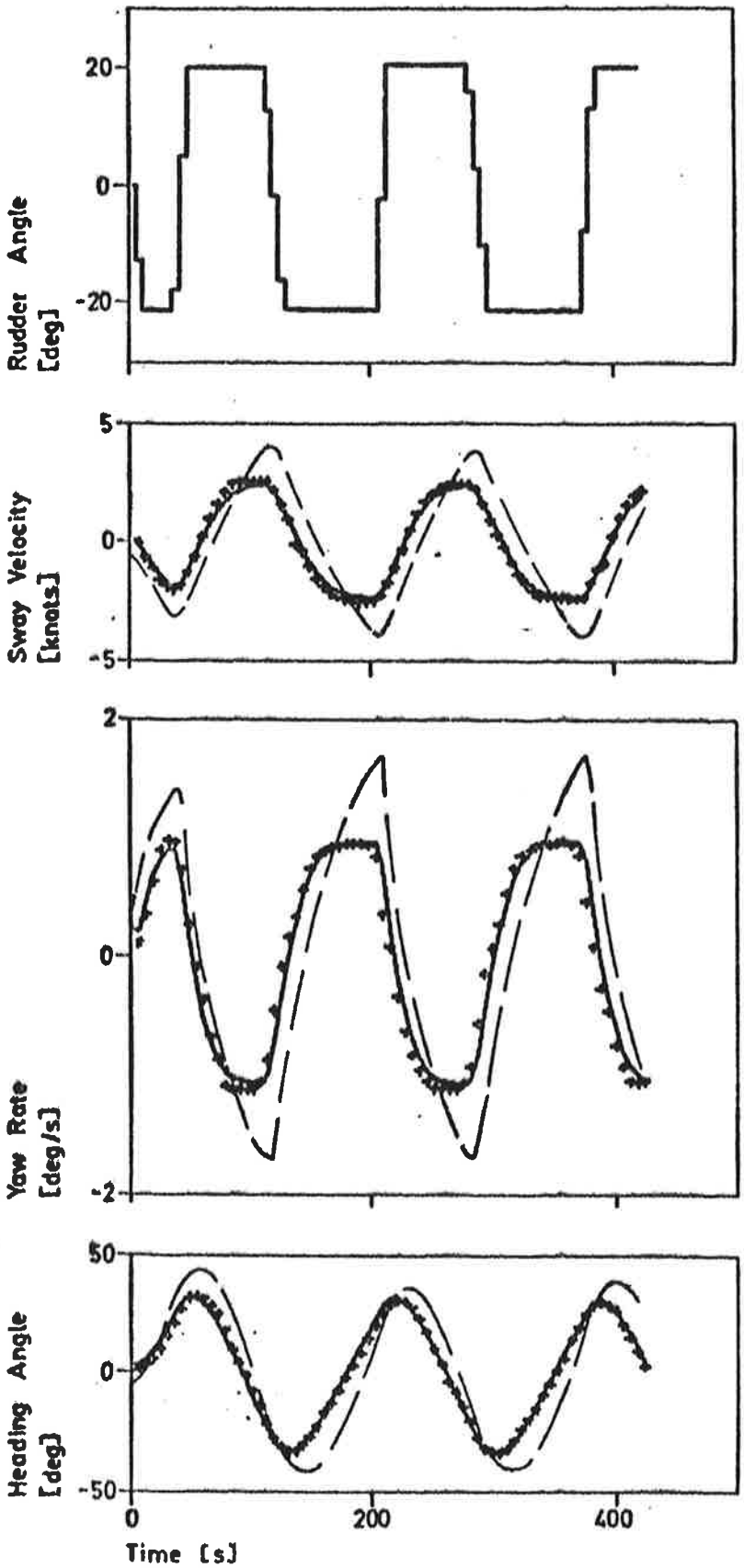

Fig. 5.10 - Results of output error identifications to data from zig-zag test 3, when the model is fixed to HyA:s linear model (the dashed lines) and when the nonlinear model is used and the linear part is fixed to HyA:s model (the continuous lines). Cf. Figs. 2.3, 4.7 and 5.7.

It is difficult to decide which of the models from zig-zag test 1 and 3 is to prefer. It is concluded from Figs. 5.3 d and 5.3 e that the residuals from experiment 1 are almost white and uncorreclated to the rudder input. The residuals from zig-zag test 3 are not as good as the ones from experiment 1 (see Figs. 5.9 d and 5.9 e). However, the value of C obtained from zig-zag test 3 (0.79) is close to the expected value 0.7, while the estimate 0.35 from zig-zag test 1 is too small. Notice that the model obtained from maximum likelihood identification to data from experiment 3 is unstable, while the model from experiment 1 and HyA:s model are stable (see Table 5.2).

The accuracy of the estimated parameter vector $\hat{\theta}$ is approximately given by

$$\text{cov}\ (\hat{\theta}) = 2V(\hat{\theta})V_{\theta\theta}^{-1}(\hat{\theta})/N \tag{5.2}$$

where V is the loss function (3.3) and $V_{\theta\theta}$ is the second derivative matrix. The following accuracies are obtained when the maximum likelihood method is applied to data from zig-zag test 1:

$$\begin{aligned}
\theta_5 &= -0.00892 \pm 0.00088 \\
\theta_6 &= -0.00817 \pm 0.00046 \\
\theta_7 &= -0.00075 \pm 0.00010 \\
\theta_8 &= -0.00100 \pm 0.00008 \\
\theta_{11} &= 0.00240 \pm 0.00009 \\
\theta_{13} &= (1.9 \pm 763.4) \cdot 10^{-7} \\
\theta_{14} &= (-4.7 \pm 0.6) \cdot 10^{-5} \\
\theta_{18} &= (4.7 \pm 17.4) \cdot 10^{-5} \\
\theta_{19} &= (2.5 \pm 2.2) \cdot 10^{-6} \\
\theta_{20} &= -1.0 \pm 0.4 \\
\theta_{21} &= (5.7 \pm 9467.0) \cdot 10^{-9} \\
\theta_{23} &= (1.1 \pm 1.1) \cdot 10^{-3} \\
\theta_{25} &= -0.48 \pm 0.07 \\
\theta_{26} &= 0.019 \pm 0.017 \\
\theta_{27} &= 0.51 \pm 0.53 \\
\theta_{34} &= 0.82 \pm 0.09 \\
\theta_{35} &= 0.35 \pm 0.04
\end{aligned} \tag{5.3}$$

The hydrodynamic derivatives $\theta_5 - \theta_8$, θ_{11}, the bias θ_{14}, the initial state θ_{25}, the parameter θ_{34} for the time delay, and the effective cross-flow drag coefficient θ_{35} are thus estimated with acceptable accuracies, while the bias θ_{13}, the parameters of the covariance matrices $\theta_{18} - \theta_{21}$, θ_{23}, and the initial states θ_{26} and θ_{27} are estimated very inaccurately.

It is illustrated in Fig. 5.11, where Figs. 2.3, 4.9 and 5.9 are put together, that the outputs from both the linear and nonlinear model are very close to the measurements, when the maximum likelihood method is applied. However, the parameters obtained when the linear model is used are far away from the expected values (see Table 4.1), while the nonlinear model gives quite reasonable parameter estimates (see Table 5.1).

The speed of the ship is changed during a $20^{\circ}/20^{\circ}$ zig-zag test. The approach speed of test 3 was 20 knots, but the speed was decreased to approximately 16.5 knots during the experiment. There were, of course, also fluctuations about the average speed. To investigate if it is possible to improve the results by using the correct value of the ship speed V at each sampling event instead of the mean value, the output error method is applied to data from zig-zag test 3 when the correct values of V are taken from Morse and Price (1961). The estimated parameters do not differ much from the values obtained when a constant ship speed is used. It is thus concluded that a constant ship speed V may be used when data from a $20^{\circ}/20^{\circ}$ zig-zag test are analysed.

The models obtained from maximum likelihood identifications to data from the 3 zig-zag tests are now further analysed. The performance of the models is investigated by fitting the bias parameters θ_{13} and θ_{14}, the initial states θ_{25}, θ_{26} and θ_{27}, and the time delay T_D to data from the 3 experiments by use of the output error method. The hydrodynamic derivatives $\theta_5 - \theta_8$, θ_{11}, and the effective cross-flow drag

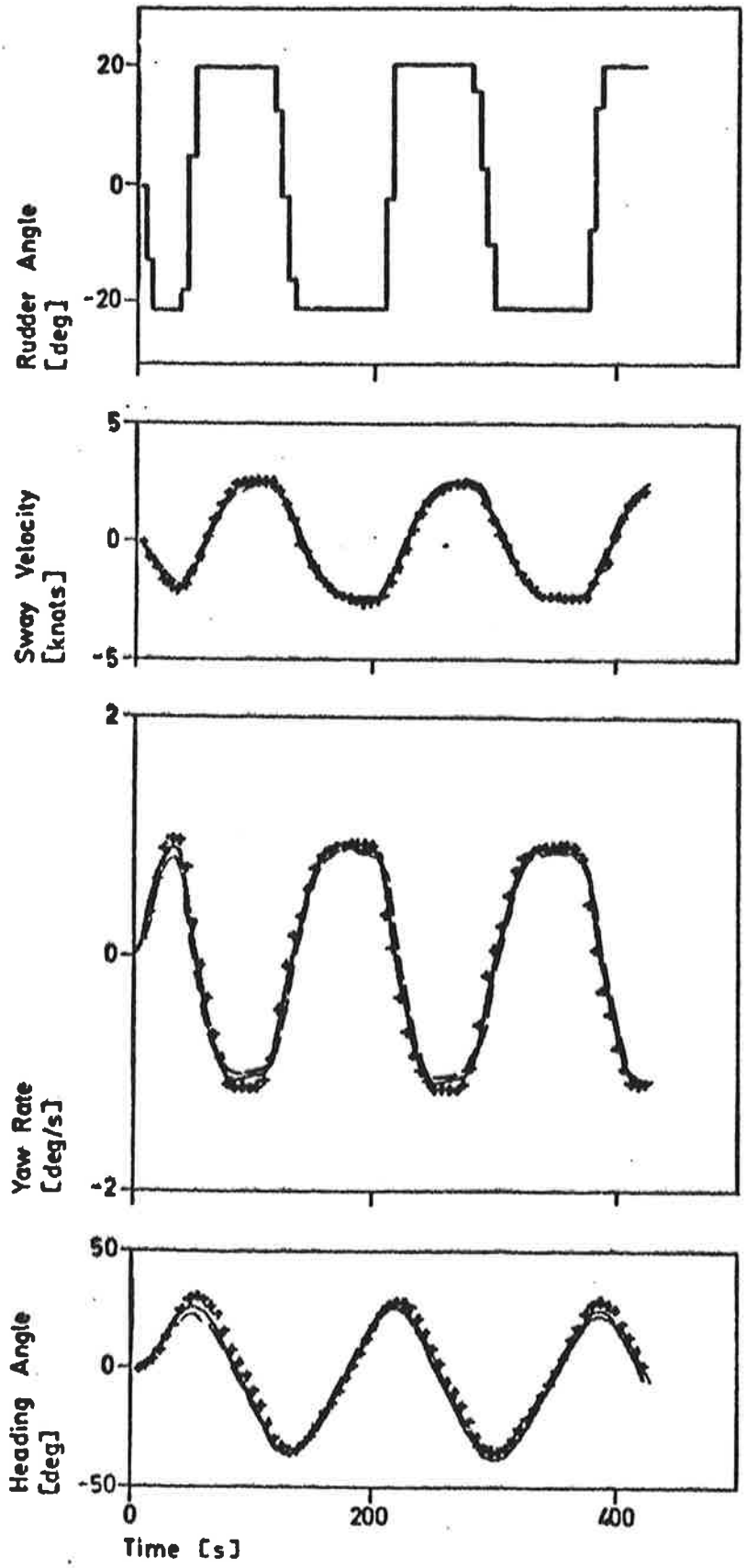

Fig. 5.11 - Results of maximum likelihood identifications to data from zig-zag test 3, when the linear model (the dashed lines) and the nonlinear model (the continuous lines) are used. Cf. Figs. 2.3, 4.9 and 5.9.

coefficient θ_{35} are then fixed. The results are summarized in Table 5.4 and the plots are shown in Figs. 5.12 - 5.20. The outputs from the 3 models are close to the measurements, and it is difficult to decide which of the models that is the best one. However, the model obtained from maximum likelihood identification to data from zig-zag test 3 is possibly to prefer, if the results are carefully considered.

Finally it is important to point out that the normalized hydrodynamic derivatives are not quite independent of the ship speed. The dependence has been investigated for a 190 000 tdw tanker by scale model tests a HyA (see Smitt and Chislett, 1973). It is thus not expected to obtain quite the same values of the hydrodynamic derivatives from the 3 different zig-zag tests, because the experiments were performed at different speeds.

		Zig-zag test 1			Zig-zag test 2			Zig-zag test 3		
		Model from test 1	Model from test 2	Model from test 3	Model from test 1	Model from test 2	Model from test 3	Model from test 1	Model from test 2	Model from test 3
Figure		5.12	5.13	5.14	5.15	5.16	5.17	5.18	5.19	5.20
Number of samples N		101	101	101	82	82	82	72	72	72
Number of estimated parameters ν		6	6	6	6	6	6	6	6	6
Loss function V		1.309	67.057	19.906	42.605	3.638	32.811	146.176	69.516	3.857
Akaike´s information criterion AIC		-33	364	242	295	93	274	368	315	106
Hydrodynamic derivatives ('prime' system, mass unit $\rho L^3/2$)	Y_v' (θ_5)	-0.00892*	-0.04886*	-0.01487*	-0.00892*	-0.04886*	-0.01487*	-0.00892*	-0.04886*	-0.01487*
	$Y_r'-m'$ (θ_6)	-0.00817*	-0.02090*	-0.00875*	-0.00817*	-0.02090*	-0.00875*	-0.00817*	-0.02090*	-0.00875*
	N_v' (θ_7)	-0.00075*	-0.00010*	-0.00123*	-0.00075*	-0.00010*	-0.00123*	-0.00075*	-0.00010*	-0.00123*
	$N_r'-m'x_G'$ (θ_8)	-0.00100*	-0.00022*	-0.00062*	-0.00100*	-0.00022*	-0.00062*	-0.00100*	-0.00022*	-0.00062*
	Y_δ' (θ_{11})	0.00240*	0.00169*	0.00178*	0.00240*	0.00169*	0.00178*	0.00240*	0.00169*	0.00178*
	N_δ' $(-\theta_{11}\theta_{12})$	-0.00115*	-0.00081*	-0.00085*	-0.00115*	-0.00081*	-0.00085*	-0.00115*	-0.00081*	-0.00085*
Cross-flow drag	C (θ_{35})	0.35*	0.46*	0.79*	0.35*	0.46*	0.79*	0.35*	0.46*	0.79*
Biases	θ_{13} [-]	$1.4\cdot10^{-4}$	$8.1\cdot10^{-4}$	$-1.1\cdot10^{-4}$	$-9.3\cdot10^{-6}$	$4.4\cdot10^{-5}$	$3.8\cdot10^{-5}$	$8.0\cdot10^{-5}$	$-3.4\cdot10^{-4}$	$-6.1\cdot10^{-5}$
	θ_{14} [-]	$-4.4\cdot10^{-5}$	$-4.6\cdot10^{-5}$	$-7.1\cdot10^{-5}$	$-4.6\cdot10^{-5}$	$-3.4\cdot10^{-5}$	$-3.9\cdot10^{-5}$	$-4.2\cdot10^{-5}$	$-2.4\cdot10^{-5}$	$-3.6\cdot10^{-5}$
Initial state	θ_{25} [knots]	-0.78	-0.30	-1.58	0.73	-0.08	-0.18	-0.79	0.17	0.01
	θ_{26} [deg/s]	0.024	0.079	0.133	0.522	0.275	0.232	0.133	0.011	0.124
	θ_{27} [deg]	1.80	-0.71	2.70	-0.32	0.19	1.32	1.72	2.45	1.00
Time delay	T_D $(T-T\lvert\sin\theta_{34}\rvert)$ [s]	1.0	0.0	0.1	1.9	0.0	0.0	2.5	3.1	2.6

* = fixed value

Table 5.4 - Parameter values from output error identifications of nonlinear models. The models are fixed to the models obtained from maximum likelihood identifications to data from zig-zag test 1,2 and 3 (cf. Table 5.1). The corresponding hydrodynamic derivatives in the 'bis' system are obtained by dividing with m' = 0.00798.

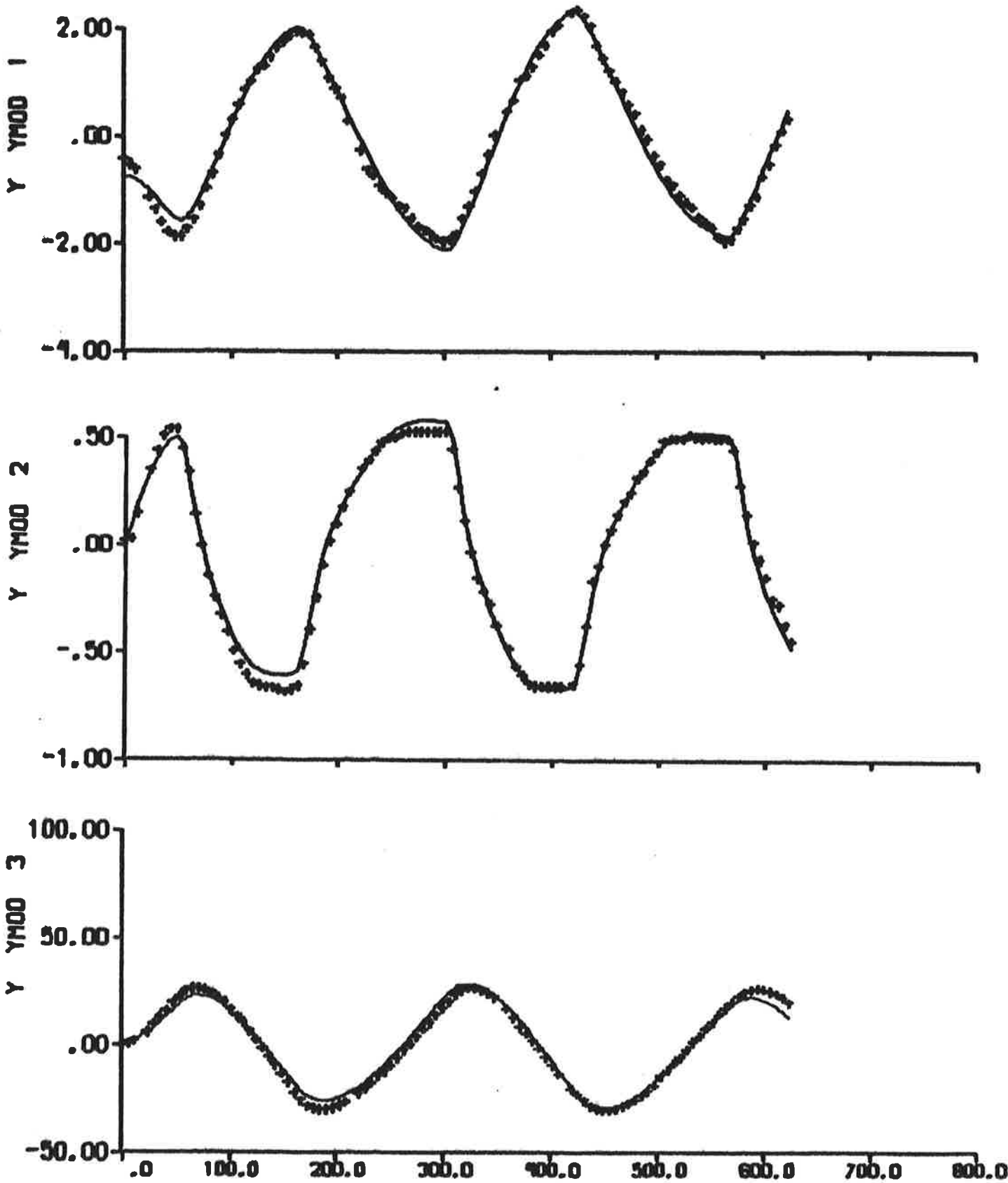

Fig. 5.12 - Result of output error identification to data from zig-zag test 1, when the model is fixed to the model obtained from maximum likelihood identification to data from zig-zag test 1. The continuous lines are model outputs. Cf. Fig. 2.1.

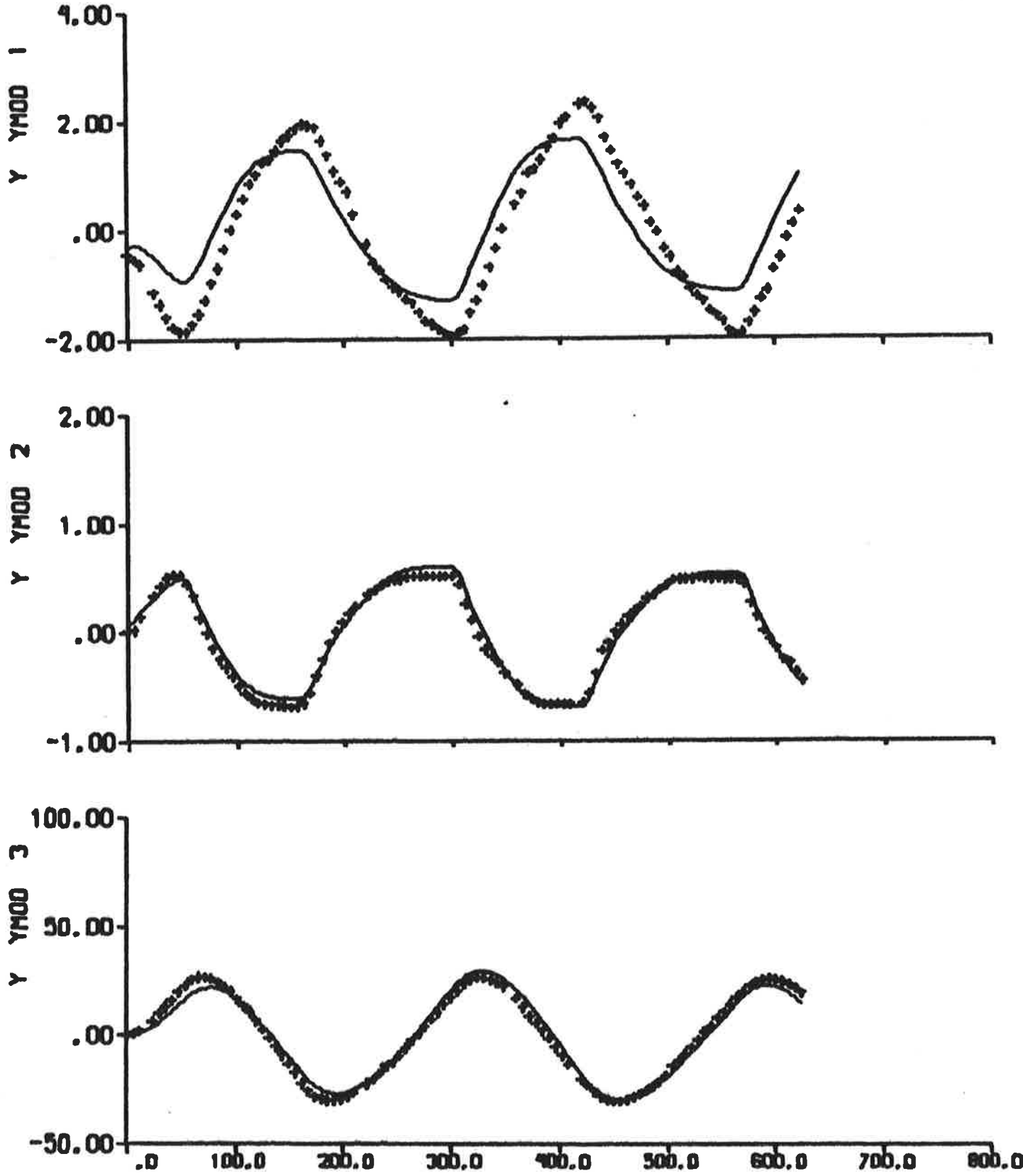

Fig. 5.13 - Result of output error identification to data from zig-zag test 1, when the model is fixed to the model obtained from maximum likelihood identification to data from zig-zag test 2. The continuous lines are model outputs. Cf. Fig. 2.1.

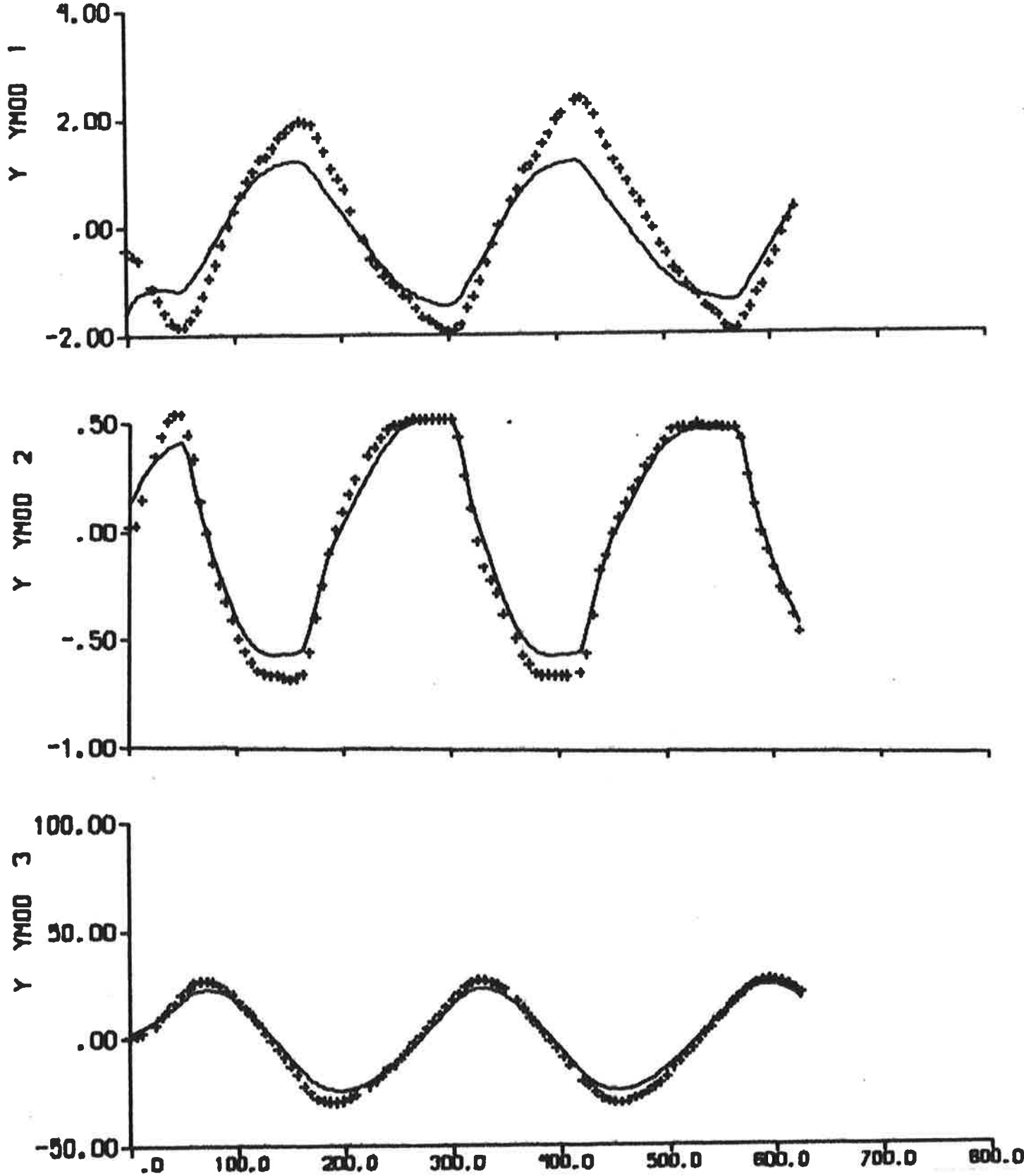

Fig. 5.14 - Result of output error identification to data from zig-zag test 1, when the model is fixed to the model obtained from maximum likelihood identification to data from zig-zag test 3. The continuous lines are model outputs. Cf. Fig. 2.1.

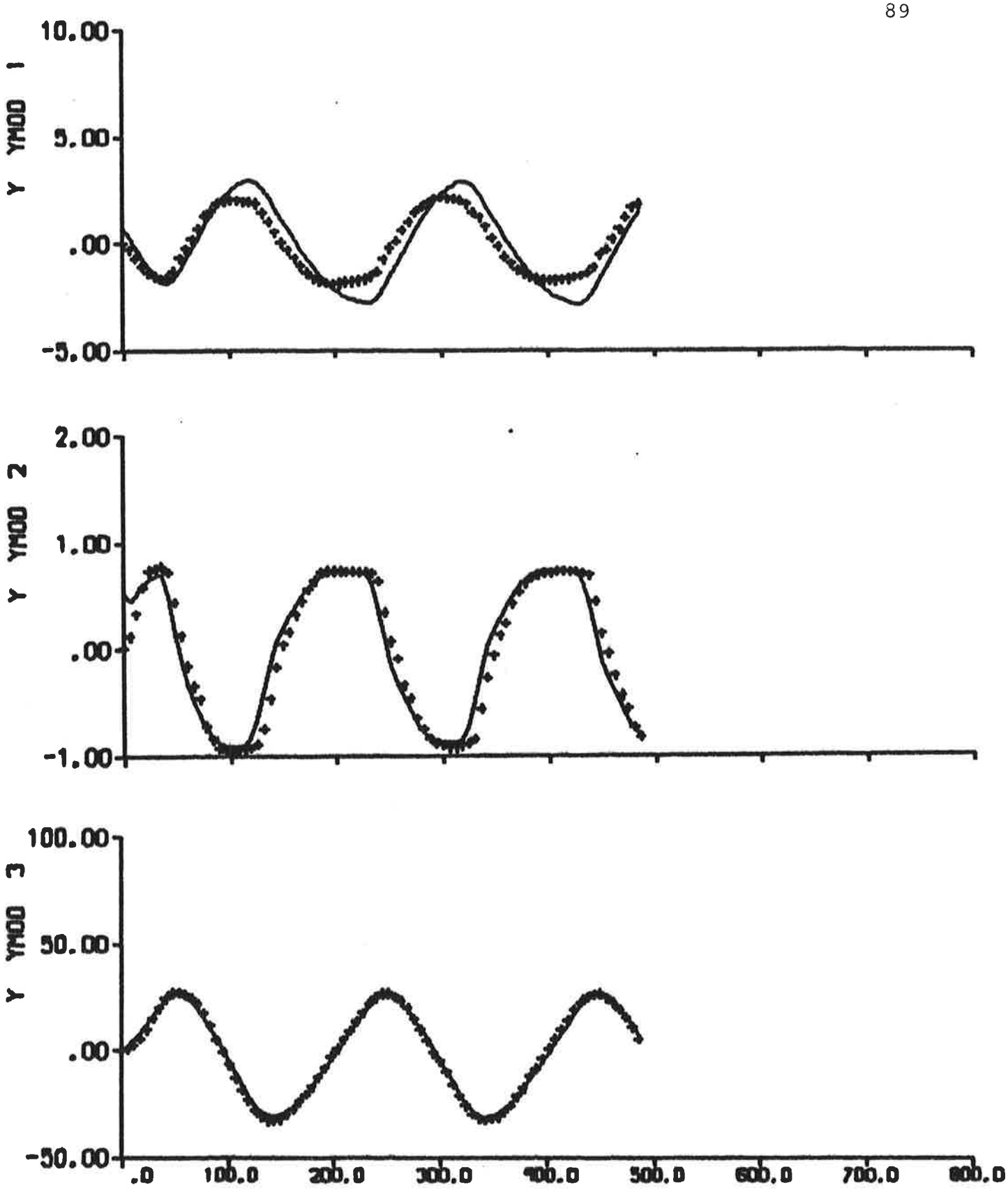

Fig. 5.15 - Result of output error identification to data from zig-zag test 2, when the model is fixed to the model obtained from maximum likelihood identification to data from zig-zag test 1. The continuous lines are model outputs. Cf. Fig. 2.2.

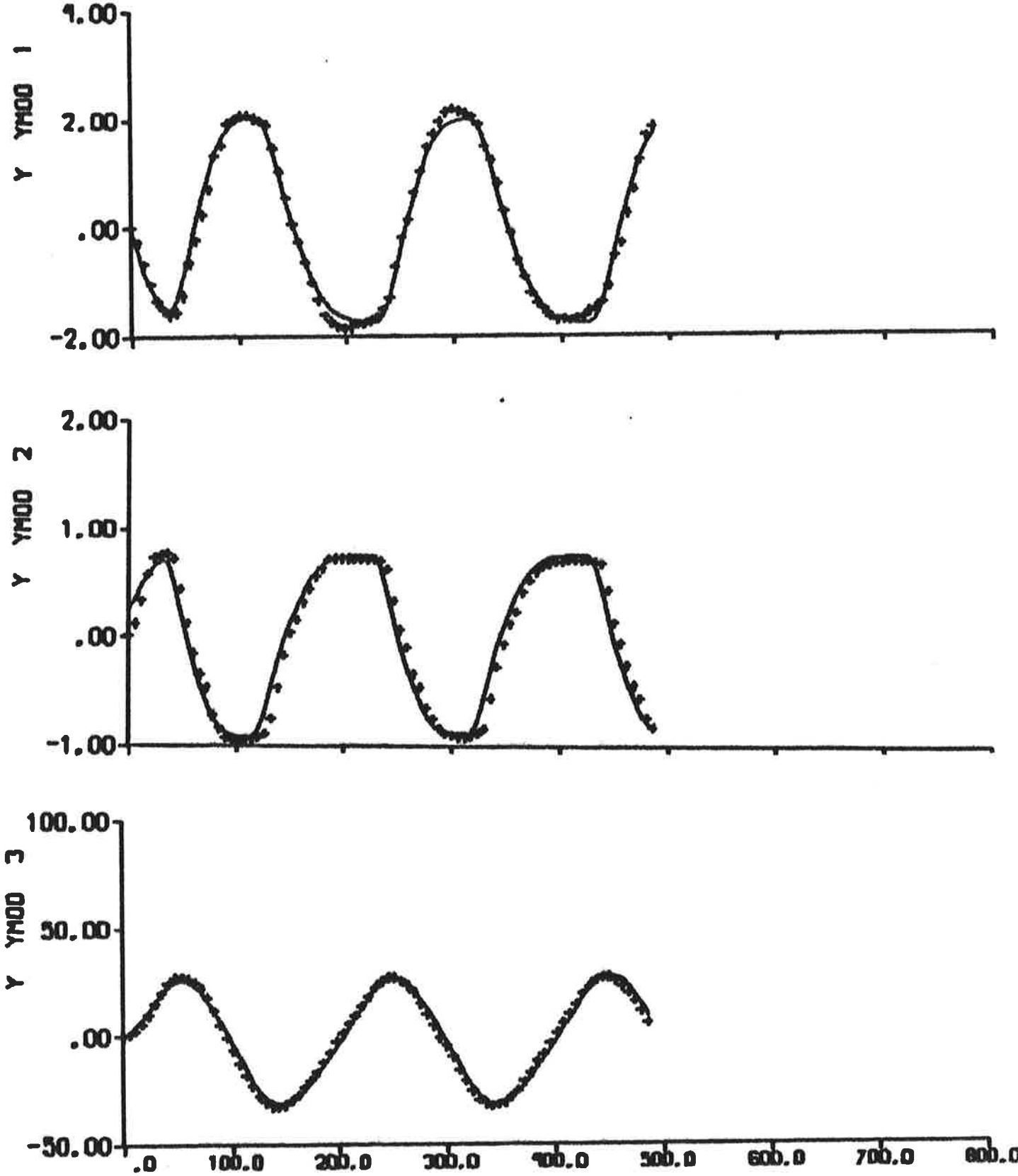

Fig. 5.16 - Result of output error identification to data from zig-zag test 2, when the model is fixed to the model obtained from maximum likelihood identification to data from zig-zag test 2. The continuous lines are model outputs. Cf. Fig. 2.2.

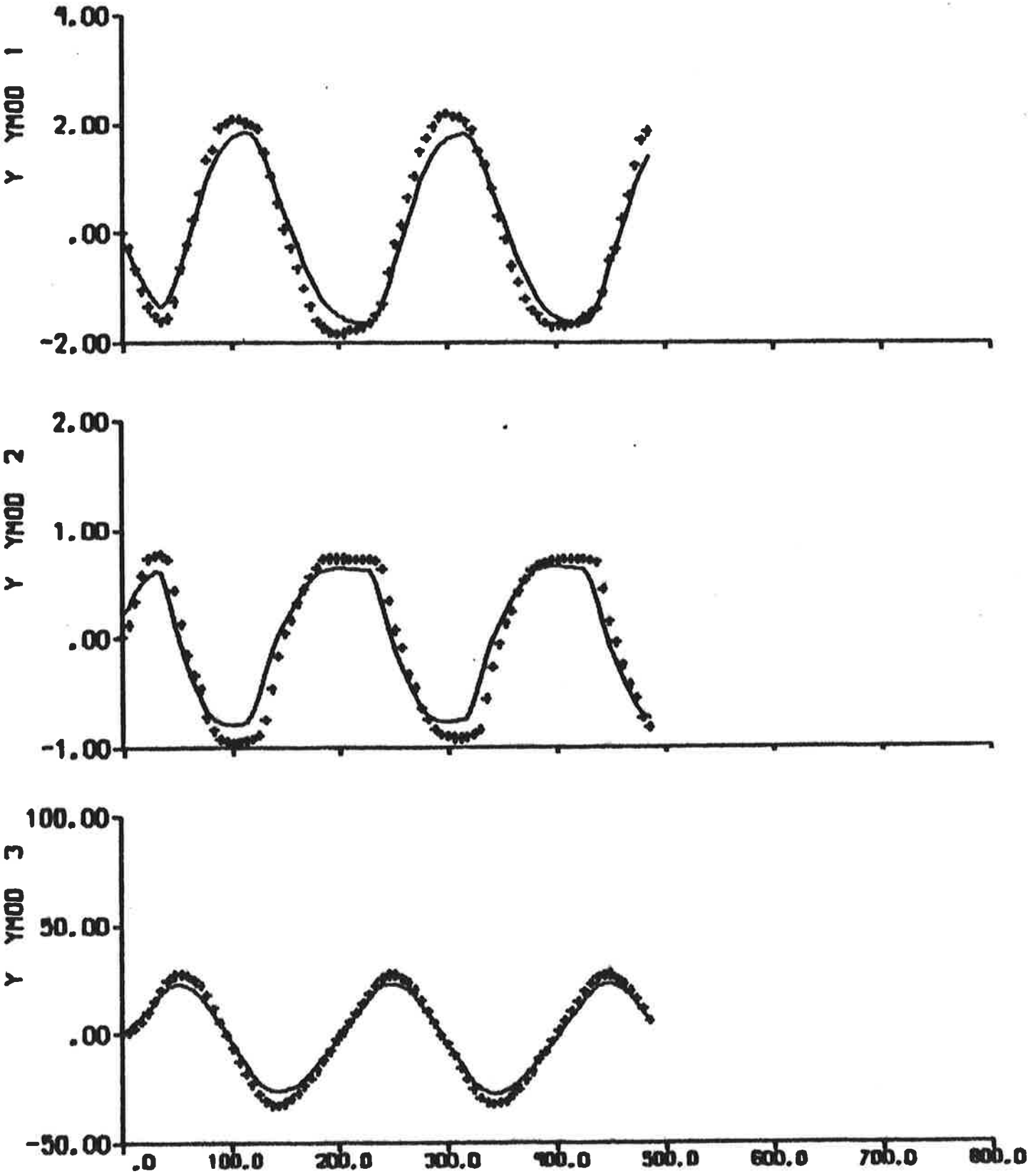

Fig. 5.17 - Result of output error identification to data from zig-zag test 2, when the model is fixed to the model obtained from maximum likelihood identification to data from zig-zag test 3. The continuous lines are model outputs. Cf. Fig. 2.2.

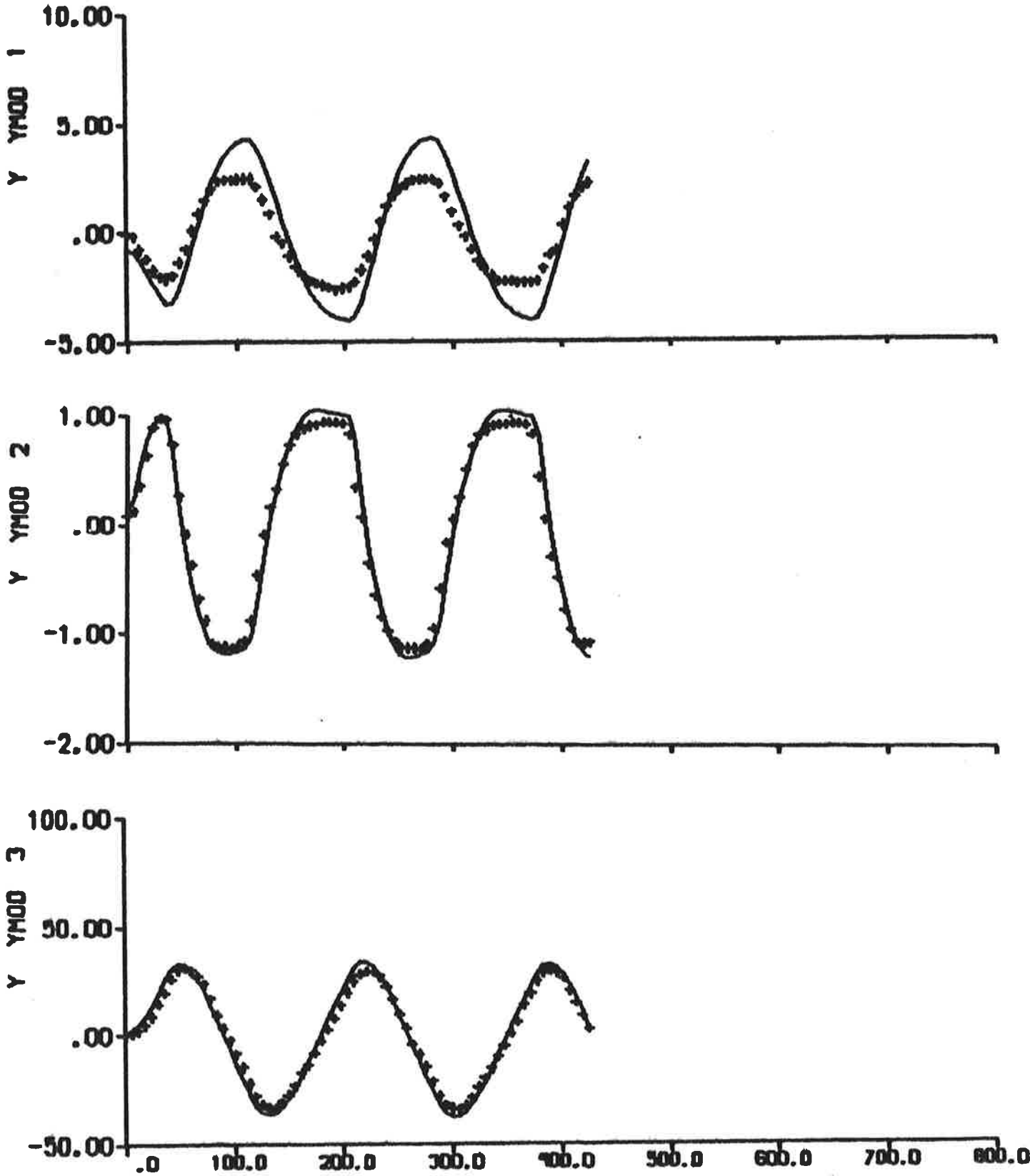

Fig. 5.18 - Result of output error identification to data from zig-zag test 3, when the model is fixed to the model obtained from maximum likelihood identification to data from zig-zag test 1. The continuous lines are model outputs. Cf. Fig. 2.3.

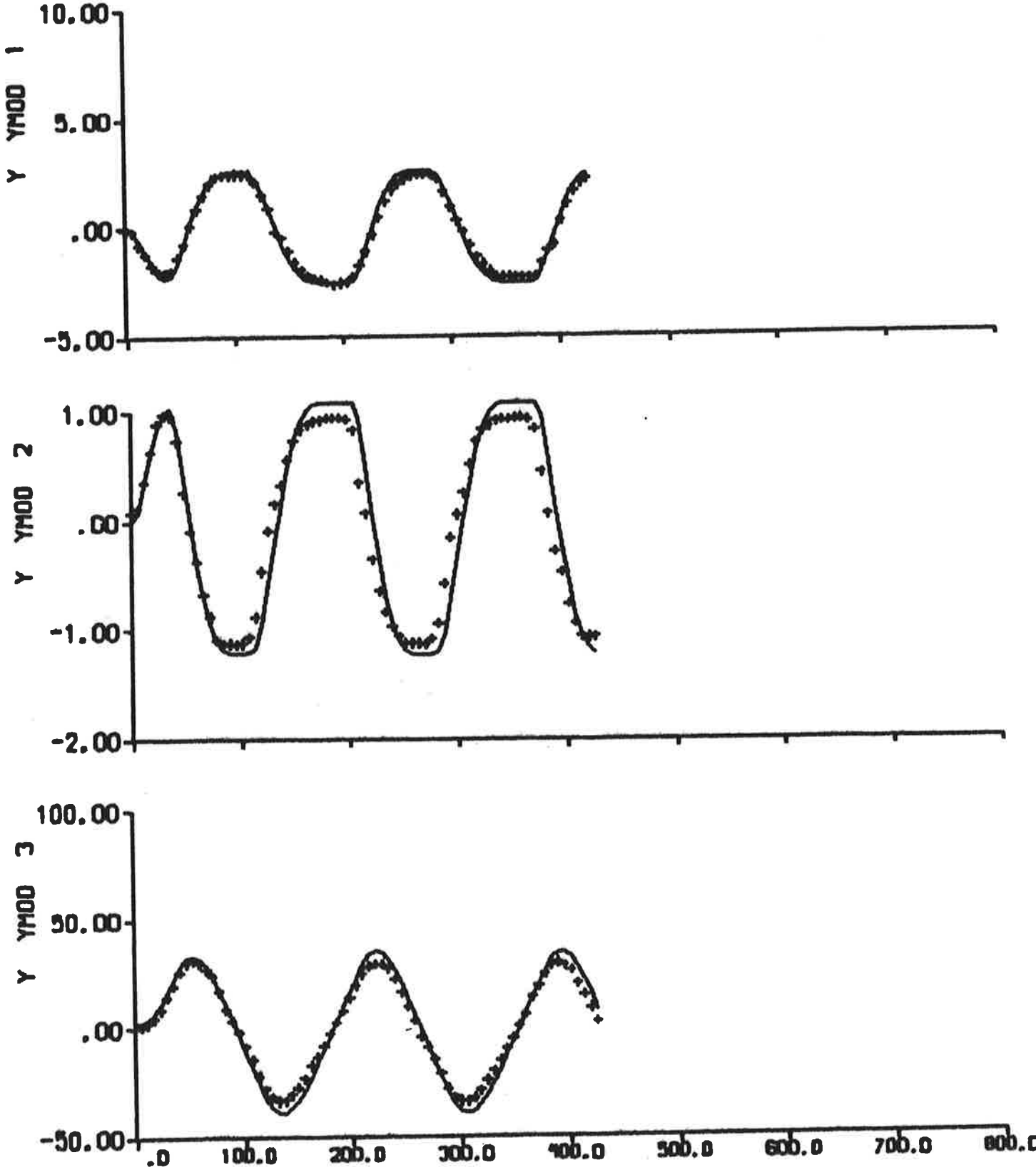

Fig. 5.19 - Result of output error identification to data from zig-zag test 3, when the model is fixed to the model obtained from maximum likelihood identification to data from zig-zag test 2. The continuous lines are model outputs. Cf. Fig. 2.3.

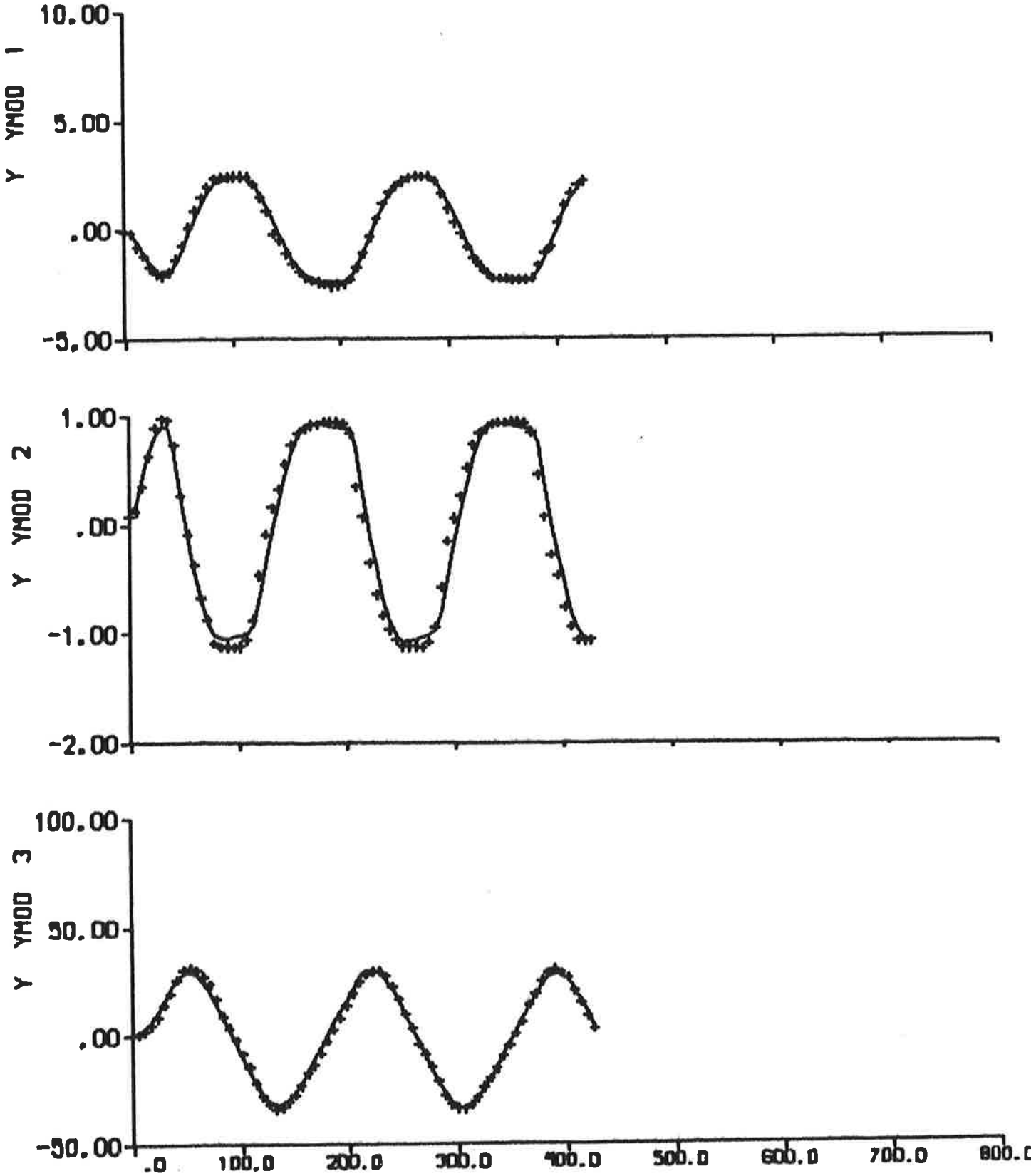

Fig. 5.20 - Result of output error identification to data from zig-zag test 3, when the model is fixed to the model obtained from maximum likelihood identification to data from zig-zag test 3. The continuous lines are model outputs. Cf. Fig. 2.3.

6. CONCLUSIONS

Three $20^{o}/20^{o}$ zig-zag tests performed with the 13 400 tdw cargo ship USS Compass Island of the Mariner class were analysed. The experiments were carried out at different speeds. The output error method and the maximum likelihood method were applied to the data by use of the identification program LISPID. The hydrodynamic derivatives of a linear steering model were determined. A nonlinear model, where the linear model is supplemented with expressions for the nonlinear cross-flow drag, was also investigated. The models obtained from system identification techniques were compared with a linear model determined by HyA from scale model tests.

Preliminary identifications showed that it was suitable to fix the relation $-N_{\delta}'/Y_{\delta}'$. It is possible to determine this relation from the hull geometry, and it was decided to use the value 0.48, which was obtained from HyA:s model. It was also concluded from the preliminary analysis that the measurement biases and the parameters of the initial state should not be estimated at the same time. It was thus decided to fix the measurement biases to zero.

The linear model was first investigated. Model outputs close to the measurements were obtained when the output error method and the maximum likelihood method were applied, but the hydrodynamic derivatives were badly estimated. This was explained by the strong influence of nonlinear effects during $20^{o}/20^{o}$ zig-zag tests. Investigations of HyA:s model also showed that a linear model could not describe the ship motion satisfactorily during such experiments.

The nonlinear model was then analysed. The effective cross-flow drag coefficient is the only unknown parameter of the nonlinear contributions. Outputs close to the measurements were now obtained from the nonlinear model, when the linear part was fixed to HyA:s model. The parameters obtained from output error

identifications and maximum likelihood identifications were reasonable. The consistency between model outputs and measurements was good in all cases. A significant improvement was thus obtained by using the nonlinear model instead of the linear model, when the $20^{\circ}/20^{\circ}$ zig-zag tests were analysed.

The models obtained from output error identifications and maximum likelihood identifications were also compared. Based on parameter estimates obtained, analysis of residuals, and Akaike´s information criterion it was concluded that the models obtained from maximum likelihood identifications were distinctly better than the ones obtained from output error identifications.

The accuracies of the parameters obtained from the maximum likelihood method were also estimated. It was concluded that the hydrodynamic derivatives and the effective cross-flow drag coefficient were estimated with acceptable accuracies, while the covariance matrices were determined with bad precision. Notice, however, that the filter gains were determined much more precisely. The parameters could probably in general be determined more accurately, if longer experiments with other rudder perturbations, for example a PRBS, were available.

The speed of the ship varies during $20^{\circ}/20^{\circ}$ zig-zag tests. It was, however, concluded that the mean value could be used as an approximation of the true speed at each sampling event, when the hydrodynamic derivatives are normalized.

It was thus possible to determine the steering dynamics of the USS Compass Island by system identification techniques applied to data from $20^{\circ}/20^{\circ}$ zig-zag tests. It was crucial to use the nonlinear model when the experiments were analysed. The maximum likelihood method proved to be advantageous compared with the output error method. The identification program LISPID proved to be a powerful tool to determine the steering dynamics of ships.

7. ACKNOWLEDGEMENTS

This work has been supported by the Swedish Board for Technical Development under Contracts 734128 U and 754053.

The manuscript has been typed by Mrs. L. Andersson and the figures are drawn by Miss B.-M. Carlsson.

8. REFERENCES

Akaike, H (1972): Use of an information theoretic quantity for statistical model identification. Proc. 5th Hawaii International Conference on System Sciences, Western Periodicals Co, North Hollywood, California, USA, pp. 249-250.

Åström, K J (1970): Introduction to Stochastic Control Theory. Academic Press, New York.

Åström, K J, and C G Källström (1973): Application of system identification techniques to the determination of ship dynamics. Proc. 3rd IFAC Symp on Identification and System Parameter Estimation, the Hague/Delft, the Netherlands, pp. 415-424.

Åström, K J, N H Norrbin, C Källström, and L Byström (1974): The identification of linear ship steering dynamics using maximum likelihood parameter estimation. TFRT - 3089, Department of Automatic Control, Lund Institute of Technology, Lund, Sweden. Also available as Report 1920-1, Swedish State Shipbuilding Experimental Tank, Gothenburg, Sweden.

Åström, K J, C G Källström, N H Norrbin, and L Byström (1975): The identification of linear ship steering dynamics using maximum likelihood parameter estimation. Publ. No 75, Swedish State Shipbuilding Experimental Tank, Gothenburg, Sweden.

Åström, K J, and C G Källström (1976): Identification of ship steering dynamics. Automatica, 12, 9.

Chislett, M S, and J Strøm-Tejsen (1965): Planar motion mechanism tests and full-scale steering and manoeuvring predictions for a Mariner class vessel. Report No. Hy-6, Hydrodynamics Department, Hydro- and Aerodynamics Laboratory, Lyngby, Denmark.

Källström, C G, T Essebo, and K J Åström (1976): A computer program for maximum likelihood identification of linear, multivariable stochastic systems. Preprints 4th IFAC Symp on Identification and System Parameter Estimation, Tbilisi, USSR, Vol. 2, pp. 508-521.

Källström, C G (1977): Identification of the linear steering dynamics of the Sea Splendour. Department of Automatic Control, Lund Institute of Technology, Lund, Sweden. CODEN: LUTFD2/(TFRT - 7129)/1-085/(1977).

Mandel, P (1967): Ship maneuvering and control. In J P Comstock (Ed.): Principles of Naval Architecture. Society of Naval Architects and Marine Engineers, New York.

Morse, R V, and D Price (1961): Maneuvering characteristics of the Mariner class ship in calm seas. Report GJ-2223-1019, Sperry Gyroscope Company, New York.

Motora, S (1972): Maneuverability, state of the art. International Jubilee Meeting on the Occasion of the 40th Anniversary of the Netherlands Ship Model Basin, Wageningen, the Netherlands.

Norrbin, N H (1976): Om en kvasi-stationär integral för icke-linjär dämpning i fartygs girmanöver. PM B187, Swedish State Shipbuilding Experimental Tank, Gothenburg, Sweden (in Swedish).

Smitt, L W, and M S Chislett (1973): Course stability while stopping. Report No. Hy-16, Hydrodynamics Department, Hydro-and Aerodynamics Laboratory, Lyngby, Denmark.